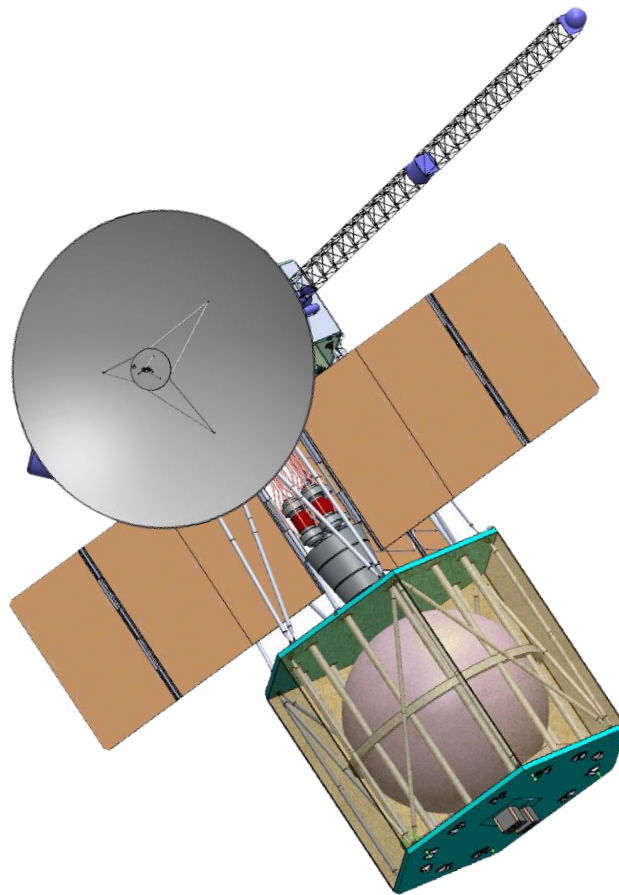


STARWORKS

VOYAGER III

DESIGN PROPOSAL



TEAM LEAD: Burton Yale
TEAM DEPUTY: Joshua Fofrich
TEAM MEMBERS: Jehosafat Cabrera-Guzman
Martin Kussler
Garrett Parham
Rohan Patel
Aayush Sareen

FACULTY ADVISOR: Dr. Navid Nakhjiri

California State Polytechnic University Pomona

Aerospace Engineering Department

Team Organization Chart



Contents

Team Organization Chart	i
List of Figures	iv
List of Tables	v
List of Equations.....	vi
Executive Summary.....	vii
1 Mission Description & Requirements	1
1.1 Requirements.....	2
1.2 Concept of Operations	5
1.3 Project Lifecycle and Mission Schedule	6
2 Scientific Objectives & Instrumentation	8
2.1 Scientific objectives.....	8
3 Configurations.....	16
3.1 Stowed Configuration	16
3.2 Mission Configuration	16
3.3 Subsystems Configurations.....	16
4 Trajectory	22
4.1 Broad Search	22
4.2 Low Thrust Trajectory Design and Optimization	25
4.3 Trajectory Coverage and Analysis	29
4.4 Launch Opportunity and Vehicle Selection.....	32
5 Propulsion Sub-System	35
5.1 Selecting a Propulsion System	35
5.2 Selecting a Thruster	37
5.3 Propulsion System in Detail	39
6 Power Sub-System	41
7 Space Environment	46
7.1 Thermal Environments.....	46
7.2 Radiation Environments.....	50
8 Structures Sub-System	52
8.1 Intro / Primary Structure Overview	52
8.2 Material Choices	52
8.3 Model Definition	52
8.4 Load Cases.....	53

8.5	Properties.....	55
8.6	MECO	58
8.7	Max Q.....	60
8.8	First Mode Approximation.....	63
9	Attitude Control Sub-System	64
9.1	Actuators and Sensors	64
9.2	Performance	67
9.3	Mass and Power Breakdown	69
10	Command and Data Handling Sub-System	70
10.1	Components.....	70
10.2	Performance	70
10.3	Fault Protection	71
10.4	Mass and Power Estimate.....	71
11	Telecommunications.....	72
11.1	Antennas.....	72
11.2	High Gain Antenna	73
11.3	Electronics.....	74
11.4	Performance	74
11.5	Subsystem Mass and Power Estimate	76
12	Systems Engineering	77
12.1	System Disposal	77
12.2	Risk Analysis and Mitigation	77
12.3	Cost Breakdown	78
12.4	System Mass & Power Breakdown	82
12.5	System Compliance.....	82
13	Future Improvements and Conclusion.....	84
13.1	Future Improvements	84
13.2	Conclusion.....	84
	Acknowledgements.....	85
	References	85

List of Figures

Figure 0-1 RETRIEVER Component Overview	viii
Figure 0-2 Trajectory Overview.....	ix
Figure 0-3 Voyager III Mission Point [73].....	x
Figure 1-1 Current Imaging Capabilities (left) [72] vs Expected Capabilities (right) [6].....	1
Figure 1-2 Concept of Operations for the Voyager III Mission	5
Figure 1-3 NASA Spaceflight Project Lifecycle [4]	6
Figure 1-4 Mission Timeline.....	7
Figure 2-1 Solar Wind Interactions [5].....	8
Figure 2-2 Solar Gravitational Lensing Focal Line [7].....	10
Figure 2-3 Mag Boom [9]	11
Figure 2-4 SWICS [10].....	11
Figure 2-5 CDA [11].....	12
Figure 2-6 ARIEL Mirror operations [12].....	12
Figure 2-7 ARIEL mirror diagram [12]	13
Figure 2-8 Output Image Resolution Grid Overlaid Over Los Angeles Airport	15
Figure 3-1 Zoom in View of Bus	18
Figure 3-2 Rotating Arc of Reactor Radiators	19
Figure 3-3 RETRIEVER Stowed Configuration Layout.....	20
Figure 3-4 RETRIEVER Mission Configuration Layout	21
Figure 4-1 Star Results Sorted by TOF, V_{∞} , and Earth Flyby Energy	23
Figure 4-2 Selected JGA Opportunities from Broad Search.....	24
Figure 4-3 Entire Trajectory (Mean Ecliptic J2000 XY View)	27
Figure 4-4 Interplanetary Trajectory (Mean Ecliptic J2000 XY View)	27
Figure 4-5 Heliocentric Velocity, Energy, and Thrust Magnitude versus Time.....	28
Figure 4-6 Earth Orbital Spatial Density versus Altitude	30
Figure 4-7 Earth Gravity Assist Perigee Error Dispersion.....	31
Figure 4-8 Earth Flyby (Left) Jupiter Flyby (Right).....	31
Figure 4-9 2044 Launch Opportunity.....	34
Figure 5-1 Contour Plot Demonstrating the Relationships Between I_{sp} , Thrust, and Power.....	38
Figure 5-2 Piping and Instrumentation Diagram	40
Figure 6-1 Power Sources Lifetime vs Output Power Level [31].....	41
Figure 7-1 Temperature Envelope for Mission Instruments.....	47
Figure 7-2 Layout and effects of ARIEL's radiation dissipation fins	48
Figure 7-3 Finite Analysis of ARIELs Thermal Isolation Techniques [12].....	49
Figure 7-4 Model of Radiation Dosage Rate vs Jupiter Orbit Altitude with Varying Shielding [38].....	50
Figure 7-5 Radiation Experienced Through Jupiter Flyby vs Titanium Thickness	51
Figure 8-1 Vertical Stiffener Cross Section.....	56
Figure 8-2 Effective Moment of Inertia of a Sandwich Panel Section	57
Figure 8-3 Moment of Inertia of a Rectangular Section	57
Figure 8-4 MECO - Total Translation.....	58
Figure 8-5 MECO - Plate Bending Moment X.....	59
Figure 8-6 MECO - PLATE Bottom Max Shear Stress	59
Figure 8-7 MECO - CBAR Axial Load.....	60
Figure 8-8 Max Q - Total Translation	61
Figure 8-9 Max Q - Plate Bending Moment X	61

Figure 8-10 Max Q - Plate Top Max Shear Stress.....	62
Figure 8-11 Max Q - CBAR Axial Load.....	62
Figure 8-12 1G Displacements	63
Figure 9-1 Placement of ACS Components in Bus.....	65
Figure 9-2 ACS Thruster Placement	66
Figure 9-3 Gyroscope used in MIMU [39]	66
Figure 9-4 MicroASC Star Tracker without Baffle [50]	66
Figure 9-5 SSOC-A60 Sun Sensor [51]	67
Figure 9-6 Pitch 90° to go from Interstellar Cruise to SGL.....	67
Figure 9-7 Roll 180° to go from SGL to Science Data Downlink.....	67
Figure 9-8 SRP Angular Impulse vs Time.....	68
Figure 11-1 Telecommunications System Block Diagram	72
Figure 11-2 Antennas of the Communications System.....	73
Figure 12-1 Architecture Risks Sorted by Likelihood and Consequence Matrix	77
Figure 12-2 Total Flight System Cost Breakdown	80
Figure 12-3 Total Project Cost Breakdown	81

List of Tables

Table 0-1 Mass Breakdown of RETRIEVER	ix
Table 1-1 System Level Requirements (SR)	2
Table 1-2 Science Objectives (SO).....	3
Table 1-3 Derived Requirements (DR)	4
Table 2-1 Science Instruments Summary.....	10
Table 2-2 ARIEL SPECS.....	13
Table 2-3 Exoplanet Selection.....	14
Table 2-4 Expected Resolution	15
Table 4-1 JPL Star Broad Search Criteria and Results	23
Table 4-2 TRAPPIST-1 Observation Target (Mean Ecliptic J2000 from the Sun).....	26
Table 4-3 Trajectory Encounter Summary	26
Table 4-4 Low Thrust Burn Schedule and ΔV	28
Table 4-5 SFL Arrival Sensitivity to Dry Mass (Assuming fixed wet mass of 14,000 kg)	29
Table 4-6 Trajectory Out of LOS Summary.....	29
Table 4-7 Galilean Moon Flybys.....	32
Table 4-8 Considered Launch Vehicles	33
Table 5-1 Propulsion Subsystem Mass Breakdown	40
Table 6-1 Primary Battery Characteristics [31]	42
Table 6-2 Battery and Solar Array Physical Values	43
Table 6-3 Solar Array Efficiencies.....	43
Table 6-4 Payload Power Required.....	44
Table 6-5 Power Sources Trade Study	45
Table 7-1 Heating Considerations per Mission Phase.....	46
Table 7-2 Steady State Heating Conditions (Cold and Hot)	47
Table 8-1 Block 1B PPL/CPL Combined Load Factors [42]	54
Table 8-2 First Mode Approximations	63
Table 9-1 Characteristics of Different Control Systems.....	64

Table 9-2 Expected Lifetime Orbit Torques	68
Table 9-3 ACS Mass and Power Current Best Estimate	69
Table 10-1 Amount of Data Possible to Collect	71
Table 10-2 C&DH Mass and Power Estimate	71
Table 11-1 Uplink to the RETRIEVER at 550 AU	75
Table 11-2 Science Data Downlink Budget from 550 AU	76
Table 11-3 Telecomm Mass and Power Estimate	76
Table 12-1 Estimation of ASRG Development and Manufacturing	79
Table 12-2 Cost Estimation Comparison (FY2020)	81
Table 12-3 RETRIEVER Mass and Power System Summary	82
Table 12-4 Architecture System Level Requirement Compliance Matrix	83

List of Equations

Equation 7-1 Maximum Temperature due to Steady State Heating	47
Equation 7-2 Minimum Temperature due to Steady State Heating	47
Equation 8-1 Equivalent Thickness Rectangular Section Representing Sandwich Panel	57
Equation 8-2 First Mode Frequency Approximation [45]	63

Executive Summary

In the effort to search for life on other planets, the main hindrance has always been how fine of detail can be resolved. In order to investigate the possible hospitability of a planet, the first aspect that must be considered is the atmospheric composition; elements such as O₂, CO₂, and N₂. Current imaging capabilities of these objects are nowhere near the level required for accurate atmosphere spectroscopy. The current best image, **Figure 1-1** (left), of an exoplanet, is not actually of the planet itself, but of its parent star. To solve this discrepancy, JPL has requested a space mission architecture proposal to utilize the concept of Solar Gravitational Lensing (SGL) to close this gap. By using the Sun's considerable gravitational attraction, a telescope would be able to increase the detail it resolves by many orders of magnitude, allowing for near megapixel image quality of a planet around another star. Much like glass lenses, the observation must happen from a focal point, for the Sun's case, this focal point is a line running from 550 AU to 1000 AU. In order to get a telescope to these distances, innovative designs must be considered, and this is why the mission is following in the legacy of the previous Voyager missions. This paper aims to provide such a vehicle to accomplish this goal.

For this mission to be viable, the spacecraft *shall* be able to reach the 550 AU mission point in under 60 years, so it has enough power to transmit back all of the science data from its 30-day mission. Another requirement to satisfy is that the spacecraft *shall* have an ACS system accurate enough to comply with the requirements from the selected telescope that *shall* have a main mirror size of larger than 1 meter.

In the process of meeting the mission goals, two candidate architectures were considered. The first design, BEAGLE, was focused around an Oberth maneuver while flying close to the Sun, 0.04 AU. This allowed the spacecraft to reach higher solar exit velocities, but the complexity involved in the thermal design made the spacecraft too risky of a design to continue. The second, and winning, design, RETRIEVER, used a combination of a 10kW nuclear reactor and Hall Effect propulsion. This, along with a series of planetary gravitational assists allowing the spacecraft to reach similar speeds as the previous design, at must less of a risk. The RETRIEVER design was selected due to its more reliable and proven mission design, simpler thermal management, and End of Life (EOL) power capabilities, which allow for secondary missions.

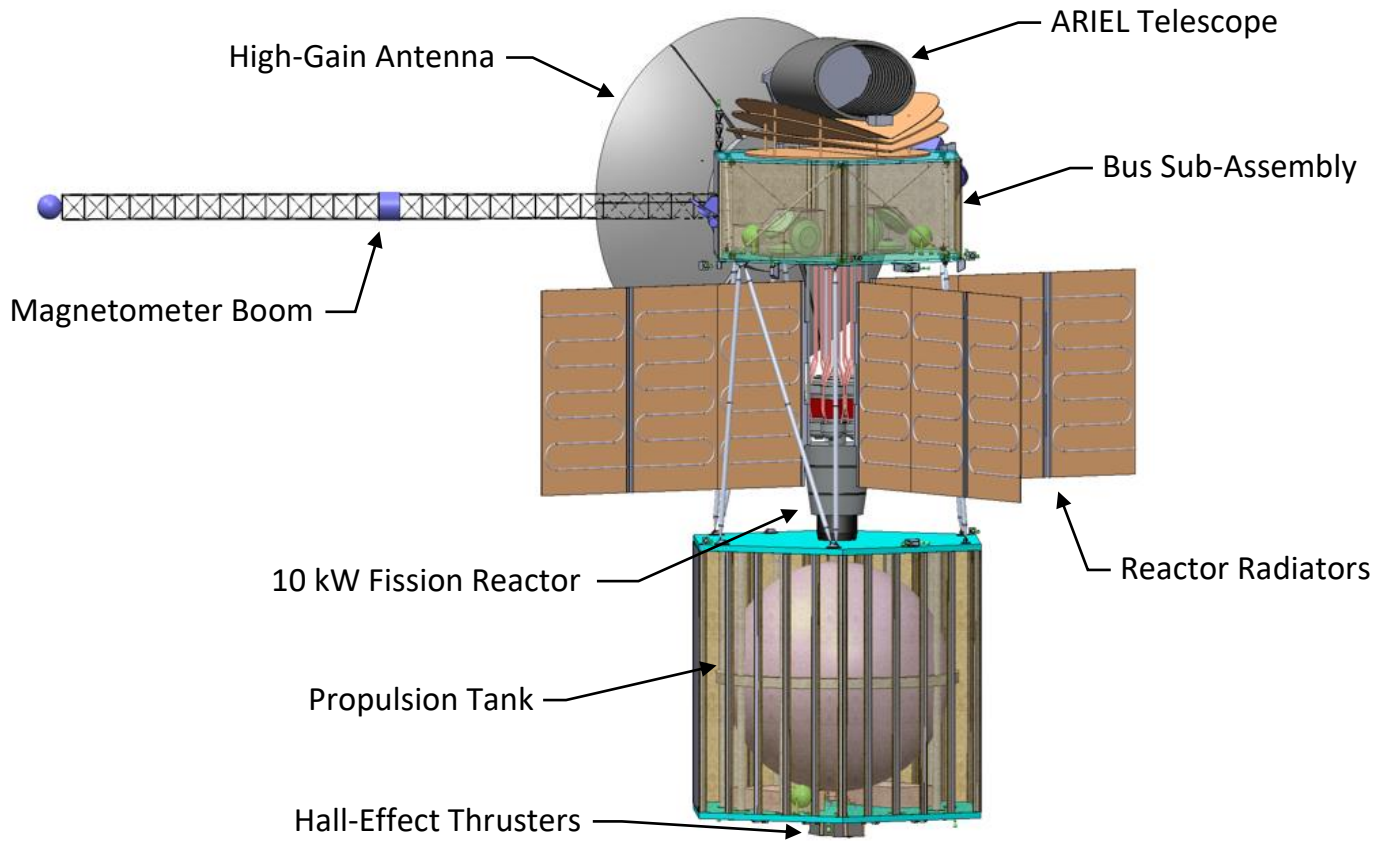


Figure 0-1 RETRIEVER Component Overview

The spacecraft is broken into three main sections, the bus which houses all of the electronics or avionics, communication equipment, and science instruments, the power assembly where the reactor and radiators are, and finally the propulsion housing where the xenon propellant and Hall Effect thrusters are mounted.

In order to minimize the time to 550 AU while maximizing the amount of science equipment, an Earth leveraging maneuver would be performed, allowing RETRIEVER to lower its C_3 from $120 \text{ km}^2/\text{s}^2$, for a direct transfer to Jupiter, to $44.89 \text{ km}^2/\text{s}^2$. After leaving Jupiter, the spacecraft will continue to accelerate using electric propulsion all the way to the 100 AU point, nearly 18 years later, with a final speed of 52.57 km/s or 11.08 AU/yr . This is nearly 3.4 times the speed of the Voyager 1 and 2 probes [1]. From there, the spacecraft would coast in a low power cruise where it would exercise its equipment for the rest of its 40-year journey. In total, RETRIEVER would be able to reach the 550 AU point and begin its mission in 2102, 58 years after its launch in 2044.

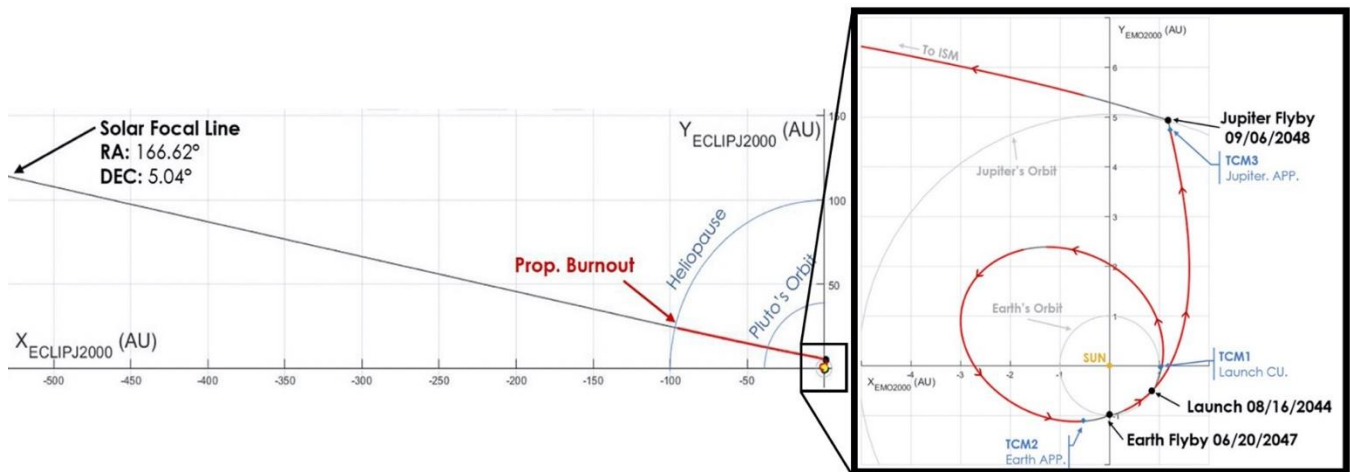


Figure 0-2 Trajectory Overview

The propulsion system, as stated, is a nuclear-electric system feeding to a Hall-Effect thruster, the Busek BHT-8000. With an on-orbit dry mass of 3200 kg, the propulsion system uses 10,800 kg of propellant in order to provide RETRIEVER with 32.4 km/s of ΔV . Another major factor of the BHT-8000 is its 8 kW power draw throughout this mission, so an adequate power system must be selected in order to meet this need.

To power the spacecraft through its long journey, there is only one energy source that will satisfy mission needs, that is nuclear energy. To satisfy the power requirements of the Hall Effect thrusters, the use of RTGs was infeasible due to a required unit count of 20. To meet the power draw of the propulsion, the 10kW version of the KiloPower nuclear fission reactor was selected.

Table 0-1 Mass Breakdown of RETRIEVER

Sub System	Mass (kg)	Power (W)
Structure/Mechanisms	440	10
Radiation Management	240	0
Thermal Management	50	10
Attitude Control	150	125
Power Management	1,445	120
Cabling	80	0
Propulsion	290	8,000
Telecommunications	50	395
Command & Data Handling	75	55
Sub-Total (margin% incl.)	3,000 (15%)	9,440 (20%)
Payload	200	150
Propellant	10800	0
LVA	415	0
Total	14,415	9,590

Due to the powerful magnetic field around Jupiter, which traps high energy particles, the spacecraft will receive a concentrated dose of radiation during its flyby. This necessitates the use of a radiation vault, akin to that seen on the spacecraft JUNO [2]. This vault protects the electronics during the Jupiter flyby, and also the rest of the mission through the interstellar medium, where the radiation environment is much more uncertain.

To communicate at distances such as 550 AU, a 3.5m Cassegrain antenna, similar to the size as seen on the Voyager probes, and high-powered traveling wave tube amplifiers, the spacecraft is able to downlink all of its data in 8 months after mission completion. For communication within the inner solar system and during low-thrust maneuvers, the spacecraft will use its three low-gain antennas to send command data and get system statuses.

In order to estimate the costs of the architecture as a whole, NASA's Project Cost Estimation Capability (PCEC) tool, a parametric cost estimator was used. Inputting RETRIEVER's mission parameters, such as flight time, sub-system complexities, and number of instruments, an approximate cost of the mission was obtained [3]. In total the RETRIEVER system, including design, manufacturing, and operation, was estimated to cost \$2.45B, excluding the cost of the launch vehicle.

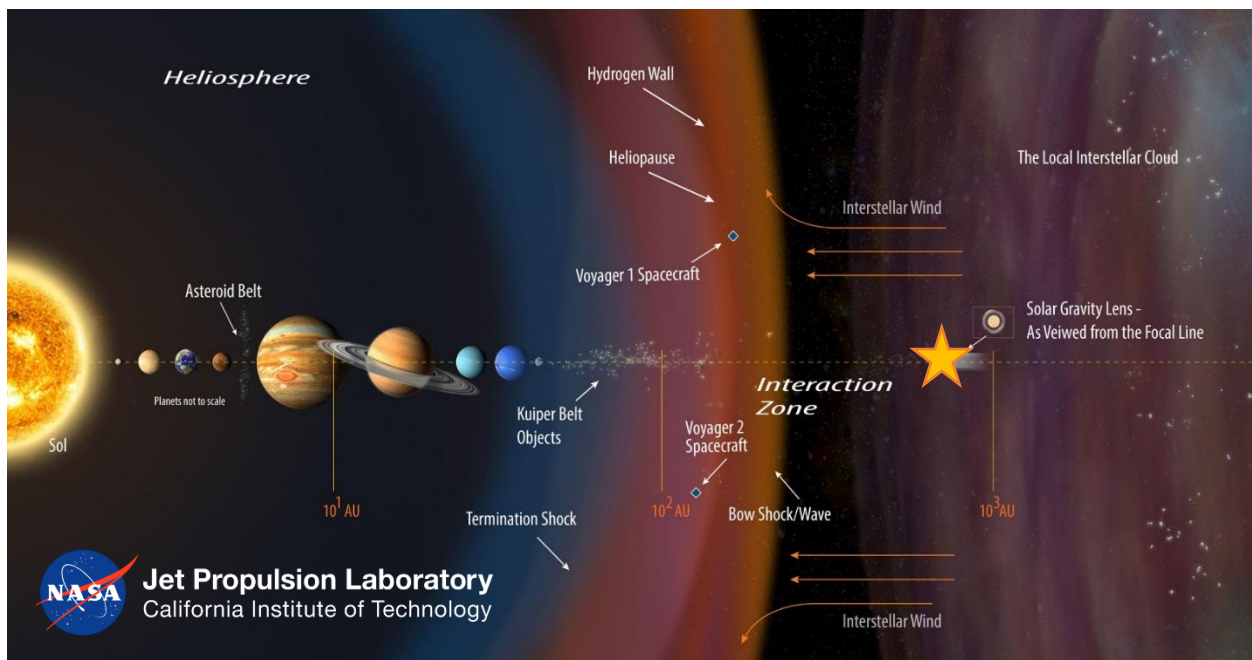


Figure O-3 Voyager III Mission Point [73]

1 Mission Description & Requirements

As part of NASA JPL's RFP to explore the interstellar medium and beyond, Voyager III will be the first spacecraft to be able to directly view a planet around another star. Both of these goals will be completed by traveling to 550 AU (3.9x farther than Voyager I), to be at the focal point for SGL, with a suite of scientific instruments to study the environment along the way. Similar to the previous Voyager missions, Voyager III aims to raise the bar in terms of new flying equipment, as they will be necessary to complete the mission within the allotted time period.

The main focus of the mission is still viewing an exoplanet, primarily to study the geology formed on other planets that, up to this point, could only be inferred upon. By using solar gravitational lensing, the spacecraft will be able to resolve enough detail to properly view the atmospheres of other planets in search of life harboring compounds.



Figure 1-1 Current Imaging Capabilities (left) [72] vs Expected Capabilities (right) [6]

In **Figure 1-1**, on the left is our current imaging capabilities of exoplanets, the image is actually a photo taken of the parent star of the exoplanet system TRAPPIST-1, taken by Kepler Space Telescope. With current capabilities being less than 1 pixel, no meaningful science data can be taken with these planets, only inferences can be placed on their possible surface features. On the right is the expected output of the mission. Once RETRIEVER gets to its mission point at 550 AU and has taken data over a 30-day span, the spacecraft will be able to return an image of approximately 1 megapixel (1,000,000 pixels). This stark difference proves the capabilities and rewards of using the Sun as a solar gravitational lens.

In order to get to this point, the vehicle must overcome many challenges, mainly stemming from its incredibly long time to mission operation. Reliability is a key issue with a mission of this duration, so redundancy is a central pillar in the design of RETRIEVER and all of its sub-systems. As well, the interstellar

medium has only been travelled by two spacecraft, so it is still a relatively untested environment for spacecraft.

1.1 Requirements

Below is the full set of requirements dictated by the RFP (system level, and science) as well as derived requirements supplied by STARWORKS for the use of better constraining architecture elements. Within the system level requirements are highlighted the driving requirements which held the greatest influence over design decisions and trade studies.

1.1.1 System Level Requirements

In the **Table 1-1** below are the system level requirements that must be met by this proposal. Additionally, all highlighted requirements were noted as driving requirements and having the largest influence on the design of RETRIEVER.

Table 1-1 System Level Requirements (SR)

SR1.0 Trajectory	
SR1.1	The launch <i>shall</i> be conducted on today's available launch vehicles (including the SLS).
SR1.2	The spacecraft <i>shall</i> reach 550 AU in less than 60 years from launch.
SR1.3	The spacecraft <i>shall</i> remain in line of sight for at least 30 days at 550 AU for SGL.
SR1.4	All required maneuvers <i>shall</i> be addressed and corrections to the orbit.
SR2.0 Observations	
SR2.1	All scientific objectives <i>shall</i> be met by the spacecraft.
SR2.2	An exoplanet system <i>shall</i> be selected for observation.
SR2.3	An exoplanet <i>shall</i> be directly imaged using solar gravitational lensing (SGL).
SR2.4	A schedule <i>shall</i> be provided for all major scientific experiments.
SR3.0 Vehicle	
SR3.1	The spacecraft <i>shall</i> withstand both the launch vehicle and space environment.
SR3.2	The spacecraft power supply <i>shall</i> be capable of transmitting all scientific data back to Earth.

SR3.3	The spacecraft's attitude control system <i>shall</i> be capable of maneuvering the telescope to perform SGL for at least 30 days.
SR3.4	The spacecraft <i>shall</i> be equipped with a 1.0 m diameter telescope and coronagraph at 550 AU.
SR4.0 Management	
SR4.1	Cost estimates <i>shall</i> be provided for all subsystems and operations of the mission.
SR4.2	A timeline of all major events and stages of the mission <i>shall</i> be provided.

1.1.2 Science Requirements

Table 1-2 Science Objectives (SO)

SO1 Solar Magnetic Fields	
SO1.1	The strength, orientation, and turbulence of the magnetic field will be measured to study the magnetic field's influence on the distribution of dust, ions, and other charge particles with an uncertainty less than ± 0.03 nT.
SO2 Solar Winds	
SO2.1	The characteristics of the boundaries of the termination shock, heliosheath, and heliopause shall be determined by measuring the pick-up ion population and energetic electrons in the range of 1 to 40 keV.
SO3 Extragalactic Background Light (EBL)	
SO3.1	The spacecraft shall measure the extragalactic background light intensities less than $0.8 \text{ nW}/(\text{m}^2\text{Sr})$ with less than 1% uncertainty within 1 – 100 μm at a minimum heliocentric distance of 10 AU.
SO4 Interplanetary Dust & Plasma	
SO4.1	The interplanetary dust composition will be determined by measuring the grain size distribution, the dust impact rates, the plasma temperatures, and the plasma density.
SO5 Solar Gravitational Lensing (SGL)	
SO5.1	Direct imaging of an exoplanet will be performed using the method of solar gravitational lensing at a minimum distance of 550 Au over a minimum wavelength of 0.1 – 20 μm .

SO5.2	A presence for the atmospheric biosignatures of O ₂ , O ₃ , N ₂ O, NH ₃ , CH ₄ , and C ₂ H ₆ shall be determined for the observed exoplanet.
-------	---------------------------------------------------------------------------------------------------------------------------------------------------------------------------------------------------------------------------

1.1.3 Derived Requirements

Table 1-3 *Derived Requirements (DR)*

DR1.0 Trajectory	
DR1.1	Earth flybys must be done at or above 500 km altitude
DR1.2	Trajectory must be able to withstand at least 1 day of missed thrusting in 100 days.
DR1.3	Planetary flybys must be unpowered with a minimum forced coast period of ± 25 days from the encounter.
DR2.0 Scientific Equipment	
DR2.1	The power draw must be under 10kW due to the current state of nuclear technology and launch mass.
DR2.2	Pointing accuracy of spacecraft must be within 17 arcseconds (1 σ radial)
DR2.3	SC must be able to sustain at least 20 years in a deep sleep low power mode
DR2.4	The telescope must provide a resolution of at least 100 km ² /pixel (from SO5.1)
DR3.0 Structure	
DR3.1	SC must be radioactive hardened to withstand planetary or solar flybys
DR3.2	Structure must be able to withstand the dynamic envelope of the launch vehicle
DR3.3	Spacecraft must be able to withstand launch vibrations
DR3.4	Bus temperature must be regulated to the operating conditions of internal components
DR4.0 Communications, Command, and Data Handling	
DR4.1	Data handling system must be able to store at least 1 Tb of data in total
DR4.2	Spacecraft must be able to transmit at least 2000 bits/second over the High Gain Antenna

DR4.3	Spacecraft must be able to transmit location data at any time requested to the DSN excluding loss of L.O.S.
DR4.5	A long term, low power cruise state must be implemented for long duration operations.

1.2 Concept of Operations

The Voyager III mission will begin in August of 2044 with a Space Launch System (SLS) Block 1B launch and heliocentric orbital injection. After a systems checkout period, RETRIEVER will begin a low thrust burn to increase its heliocentric energy in preparation for the Earth flyby. During the interplanetary orbit and Earth gravity assist, which occurs in 2047, the spacecraft can conduct science and calibrate its onboard instruments. After another checkout period, RETRIEVER will then restart its low thrust engine and head towards Jupiter in 2048 for another gravity assist, offering imaging science of the Galilean moons. A long-duration low-thrust burn, which will deplete all remaining propellant, will be conducted after the flyby and RETRIEVER will be sent to the interstellar medium. Additional science measurements will be conducted along the way and periodic equipment exercising and communication will commence. After 58 years from launch, RETRIEVER will finally reach the solar focal line and image the TRAPPIST-1 exoplanet system. The data will be sent to Earth, and the possible extended mission and disposal protocol will begin. Figure 1-2 summarizes the critical phases of the mission in the order they will occur.

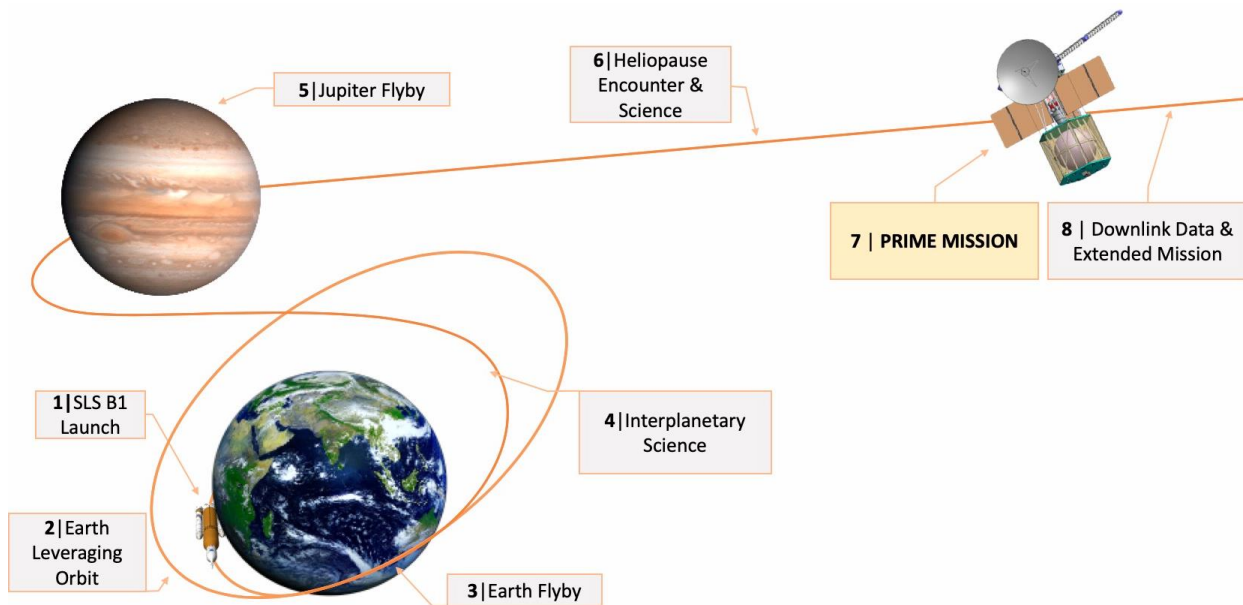


Figure 1-2 Concept of Operations for the Voyager III Mission

1.3 Project Lifecycle and Mission Schedule

Currently, the project has passed the Preliminary Design Review (PDR). The next milestone is the Critical Design Review, where a detailed analysis of each subsystem and project element will be reviewed. **Figure 1-3** illustrates the NASA project life cycle timeline in terms of project phases and technical reviews. Phase B is completed as of PDR, and Phase C will begin. Certain fabrication elements will be coordinated, and the design will be finalized.

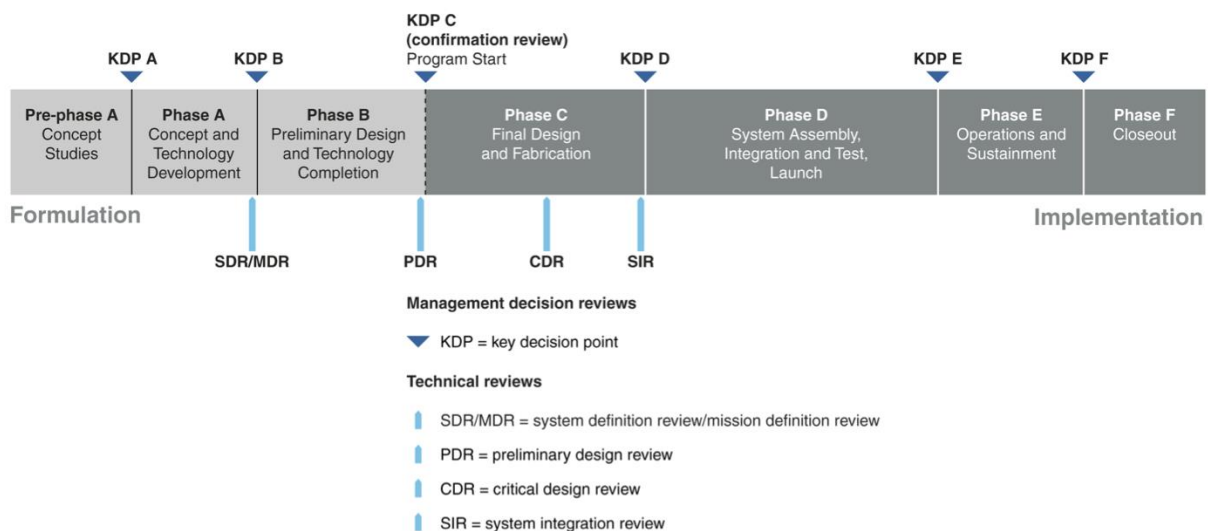


Figure 1-3 NASA Spaceflight Project Lifecycle [4]

Figure 1-3 highlights key events of the mission design to their radial distances and time. The anticipated launch period is between August 4th and August 23rd. After the second stage cutoff from the SLS and a nominal heliocentric orbit injection, the vehicle will be oriented for the acquisition of the signal. Once done, the radiator panels and magnetometer boom will extend, and the systems checkout period will begin. A trajectory correction maneuver (TCM) will be performed on the attitude control system to correct for any launch injection errors. The first low thrust burn will begin and routine uplinks and downlinks with the spacecraft will commence. The burn will finish in June of 2045 and a 2-month coast period will begin. Interplanetary and parallax science can be conducted in this window. There is a solar conjunction occurring on July 19, 2045 for 19 hours and 16 minutes. Any thrusting or TCMs are prohibited out of line of sight (LOS) due to a lack of ground intervention in the event the spacecraft goes into safing. The second burn will be conducted up until the pre-flyby forced coast period for planetary protection. A TCM will be performed and the Earth flyby will yield a valuable opportunity to calibrate the telescope and other science equipment. After the flyby, the low-thrust engine will be restarted and a short coast period

to Jupiter will begin. The Jupiter flyby will be preceded by a TCM, and scientific instruments will be reactivated to collect data on the environment and Jovian moons through the flyby. On the solar system escape portion of the trajectory, the low thrust engine will be restarted and after 10 AU (radial distance from the Sun) the second major interplanetary science mission to investigate the Extragalactic Background Light (EBL) will begin. The spacecraft will routinely exercise its reaction wheels and instruments onboard while relaying engineering data via the low gain antenna (LGA). Another scientific mission opportunity will be encountered at the heliopause and data will be transmitted via the high gain antenna (HGA). From the heliopause (100 AU) to the solar focal line (550 AU), the spacecraft will enter a long duration low power cruise with minimal ground staffing. Engineering data will be periodically transmitted via the LGA and equipment intermittently exercised. In preparation for the prime mission, the attitude control system will be tested and verified. Data will be relayed to Earth and the telescope will begin another calibration phase. The prime mission is expected to take 30 days, beginning in August of 2102. After the prime mission, the data will be relayed via the HGA for roughly 0.7 years. Any extended mission opportunities will be conducted afterward. System disposal is not prioritized by any planetary protection regulations as the spacecraft is already on a solar system escape trajectory. The legacy of the existing Voyager missions can be continued on RETRIEVER with another golden plaque representing humanity to those out in the interstellar medium.

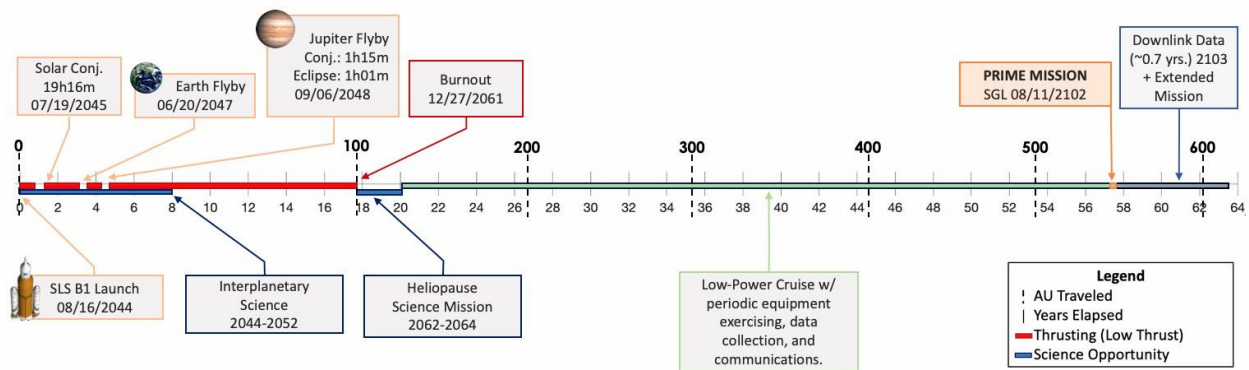


Figure 1-4 Mission Timeline

2 Scientific Objectives & Instrumentation

2.1 Scientific objectives

This section briefly summarizes the scientific objectives RETRIEVER has been designed to complete. The primary scientific goal of the spacecraft is to directly image an exoplanet using Solar Gravitational Lensing, but multiple scientific experiments will occur along the way to obtain further knowledge of the interstellar medium.

The first objective is to measure planets' magnetic field strength and orientation. Furthermore, the spacecraft will measure the flow behavior in the distribution of dust, ions and charged particles due to the influence of magnetic strength.

The second objective is to measure any pick-up ion or energetic electrons charges and population. As RETRIEVER cruises towards the ISM and measure charged particles and dust, it provides data to determine the boundaries of the Heliopause, and the termination shock at the Heliosheath, which is currently believed to be at 120 AU and 80 to 100 AU, respectively [5]. The difference in the intensity, relative velocity, and impact of solar wind and dust particles will determine these boundaries. As RETRIEVER reaches the termination shock, the spacecraft enters the heliosheath where the spacecraft will begin to measure magnetic field strength and magnetic influence on particles in ISM. Additional understanding of the heliopause, the region where the solar wind particles and interstellar wind particles come to rest, will be obtained during this portion of the spacecraft's trajectory. **Figure 2-1** below depicts a model of the upwind heliosphere in the magnetized interstellar wind [5].

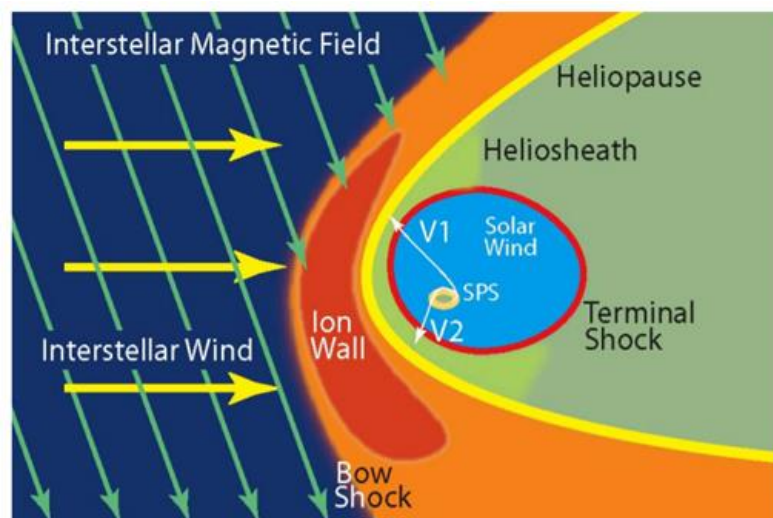


Figure 2-1 Solar Wind Interactions [5]

The third objective for the mission is to obtain the EBL spectrum and brightness for both optical and IR wavelengths with intensities less than $0.8 \text{ nW}/(\text{m}^2\text{Sr})$ with less than 1% uncertainty. This objective must be conducted beyond 10 AU to reduce zodiacal light effect. The EBL spectrum captures cosmological backgrounds such as cosmic microwave background (CMB), or photons emitted by near galaxies and star due to radiative particles and processes.

The final science objective, apart from the prime mission, is to collect and measure dust particles and plasma intensity during interplanetary cruise. As RETRIEVER cruises through the heliosphere, dust and grains around planets will be measured to understand grain sizes and distribution around the magnetosphere of the planet. When RETRIEVER reaches the ISM, there is an opportunity to quantify plasma intensity, temperatures and, dust impact rates within solar wind and interstellar wind. Modelling the plasma density variations in heliosheath and interstellar medium can provide data for determining the boundaries of ISM.

As the spacecraft reaches 550 AU, the prime mission of the design begins, and RETRIEVER will directly image an exoplanet. RETRIEVER must also search for biosignatures of the exoplanets, which will be covered in further detail in the Exoplanet System section of this report. The presence of any biosignatures will be achieved by obtaining spectroscopic and IR images over the wavelength ranges provided by the RFP between 0.1 to $20\mu\text{m}$. The focus of RETRIEVER is to image an exoplanet by reaching 550 AU. The spacecraft has to remain in the radius of deflected rays from Einstein ring to utilize Solar Gravitational Lensing (SGL) to increase the effective focal length of the telescope, which, in return, enhances the product resolution of the exoplanet by over one million times. In geometrical optics, rays of light in the vicinity of mass such as Jupiter are deflected from their initial direction at a rate θ , where these rays typically with some impact parameter converge at a focal line, where the light intensity is amplified by a factor of $2GM/c^2\lambda$ [6]. This phenomenon and the focal point acts as gravitational lens. Gravitational lens having spherical aberration forms a focal line of the light rays converging from the body. Any star that is massive and compact enough for the light rays to deflect to the focal line due to gravitational deflection acts similar to a lens of a telescope. Its focal line begins at 547.8 AU and spans to 650 AU. The thickness of the Einstein Ring at 550 AU starts at 1000 km, but only gets larger and easier to view, the further the focal point. The figure below provides an illustration of SGL [7].

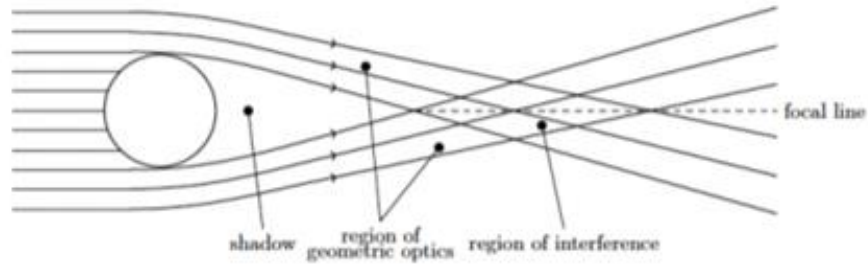


Figure 2-2 Solar Gravitational Lensing Focal Line [7]

The reason for the large amplification of the SGL is that it forms an envelope of light rays deflected from the sun in its focal area, whereas a normal optical lens forms a single focal point. To be a gravitational lens, the wavelength of the light rays must be smaller than the Schwarzschild radius at a given distance, which happens beyond 548 AU, where wavefront in focal region is dominated by caustic. Thus, a spacecraft that is capable of reaching 550 AU can utilize Solar Gravitational Lensing in order to magnify any light from distant objects to directly observe exoplanets.

2.1.1 Payload

The RETRIEVER spacecraft utilizes a several instruments to meet all the scientific objectives of the mission. The payload instruments are shown in **Table 2-1**. The payload is designed to analyze the strength of magnetic fields, analyze interplanetary dust and grains, and measure plasma waves as the spacecraft cruises through the ISM to 550 AU where the ARIEL Telescope will be used for solar gravitation lensing for 30 days. The payload of RETIREVER has many inputs to the payload power efficiency compared to legacy spacecraft, such as Cassini with instruments drawing only 157 watts of power while utilizing some of the same instruments that were used for the Cassini mission [8]. The instruments are designed to endure the low temperature environments associated with the long duration travel through the ISM [8].

Table 2-1 Science Instruments Summary

Instrument Name	Mass (kg)	Power (W)	Temperature Limits (°C)
MAG – 3 [9]	0.1	0.03	-55 to 85
Solar Wind Ion Composition Spectrometer (SWICS) [10]	6	6	-10 to 40
Cosmic Dust Analyzer [11]	16	11	-10 to 40
ARIEL Telescope & Coronagraph [12]	180	140	-233 to -203

2.1.1.1 MAG – 3

The MAG-3 is designed to be a 3-axis fluxgate magnetometer to act as a highly-sensitive deep space compass to precisely record the magnetic field strength around the spacecraft as it cruises through the planet's magnetosphere region [9]. The MAG-3 was used on Cassini and has a TRL of 9 [9]. As RETRIEVER cruises past planets to perform Jupiter



Figure 2-3 Mag Boom [9]

and Earth gravity assists to slingshot the spacecraft into the ISM, MAG-3 will be operating continuously throughout the journey for navigation. MAG-3 will be recording magnetic field strength from Jupiter to any magnetic field influence from outer stars on particles, dust, and grains during the cruise past the Heliosheath towards the ISM. MAG-3 has a sensitivity of $100 \mu\text{V/nT}$, and accuracy of 0.0075 nT , and can be sensitive to any magnetic, radio waves produced from the spacecraft. To mitigate the risk of reading signals produced by the spacecraft, MAG-3 will be installed on 6.5-meter-long arm Mag Boom shown in **Figure 2-3**.

2.1.1.2 Solar Wind Ion Composition Spectrometer (SWICS)

SWICS instrument will be utilized to measure any particles detected within the solar and interstellar wind. The SWICS instrument is flight-proven since it was used on the Cassini spacecraft [10]. As RETRIEVER passes through the heliosphere and enters the termination shock, SWICS will be continuously detecting and measuring the



Figure 2-4 SWICS [10]

composition, density, temperature and flow velocity of ions, low-charged ions and high-charged particles. The differently charged particles with different flow velocities can help determine the boundaries of heliopause and termination shock while generating data to further understand the behavior of interstellar wind. SWICS instrument consists of an electron spectrometer to measure low-charged particles and an ion beam and mass spectrometer, which can measure different high-end energy spectrum of charged mass and particles. The SWICS instrument exceeds the requirements of being capable of measuring charged particles between $1 - 40 \text{ keV}$ by having a measurement range of $0.16 - 70 \text{ keV}$ [10].

2.1.1.3 Cosmic Dust Analyzer (CDA)

The CDA instrument will provide direct observations and measurements of any dust grains emitting from the atmosphere of planets. The trajectory through Jupiter's magnetosphere contains an opportunity to directly observe the atmosphere around the Jovian Moons. **Figure 2-5** shows the CDA in its data gathering configuration. This instrument measures the amount, velocity, impact rates, and mass of charged ions and dust particles. The CDA instrument is capable of measuring impact rates up to 1 particle per second, for speeds of 1-100 km/s. The CDA can measure particles of mass within the range of 10^{-15} to 10^{-6} kg. The CDA will be operating most of the mission duration to obtain as much data on the behavior of particles as possible [8].



Figure 2-5 CDA [11]

2.1.1.4 ARIEL Telescope

ARIEL Telescope is a Cassegrain telescope (M1 being primary parabolic and M2 being secondary hyperbolic mirror) with M3 mirror aligning the beams [12]. As described by ESA, ARIEL is also provided with an additional M4 mirror that helps direct the collimated beam to the optical bench as shown in **Figure 2-7** below [12].

The aperture stop is located at M1 as the primary coronagraph, which acts as first line of defense to block out-of-field-light. Then an additional baffle is positioned on M2 which further blocks any dust particles and direct view of the sky from M2. The M2 has a refocus mechanism which can be actuated in 3 degrees of freedom which helps correct one-off movements due to cool-down and loads. This refocus mechanism helps move M2 to direct the spectrum to be collected by ARIEL's sensors, AIRS and FGS. This mechanism provides the Cassegrain focus. According to ESA, after Cassegrain focus, the beam is aligned towards M3, which is then collimated to a 20 mm x 13.3 mm beam size and then directed to M4 which passes the beam to optical bench [12]. This beam continues traveling to a folding mirror (M5), which is used to deflect the beam back at an angle towards the AIRS sensor input

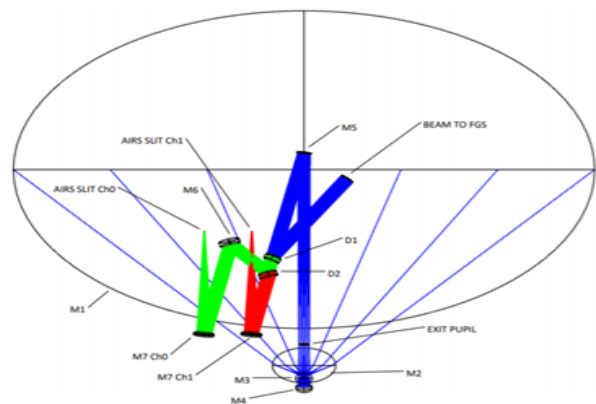


Figure 2-6 ARIEL Mirror operations [12]

optics and dichroic (showing different visible rays) beam, which is then injected into single beam through a small hole in the center of the mirror as shown in **Figure 2-6** [12].

With the given mechanism and Focal length of 14.17 m, ARIEL telescope is able to achieve an angular magnification of 55 and focal ratio of 13 and 18.9 respectively for M1 & M2 [12]. This coupled with SGL provides the imaging magnification of over a million pixels. The

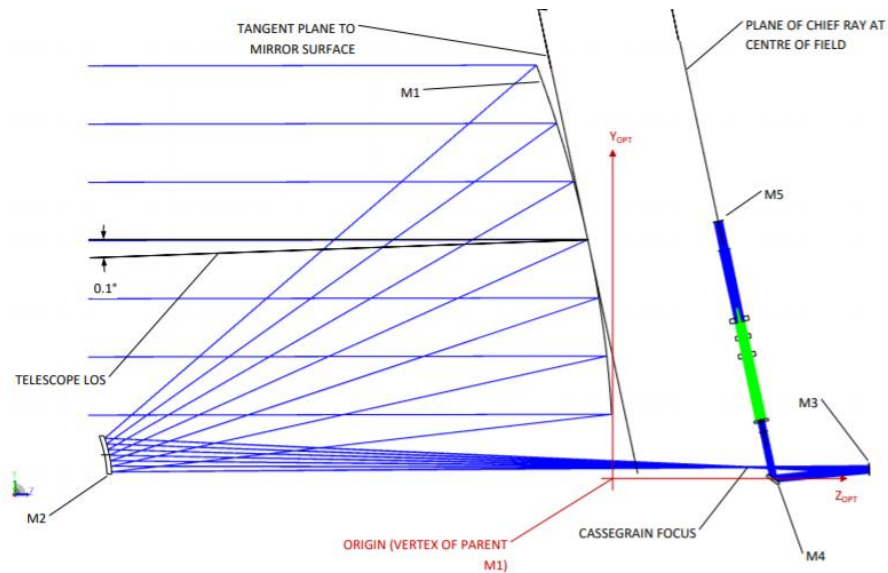


Figure 2-7 ARIEL mirror diagram [12]

Table 2-2 below provides simple specs for the telescope [12].

Table 2-2 ARIEL SPECS

Criteria	ARIEL's Capability (0.95 m diameter)
Focal Length (m)	(M1 & M2): 14.17
Angular Magnification	55
Focal Ratio	Mirror 1: 13.0 Mirror 2: 18.3
Wavelengths (μm)	0.03-18
Linear Resolution	<0.1 μm
FoV science pixel (")	6.4 x 26.8

2.1.2 Additional Science opportunities

The 58-year total mission time provides the science team numerous opportunities to conduct more scientific investigations. The RETRIEVER spacecraft has countless opportunities to conduct additional science experiments to exceed the requirements outlined in the RFP. As RETRIEVER performs a gravitational assist at Jupiter, RETRIEVER’s instruments, such as ARIEL and CDA will be turned on to collect images and analyze the dust particles emitted from Jovian moons. Turning on the telescope throughout the journey provides the spacecraft with another opportunity to perform parallax science to accurately measure the distance of distant stars at different points and time. Furthermore, turning on SWICS, even after exiting heliopause and entering the ISM, can provide valuable data of any interactions happening within the interstellar wind due to other stars.

2.1.3 Exoplanet System

At 550 AU the spacecraft will begin to directly image the exoplanet. Due to trajectory constraints limiting the declination angle, the two possible exoplanet systems to image were TRAPPIST-1 and K2-285. A trade study between these two exoplanet systems was performed, where the imaging resolution was the most important criteria.

Table 2-3 below shows the trade study performed between TRAPPIST-1 and K2-285 systems.

Table 2-3 Exoplanet Selection

Criteria	K2-285	TRAPPIST-1
Distance (Parsecs)	156	12
Number of Exoplanets	4	7
RA (deg.)	349.384	346.622
DEC (deg.)	1.300	-5.041
Imaging Resolution	19.34km/px 373.84 km ² /px	1.8km/px 3.24 km ² /px

With the increased focal length due to solar gravitational lensing and ARIEL’s angular magnification, the imaging resolution for both TRAPPIST-1 and K2-285 were calculated. The TRAPPIST-1 system was chosen due to its expected resolution, as it is over five times greater than the minimum

resolution required by the RFP. This system would allow for more opportunities to image more Earth-like exoplanets, since there are 7 exoplanets to target in that system. In **Figure 2-8**, the expected resolution of the output image can be seen. The reason for the significant difference in resolution was that TRAPPIST-1 is 12 parsecs away compared to K2-285 being 156 parsecs away. Below in **Table 2-4**, the expected resolution of TRAPPIST-1 based on the operated wavelengths of ARIEL telescope is provided [13].

Table 2-4 Expected Resolution

$\theta_{\text{resolution}}$ (arcsec)	Wavelength (μm)	Frequency (m^{-1})	Spatial Resolution (km)	Image Resolution (km/pixel)
4.36E-10	0.03	1.0E+08	1.98E+03	1.98
2.18E-09	0.05	2.0E+07	1.87E+03	1.87
4.36E-09	0.1	1.0E+07	1.79E+03	1.79
1.31E-08	0.3	3.333E+06	1.82E+03	1.82
4.36E-08	1	1.0E+06	2.67E+03	2.67
2.18E-07	5	2.0E+05	5.98E+03	5.98
4.36E-07	10	1.0E+05	6.23E+03	6.23
7.85E-07	18	5.556E+04	7.15E+03	7.15
8.73E-07	20	5.0E+04	7.37E+03	7.37

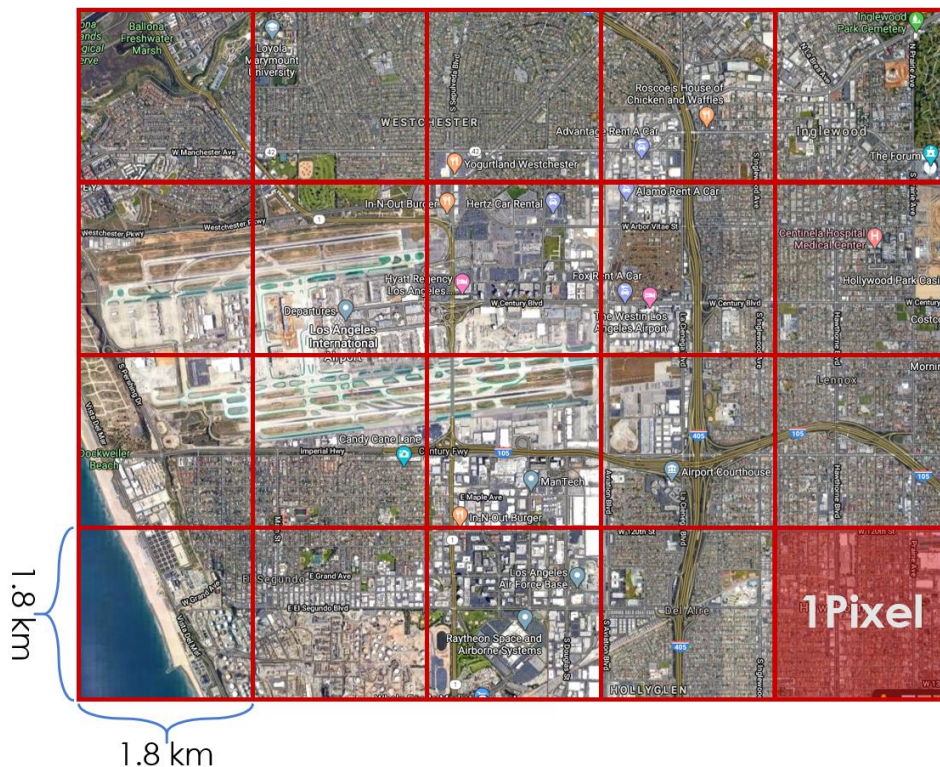


Figure 2-8 Output Image Resolution Grid Overlaid Over Los Angeles Airport

3 Configurations

In this section the different configurations of RETRIEVER will be discussed as well as the placement of subsystems and their components. It is important to determine the locations of the science instrumentation and provide them with the appropriate field of view to conduct their mission objective.

3.1 Stowed Configuration

The stowed configuration is shown in **Figure 3-3**. The important things to note from this figure are the clearances of the spacecraft from the inner membrane of the fairing. When RETRIEVER is stowed inside there is a maximum and minimum clearance of 2.35 m and 1.30 m, respectively from the side and a clearance of 9.37 m from the top of the spacecraft to the inner ceiling of the fairing. The three key differences in this configuration from the mission configuration are the nuclear reactor radiators, the magnetometer boom, and ARIEL Telescope. For the spacecraft to fit inside of the SLS B1B fairing [14], the magnetometer boom will be compressed and stowed inside of its compartment attached to the side of the bus. The optical opening of ARIEL will be covered in order to prevent any debris from damaging the lenses and coronagraph inside of the shroud. The reactor radiators are separated in three sections. The configuration of the subsystems will be further discussed in detail in the following sections. In this configuration, the spacecraft will be attached to the payload adapter fairing using an array of tie-rods separating RETRIEVER from the PAF by 0.40m.

3.2 Mission Configuration

In **Figure 3-4** the mission configuration of RETRIEVER is shown. In this configuration the magnetometer boom is extended out exposing both of its magnetometers to space to conduct science. The boom will extend 6.5m out from one side of the bus. The reactor radiators will be folded out to dissipate heat generated by the reactor and ARIEL Telescope will be uncovered.

3.3 Subsystems Configurations

To mitigate thermal, structural, and field of view design risks, it is important to have all science instrumentation close to one another. When deciding on the placement of all science equipment, this was the primary consideration.

The main instrument, the ARIEL Telescope, was mounted to the top the honeycomb panel of the bus. This allowed the telescope a clear line of sight to conduct the science required and transmitting data

back to Earth. Three of the six sides of the bus are covered in multi-layer insulation (MLI) and the other three are honeycomb paneling. The honeycomb panel provides adequate structural support to the components mounted on the sides of the bus. The SWICS instrument was placed on the left-hand side of the bus as well as the magnetometer boom. On the other side of the bus, the Cosmic Dust Analyzer (CDA) from Cassini was placed as well as a low gain antenna (LGA) facing towards the propulsion housing. In order to provide an inertial reference, there are two star-trackers attached on top of the bus. One star tracker faces towards the left side and another faces upwards on the opposite side. Another LGA can be found on the front of the bus towards the left side of the front face. This antenna is not centered to prevent the attitude control thrusters from interfering with its line of sight.

There are a total of 8 ACS thrusters on the outside of the bus. Four thrusters are facing upwards to provide pitch to the spacecraft. One set is directly facing upwards and was placed towards the back of the ARIEL Telescope on the top face of the honeycomb panel. The other two are attached to the bottom honeycomb panel of the bus. They were not placed opposite to the other set to prevent blocking the field of view of the telescope. Two thrusters, one on each side of the bus, face towards the front on the spacecraft to provide roll and the last two are attached to a mount in the front of the bus to provide yaw control. As shown in **Figure 3-1** there are two small propellant tanks provide the attitude control system with propellant. Inside of the bus there is a two sets of reaction wheel assemblies (RWA's). Within their radiation shielding, are four reaction wheels. Three are mounted perpendicular to each other and a fourth one is mounted off-axis thus allowing redundancy if one of the other three were to fail. A radiation vault was attached to the back panel of the bus.

The radiation vault protects all major electronics and computers pertaining to command and data handling, ACS, and telecommunications from the thermal and radiation environments of space. The telecommunications subsystem requires for all components of the subsystem to be close together, therefore the 3.5m high gain antenna is attached to the back panel of the Bus on the other side of the radiation vault.

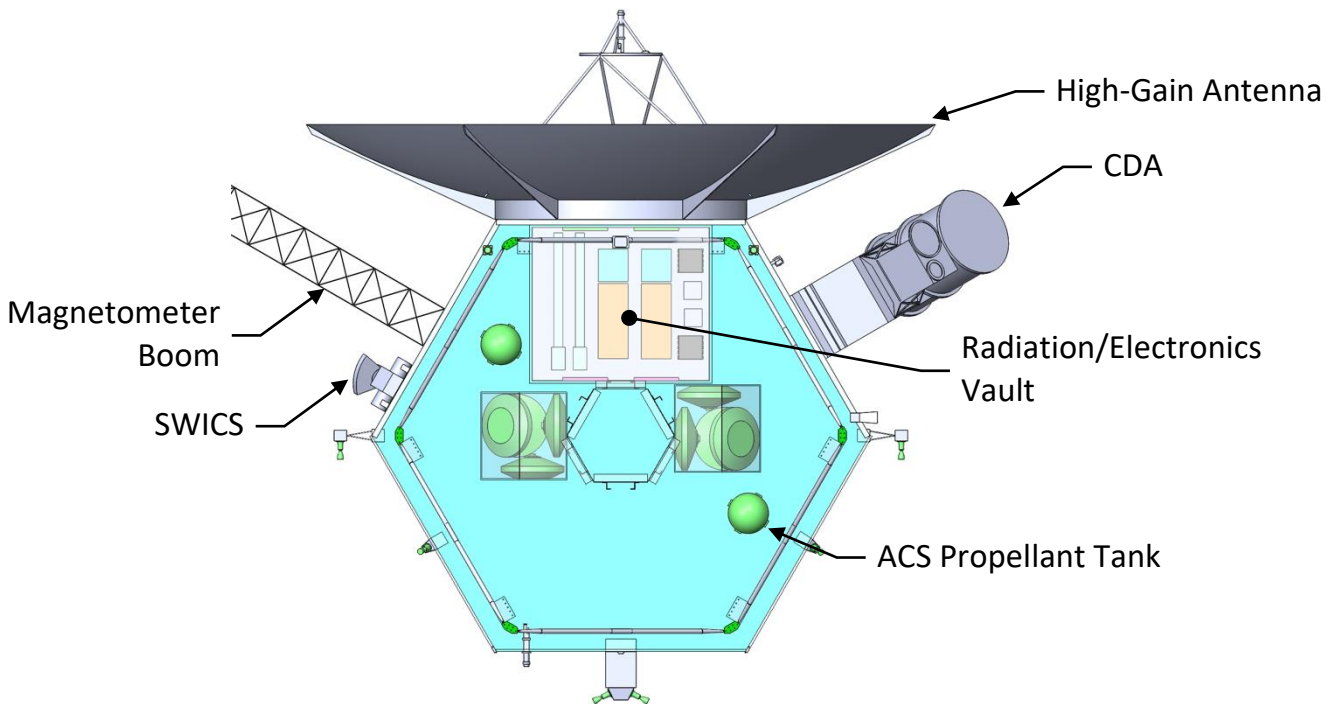


Figure 3-1 Zoom in View of Bus

Following the bus is the KiloPower nuclear reactor which provides power to the different subsystems of the spacecraft. The reactor is shown in its mission configuration in **Figure 3-4**. In this configuration, as previously stated, the reactor radiators are extended out. There are three radiator assemblies attached to the core of the reactor in a T-like configuration. This configuration was chosen to allow for enough space on the back of the bus for the HGA to be attached to. Each radiator assembly consists of three 2.22m x 1m panels for a total area of 20m². The first two panels are held rigidly in place and the third panel is capable of folding in. This configuration allows the spacecraft to fit inside the dynamic envelope of the SLS B1B payload fairing and reduces the amount of moving mechanisms. The arc path that the third panel traces as it folds is shown in **Figure 3-2**. This shows that the radiators will not come in contact with the intermediate structure while reducing the transverse moments of inertia. In order to help dissipate heat uniformly, heat pipes were modeled running through each of the radiator assemblies. Each heat pipe starts at the root panel attached to the radiator core and ends at the last panel in the sequence, forming a vertical slalom path. An intermediate structure made up of tie-rods had to be designed for RETRIEVER. The tie-rods are attached to clevises on the bottom honeycomb panel of the Bus and to the top honeycomb panel of the propulsion housing. Due to the bus being smaller than the

propulsion housing, the tie-rods are positioned at an angle however proper structural considerations were taken and will be discussed later.

The propulsion housing is attached to the bottom of the KiloPower Reactor. On the top honeycomb panel of the housing, two sets of ACS thrusters were placed. One set faces forward to provide roll to the spacecraft and another set is attached to a mount platform in the front of the panel to provide yaw. Each of the six faces of the housing is covered by an aluminum sheet 0.032" thick. Additional

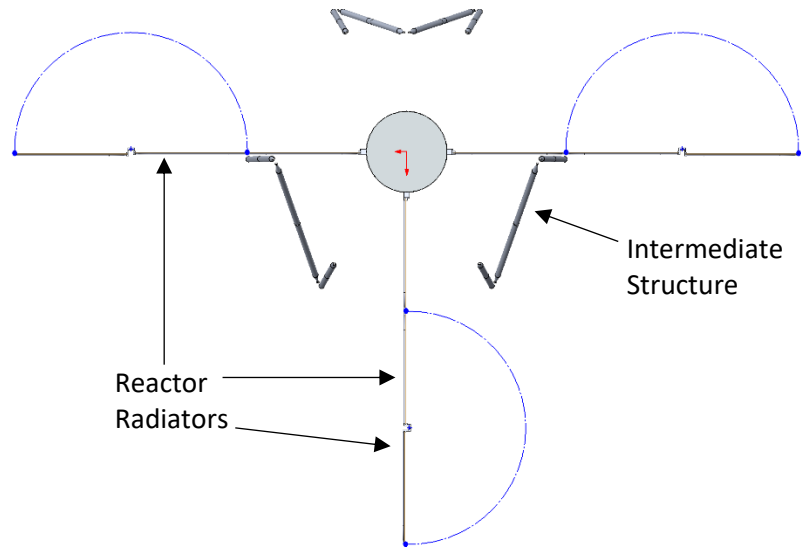
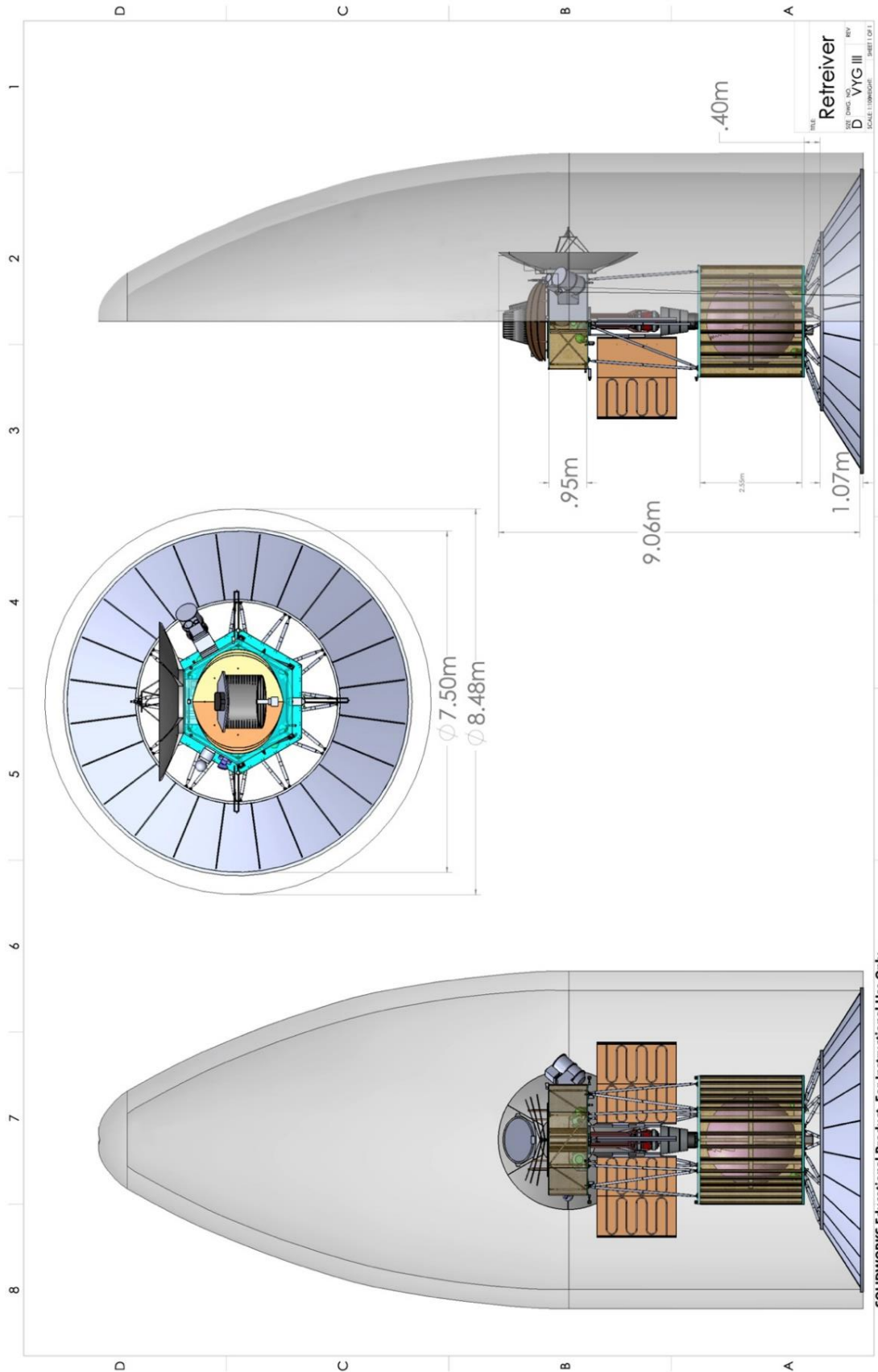


Figure 3-2 Rotating Arc of Reactor Radiators

structural support was provided with thirty stiffeners connecting the top honeycomb panel of the housing to the bottom one along the aluminum sheets. Inside of the housing, the propulsion tank was centered with 12 tubes attached to a ring-like structure holding the tank in place. On the bottom of the tank, two additional ACS propellant tanks were placed alongside two PPU's each connected to a Busek BHT 8000 Hall Effect Thruster. The thrusters are mounted at a 1.5 degree offset from the horizontal mount on the bottom honeycomb panel of the housing. As the xenon inside of the propulsion tank decreases, the center of mass of the vehicle moves upward. The offset takes into consideration the average change in distance of the center of mass to ensure the thrust passes through this average center point. Another two sets of thrusters are attached to the bottom of the propulsion housing to provide pitch control to the spacecraft for a total of 16 ACS thrusters on RETRIEVER.



SOLIDWORKS Educational Product. For Instructional Use Only.

Figure 3-3 RETRIEVER Stowed Configuration Layout

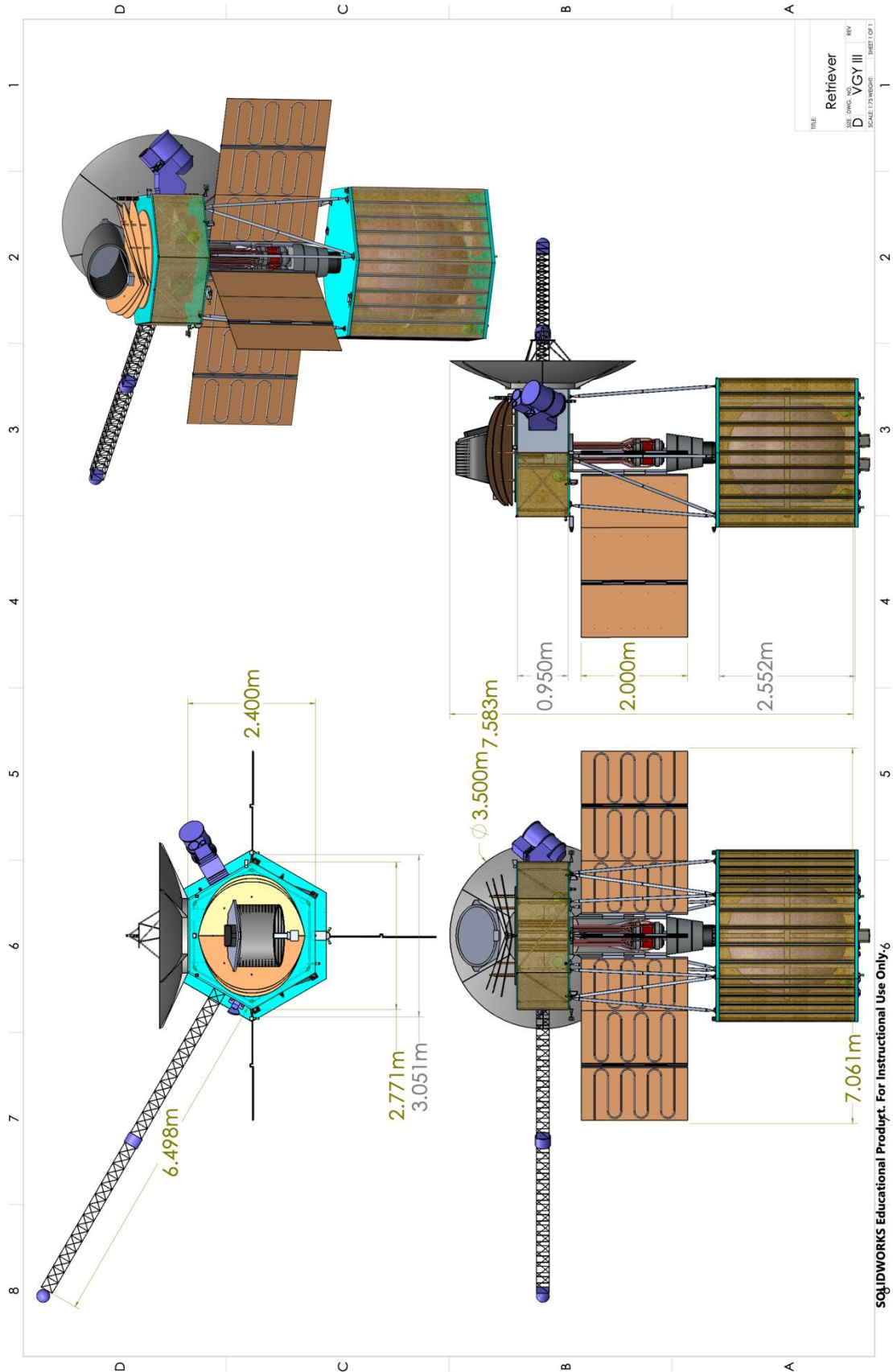


Figure 3-4 RETRIEVER Mission Configuration Layout

4 Trajectory

The primary goal of the trajectory design is to be able to target and fly past a specific point in space directly opposite of the TRAPPIST-1 star system. This point would have a fixed radial distance from the Sun of 550 astronomical units (AU). It would be oriented in space with a specific right ascension of 166.62 degrees and a declination angle of 5.04 degrees with respect to the Mean Ecliptic J2000 reference frame. The trajectory accuracy must be within 1 km by 1 km, as requested by the RFP issuer.

Another key objective of the trajectory design is to maximize the solar system heliocentric velocity in order to reach the solar focal line in a reasonable time. Current concepts to achieve escape velocities in excess of 12 AU/year include: large solar sails flown close to the Sun to leverage solar radiation pressure, and the option to use a large ΔV maneuver, on the order of 5-8 km/s, very close to the Sun (~ 0.04 AU) [15] in order to utilize the Oberth effect [16]. While these concepts yield times of flight under 50 years [15], they rely on low TRL technology and mission design practices not yet conducted. The thermal considerations, required solar sail area, and maneuver design accuracy shortcomings are some of the setbacks. Therefore, a more conventional approach was utilized. Planetary gravity assists can help boost the spacecraft's velocity post flyby, but still a significant amount of ΔV is required. Therefore, a low-thrust, long-duration burn trajectory was considered for this mission design. By combining classical interplanetary trajectory design with flight proven Hall Effect engines, a reasonable time of flight was achieved.

4.1 Broad Search

A multi-gravity assist, broad trajectory search was conducted before the optimization process to find possible flybys that would maximize the solar system escape velocity. This data was provided by the Jet Propulsion Laboratory's broad search algorithm named Star. Lambert arc fits would be used to join multiple bodies. Each leg would have discontinuous endpoint velocities, but a ΔV is assumed to be applied by an optimized flyby. Trajectories are forward and backward solved to reduce the number of tree nodes, and individual legs are grouped by date characteristics and velocities to reduce the computation time [17].

Table 4-1 summarizes the input and outputs from the broad search.

Table 4-1 JPL Star Broad Search Criteria and Results

Input Criteria	
Search Years	2030-2060
Earth Departure Characteristic Energy (C3)	<120 km ² /s ²
Flyby Bodies	Jupiter, Saturn, Uranus, Neptune
Goal	Maximize Final Body Inbound V _∞
Output Summary	
Number of Resulting Trajectories	10,706
Gravity Assist (GA) Body Sequences Yielded	JGA (Jupiter Only), JSGA (Jupiter to Saturn) SGA (Saturn Only) JUGA (Jupiter to Uranus)

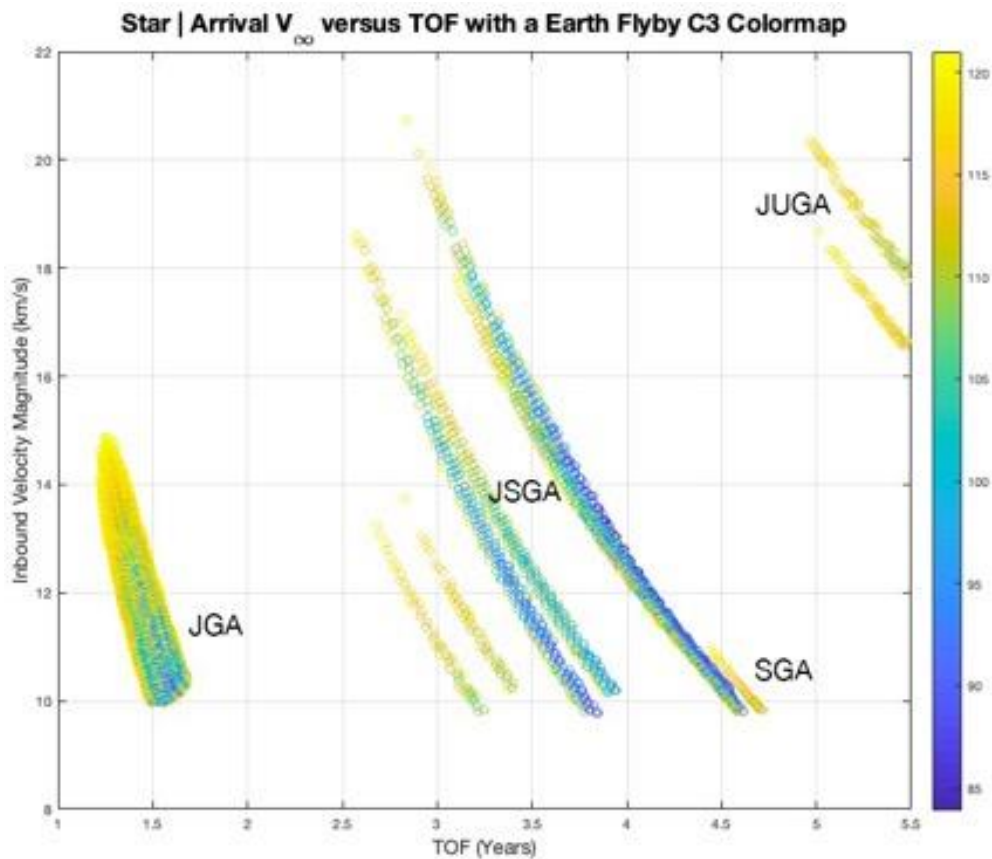


Figure 4-1 Star Results Sorted by TOF, V_∞, and Earth Flyby Energy

Figure 4-1 plots the resulting trajectory possibilities by their time of flight, inbound relative velocity, and the required Earth departure characteristic energy. The search yielded several sets of gravity assist combinations which were traded based on their inbound relative velocity (V_{∞}), right ascension of the final body at the encounter, maximum achievable turn angle (assuming a planar flyby and close approach altitude of no less than 5000 km), and the encounter year. The Saturn only gravity assist trajectories were

immediately dropped for their maximized Earth departure C3 and their low V_∞ values. In the search, three different candidates were analyzed for preliminary investigation: a JGA with the Jupiter encounter in January of 2048, a JSGA with the Saturn encounter in November of 2059, and a JUGA with the Uranus encounter in 2039. The JSGA and JUGA trajectories offer higher inbound V_∞ values of 20.73 and 20.35 km/s, respectively, compared to the 14.03 km/s from a single Jupiter flyby. This, coupled with the fact that the spacecraft can potentially collect more science data through additional planetary flybys, made these options more attractive in the beginning. However, there were certain limitations in these flyby body candidates. Both GA combinations had post flyby right ascension differences, with respect to the target, of greater than 11 degrees. This meant that the low thrust propulsion system would have to change the direction of travel and boost the heliocentric velocity of the spacecraft, resulting in a slower burnout velocity. Also, a more aggressive design and manufacturing timeline would be necessary for the JUGA trajectory as it encounters Uranus in 2039. This means that the Earth launch would have to be in the late 2020s in order to accommodate for ΔV leveraging flybys and the transfer to Jupiter. Subsequently, the JSGA opportunity encounters Saturn, which is only roughly 9.6 AU from the Sun, in 2059. With these considerations, and the fact that the launch period becomes much more sensitive to the multi-flyby mission design, a Jupiter only gravity assist trajectory selected for optimization.

It is important to note that despite only being roughly 5 AU from the Sun, Jupiter's offset from the required heliocentric outbound right ascension is significant enough to account for in the broad search trajectory selection. Of the nearly 8,800 Earth-Jupiter opportunities, two had post flyby heliocentric right ascensions that matched the target conditions. **Figure 4-2** displays these two opportunities and their differences in the required post flyby right ascensions after a 20-year propagation.

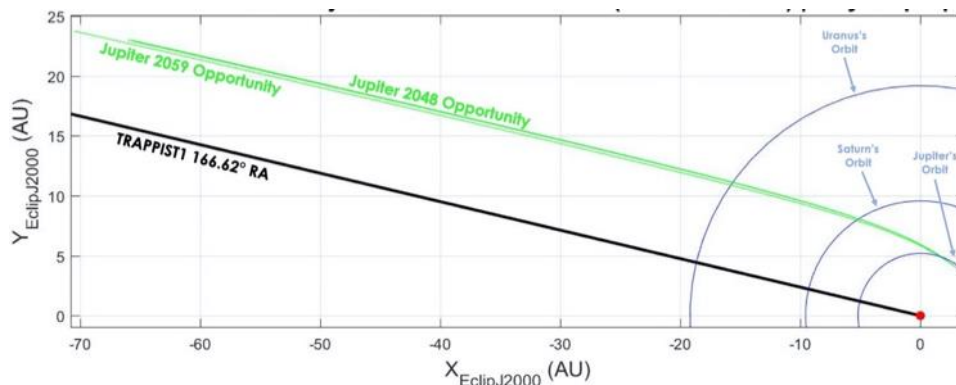


Figure 4-2 Selected JGA Opportunities from Broad Search

The calculated offset, in order to intercept the SGL point, from Jupiter was 0.4798 degrees (resulting in a searched right ascension of 167.099 degrees for all prograde trajectories). These two opportunities were within 0.015 degrees of this new target. The 2048 JGA opportunity was then selected for the low thrust optimization portion of the trajectory design due to its earlier encounter year.

4.2 Low Thrust Trajectory Design and Optimization

The trajectory optimization process began with an investigation into the current capabilities of electric propulsion engines. Hall Effect thrusters were considered due to their increasing efficiency, nearing 60%, and output thrust, in excess of 0.4 N [18]. All candidate trajectories were designed with the output thrust as the driving propulsion parameter, and it was preferred to exhaust the propellant as soon as possible after the Jupiter flyby as this would reduce the amount of time the power system would have to deliver the large input power.

The Jet Propulsion Laboratory's Mission Analysis Low Thrust Optimizer (MALTO), which is a preliminary mission design tool, was utilized for trajectory optimization. It models low thrust arcs as a series of impulsive maneuvers segments, and patches together the trajectory by forward and backward propagations from control points. Control points can be either planets or defined points in space given the orbital elements, valid times, and reference body.

The broad search found the Earth to Jupiter (EJ) portion of the trajectory at the maximum C3 (120 km^2/s^2). This direct transfer would be possible on deep space launch vehicles, but the mass delivered would be too small for the spacecraft design. The initial estimate for RETRIEVER was on the order of 2500 kg dry and in excess of 12,000 kg wet. Preliminary analysis into a STAR-37 kick stage was conducted to see if having a third stage could improve performance. However, after using the Tsiolkovsky ΔV equation, it was found that a kick stage could only deliver roughly 230 m/s, which is not enough for the leveraging orbit injection. Therefore a ΔV -EGA trajectory that utilizes a deep space maneuver (DSM) and an Earth flyby, similar to that of the Juno Mission [19], was utilized. The advantage of this approach is that it only relies on Earth gravity assist(s), and so targeting specific flyby parameters is simplified. However, one significant limitation is that the spacecraft will be carrying nuclear substances and conducting these flybys. Mission implications and subsequent analysis for the EGA are discussed further on. A 3:1⁻ Earth Leveraging orbit, discussed by Sims and Longuski in [20] was selected for this trajectory as it was a reasonable compromise between the amount of time spent interplanetary, and required launch energy. It is important to note that the analysis covered by Sims and Longuski are designed to rendezvous with

Jupiter. RETRIEVER’s trajectory is aiming to maximize the incoming relative velocity. This means that it would be more optimal to use the 3:1⁻ as a starting point and let the optimizer build heliocentric energy by running the electric propulsion engine during the EJ transfer to maximize the incoming heliocentric velocity. The only limitation in this was the derived requirement for mandatory forced coast periods before and after flybys for planetary protection and to prevent powered flyby maneuver errors. These considerations were applied in the MALTO trajectory, and the deep space maneuver would be replaced by a long duration low-thrust burn to prevent the need of carrying a kick-stage. The final portion of the trajectory was targeting the correct heliocentric right ascension and distance. A user-defined control point in space was created with the following Keplerian orbital elements in **Table 4-2**.

Table 4-2 TRAPPIST-1 Observation Target (Mean Ecliptic J2000 from the Sun)

Orbital Element	Value
a (AU)	550
<i>e</i>	0.00
<i>i</i> (°)	5.04
Ω (°)	76.66
ω (°)	90.00
ϑ (°)	0.00

Ultimately, the vehicle mass was capped at 14,000 kg wet. After an extensive trajectory optimization period and tweaking date and mass limits, the trajectory converged. With the tolerances, the largest trajectory discontinuity between matchpoints in the position was 0.05 km and the largest velocity discontinuity was on the order of 10⁻⁹ km/s. **Table 4-3** provides a summary of all various trajectory parameters.

Table 4-3 Trajectory Encounter Summary

Event	Epoch (MM/DD/YYYY)	TOF (years)	V_{∞} (km/s)	Mass at Enc. (kg)	Flyby Alt. (km)	B•R (km)	B•T (km)
Launch	08/16/2044	0.00	6.70	14,000.00	-	-	-
EGA	06/20/2047	2.83	14.43	12,520.95	1250	-255.9	-9343.6
JGA	09/06/2048	4.04	17.32	11,774.22	43199	33,810.7	329,878.0
Prop. Burnout	12/27/2061	17.37	52.57	3200.00	-	-	-
SGL	04/28/2102	58.01	52.57	3200.00	-	-	-

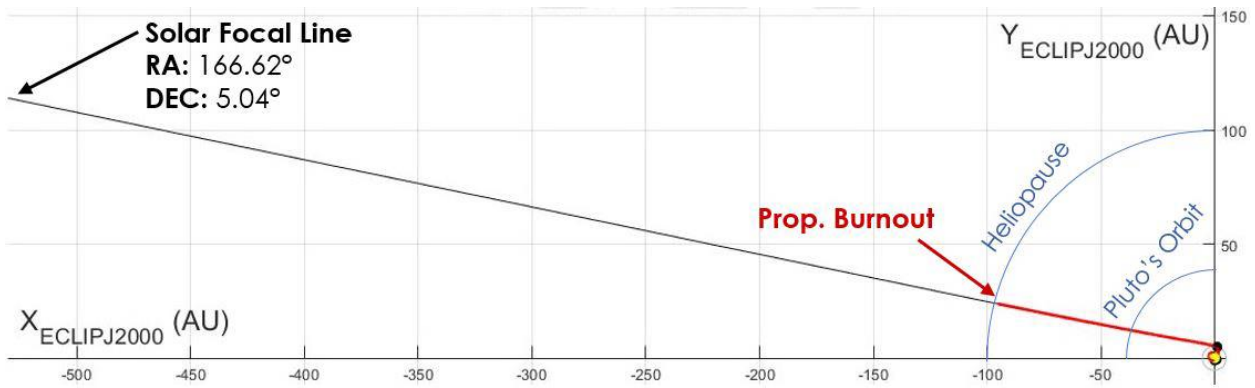


Figure 4-3 Entire Trajectory (Mean Ecliptic J2000 XY View)

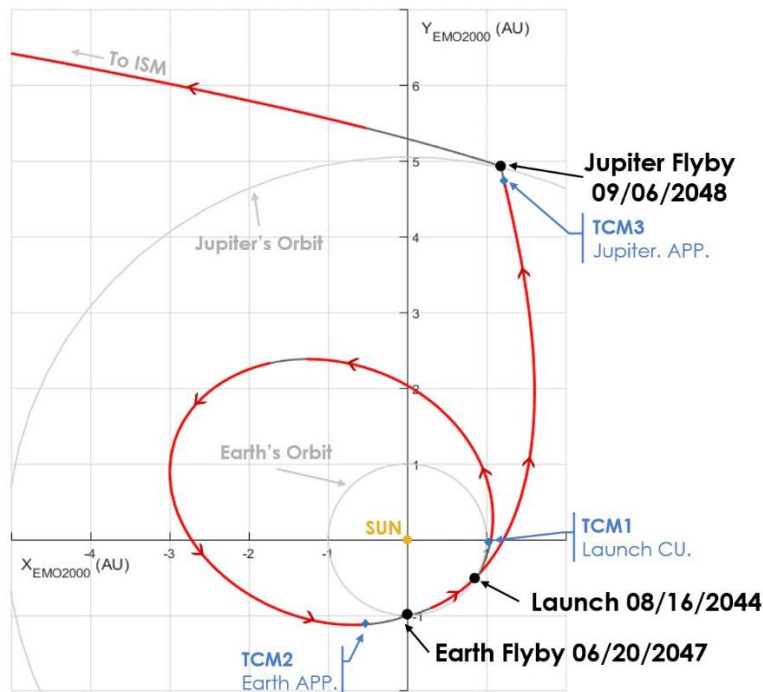


Figure 4-4 Interplanetary Trajectory (Mean Ecliptic J2000 XY View)

Figure 4-3 displays the entire trajectory. Notice that the propulsion burnout occurs near the Heliopause at roughly 97 AU. **Figure 4-4** contains the interplanetary portion. Arrows are added to follow the direction of the spacecraft. The first low thrust burn occurs shortly after launch and the first clean up trajectory correction maneuver (TCM). The Earth leveraging orbit requires thrusting as a chemical deep space maneuver is not executed. There is a break in thrusting momentarily, and this can be used for additional science experimentation. Also, the thruster restart post JGA is delayed for an additional science opportunity. There are regions of the interplanetary trajectory where the spacecraft is restricted from thrusting. As mentioned earlier, these are forced coast periods added to ensure the flybys would not be powered to reduce state errors post flyby and for planetary protection. Additional TCMs are added before

the EGA and JGA which were assumed to be <2 m/s as per [19]. There are four main engine burns that are summarized in **Table 4-4**.

Table 4-4 Low Thrust Burn Schedule and ΔV

Low Thrust Burn #	Start Epoch	Stop Epoch	ΔV (m/s)
LTB 1	09/15/2044	06/26/2045	803
LTB 2	08/19/2045	05/25/2047	1,936
LTB 3	07/05/2047	08/22/2048	1,346
LTB 4	12/17/2048	12/27/2061	28,291

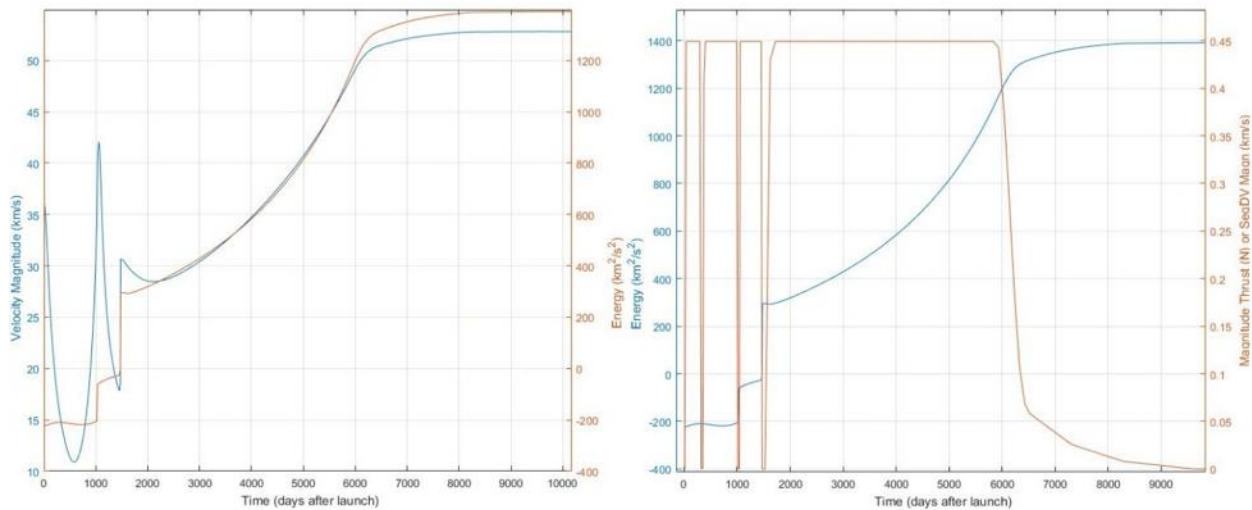


Figure 4-5 Heliocentric Velocity, Energy, and Thrust Magnitude versus Time

Figure 4-5 shows the heliocentric velocity and energy as well as the thrust required versus time. The blue spike around 1000 days on the left-hand plot is the Earth gravity assist, and the second is the Jupiter flyby. It is important to note just how dependent the trajectory is on propulsion system that can run for long durations and provide relatively high thrust (seen on the right-side plot). The expected heliocentric energy will be roughly 1400 km²/s² which equates to 11.08 AU/year.

RETRIEVER's dry mass was varied in optimizations between 3000 kg to 3200 kg as the mass of the spacecraft grew. The maximum available thrust was set to 0.45N, which is 0.15 N less than the maximum output of the Busek BTH-8000 at 8kW input power for contingency, discussed in propulsion. The trajectory can also withstand a missed thrust day for every one hundred days of operation by MALTO's missed thrust definition. **Table 4-5** contains trajectory parameters as the dry mass was varied.

Table 4-5 SFL Arrival Sensitivity to Dry Mass (Assuming fixed wet mass of 14,000 kg)

Dry Mass (kg)	SFL Encounter Epoch	TOF (years)	V_{∞} (km/s)	V_{∞} (AU/year)
3000	01/14/2102	57.44	53.05	11.18
3100	04/28/2102	57.72	52.75	11.12
3200	11/3/2102	58.01	52.22	11.01

The trajectory discontinuities, as discussed above, were deemed acceptable as MALTO is a preliminary mission design tool. While it is powerful in its capability, MALTO has underlying assumptions built into its astrodynamics computation making it useful for rapid prototyping of trajectories. The trajectory would need to be further developed in higher fidelity applications such as JPL’s MYSTIC. For this reason, the trajectory cannot be guaranteed at this point of the analysis to meet the RFP issuer’s 1 km by 1 km trajectory accuracy at the solar focal line. Orbit determination uncertainties are likely to be greater than this limit and so, for the scope of this investigation, the accuracy was forgone.

4.3 Trajectory Coverage and Analysis

With a converged MALTO solution the next goal for the trajectory design was to analyze the flybys in detail and check for occultations, eclipses, and solar conjunctions. Analytical Graphics Incorporated’s (AGI) Systems Tool Kit (STK) was used, and with the Astrogator extension, interplanetary trajectory modelling and SPK (Satellite and Planetary Kernel) file reading was accessible. Three scenarios were setup. The first was reading the generated position and velocity data from the MALTO produced SPK file to find the solar conjunctions that could occur along the entire trajectory. The second and third scenarios were of the Earth and Jupiter flybys. These scenarios began out of the planet’s SOI and used Astrogator’s Mission Control Sequence (MCS) to target the flyby B-Plane and epoch parameters (listed in section 6.2). **Table 4-6** lists all the out of line of sight (LOS) coverage times and durations.

Table 4-6 Trajectory Out of LOS Summary

Event	Start Time (UTCG)	End Time (UTCG)	Duration (HH:MM:SS)
Solar Conjunction	19 JUL 2045 14:33:33	20 JUL 2045 12:16:59	21:43:26
Earth Eclipse	None	None	N/A
Jupiter Eclipse	24 SEP 2048 00:54:09	24 SEP 2048 02:05:17	01:11:08
Jupiter Conjunction	24 SEP 2048 01:08:11	24 SEP 2048 02:30:11	01:28:00

The trajectory design included supplemental preliminary analysis for the EGA as the spacecraft is going to carry nuclear substances through the flyby. The Cassini mission, which contained 78 kg of plutonium, underwent extensive scrutiny by the public and Congress for carrying these through its Earth flyby, and so mission designers had to conduct extensive analysis to prove minimal impact probability [21]. It was considered to replace RETREIVER's EGA with other flyby combinations, but the <60 years TOF derived requirement did not allow for this. The flyby was restricted to an altitude that limited the spatial density of orbiting objects around Earth. **Figure 4-6**, originally from [22], plots different NASA robotic missions that conducted an Earth flyby and has RETRIEVER's expected flyby altitude. By selecting 1250 km, the risk of hitting existing orbital debris is limited.

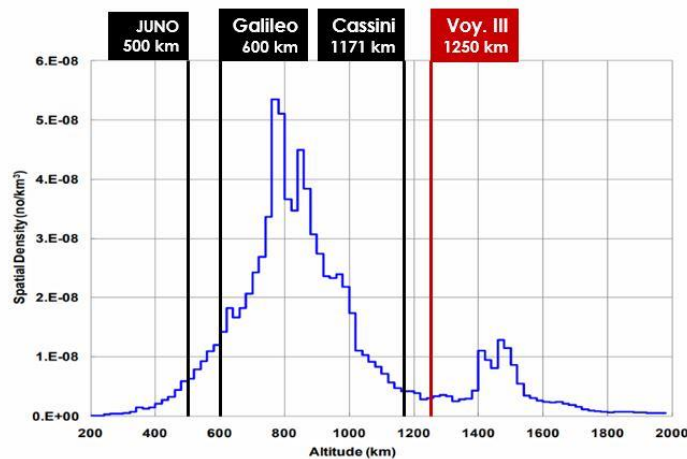


Figure 4-6 Earth Orbital Spatial Density versus Altitude

The next method of supplemental analysis was introducing position and velocity errors from the deterministic trajectory before the flyby and propagating them out to perigee. This was done by first querying the state and epoch of the spacecraft roughly where it crossed Earth's SOI (assumed to be 925,000 km). 3000 error samples were created with the assumption that 99.7%, or 3σ , of state errors were within a sphere 100 km in radius from the deterministic position, and 3.5 m/s from the velocity. To put these numbers into context, the original Voyager missions had a delivery accuracy of 100 km after 47.65 AU of travel [1]. The state errors are significantly exaggerated to determine the absolute worst case scenario as no existing data was found publicly regarding this topic at the time of analysis. **Figure 4-7** plots the dispersion of the perigees. It is important to note that the mission would be most likely be compromised if the spacecraft were to fly at any of these extremes, despite having a low thrust propulsions system to correct the errors.

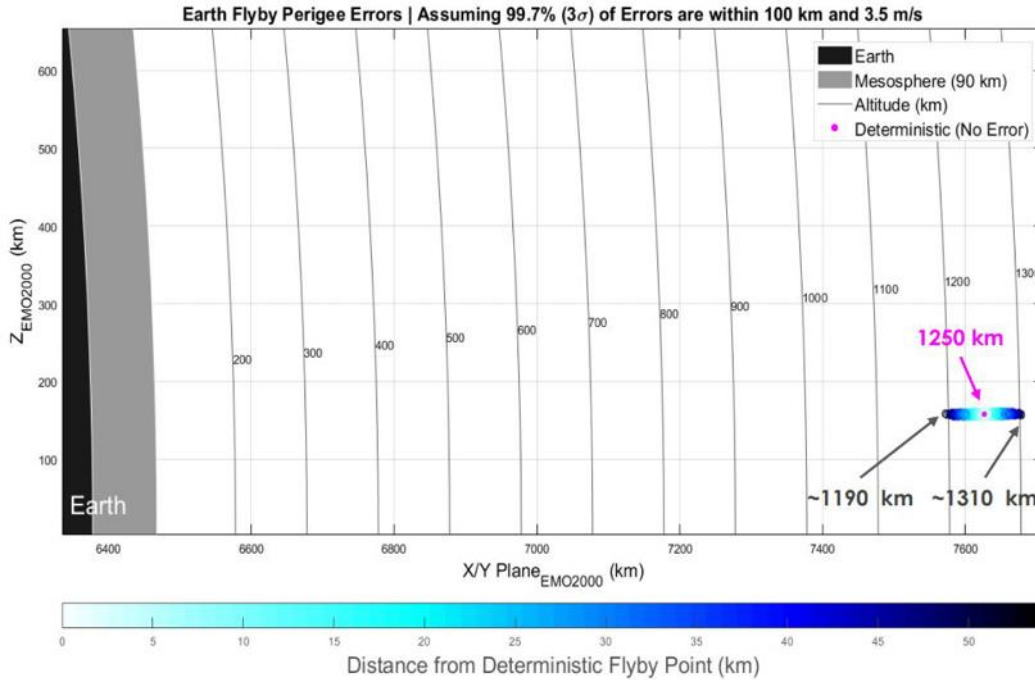


Figure 4-7 Earth Gravity Assist Perigee Error Dispersion

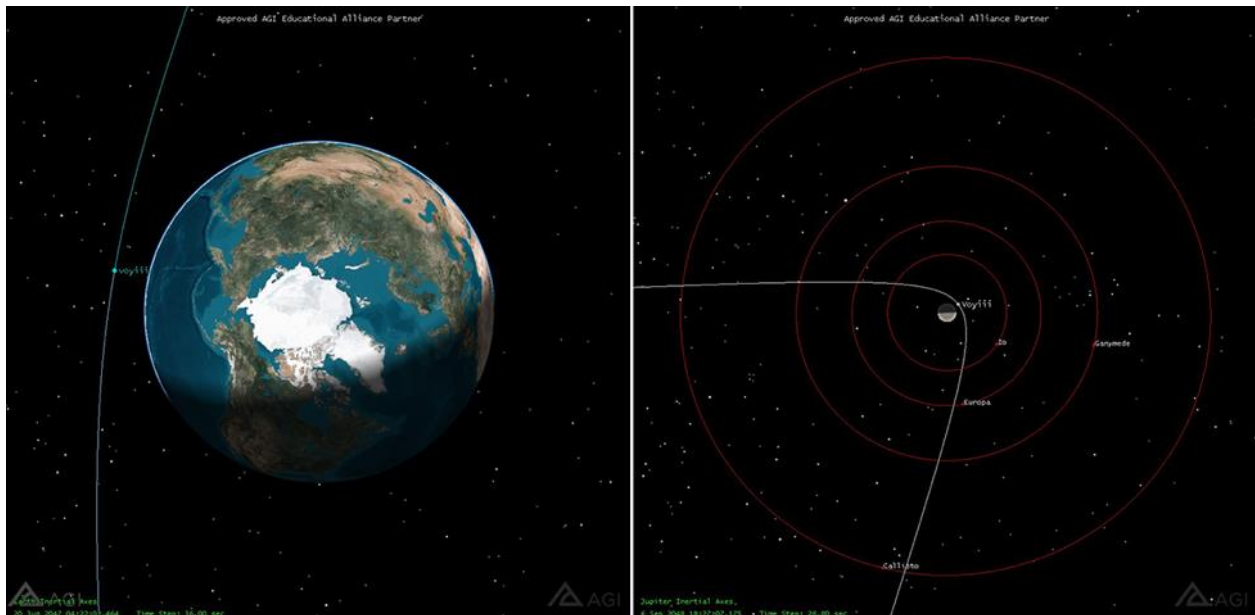


Figure 4-8 Earth Flyby (Left) Jupiter Flyby (Right)

Besides studying the interstellar medium and conducting interplanetary science, an additional opportunity for science was discovered in the trajectory analysis. The Jupiter flyby allows for the chance to study the Galilean moons. **Table 4-7** covers the close approaches of each of the four moons.

Table 4-7 Galilean Moon Flybys

Moon	Close Approach Epoch (06 SEP 2048 UTCG)	Distance (km)	Sunlit Opportunity
Callisto	00:27:00	753,360	Partial
Ganymede	15:57:00	878,734	Partial
Europa	12:44:35	244,446	Full
Io	14:43:00	78,436	Full

There is sufficient time between each close approach for reorienting the spacecraft for imaging and Io and Europa are prime candidates for a full disk image.

4.4 Launch Opportunity and Vehicle Selection

The trajectory design and weight of the spacecraft significantly limited the available launch vehicles. Because of the time of flight derived requirement, the trajectory requires a high launch C3 of $44.89 \text{ km}^2/\text{s}^2$ (V_∞ of 6.70 km/s). It is assumed that the launch vehicle will deliver this entirely in order to save the spacecraft’s propellant, and to not have to use a kick stage. Existing Evolved Expendable Launch Vehicles (EELV) like ULA’s Delta IV Heavy and Atlas V 551 were considered for their reliability and nuclear carrying capability. SpaceX’s Falcon Heavy in the recoverable and fully expendable configurations were also investigated due to their cost. Still, these vehicles are not nuclear rated and have only launched twice at the time of analysis. Finally, the NASA/Boeing Space Launch System (SLS) Block 1B and 2 were traded as these are heavy lift, assumed nuclear-capable, vehicles designed for deep space missions with high launch energy requirements. **Table 4-8** reviews the properties of the launch vehicles that were considered. Note that options such as Blue Origin’s New Glen, SpaceX’s Starship, and ULA’s Vulcan were not considered due to a lack of available data. Starship and New Glen could be prime contenders for this mission as they are intended to compete with the SLS for deep-space heavy-lift missions.

Table 4-8 Considered Launch Vehicles

Properties	NASA/Boeing SLS B2 [14]	NASA/Boeing SLS B1B [14]	SpaceX Falcon Heavy (RTLS) [23]	SpaceX Falcon Heavy(Expend.) [23]	ULA Delta IV Heavy [24]	ULA Atlas V-551 [25]
Image						
Mass deliv. at C3 req. (kg)	24200	17600	1350	5800	4200	2350
Nuclear Cap.	✓	✓	✗	✗	✓	✓
Launch Reliability	In Development	In Development	3/3	3/3	9/10	83/83
Launch Site	KSC	KSC	KSC VBG	KSC VBG	KSC VBG	KSC VBG
Cost/Launch FY2020	unknown	\$2.5B	\$90M	\$150M	\$450M	\$110M
Launches/Year	1	1	2	2	2	4

The SLS is expected to launch NASA’s flagships in the coming future, such as Europa Clipper and a few of the Artemis program’s missions. Despite the launch cost and development status, the SLS Block 1B was chosen as it is the only physical vehicle able to meet the mass and energy requirements. RETRIEVER can be comfortably accommodated in the B8.4m-27000 fairing due to its large 7.5-meter diameter dynamic envelope and over 18-meter tall fairing [14]. Also, the spacecraft and launch vehicle adapter is estimated to be <14,500 kg, allowing for a 3,100 kg mass margin. Once again, the private sector’s heavy lift deep space vehicles can likely be contenders for this mission, but due to their performance uncertainty at the time of analysis, they were not considered. The SLS Block 1B will launch RETRIEVER.

By parametrically varying the launch date in MALTO, a study was conducted in order to determine the launch opportunity and its effects on time of flight and required C3. **Figure 4-9** illustrates the available launch opportunity for RETRIEVER. The time of flight derived requirement is also plotted to show the maximum bounds for the solution.

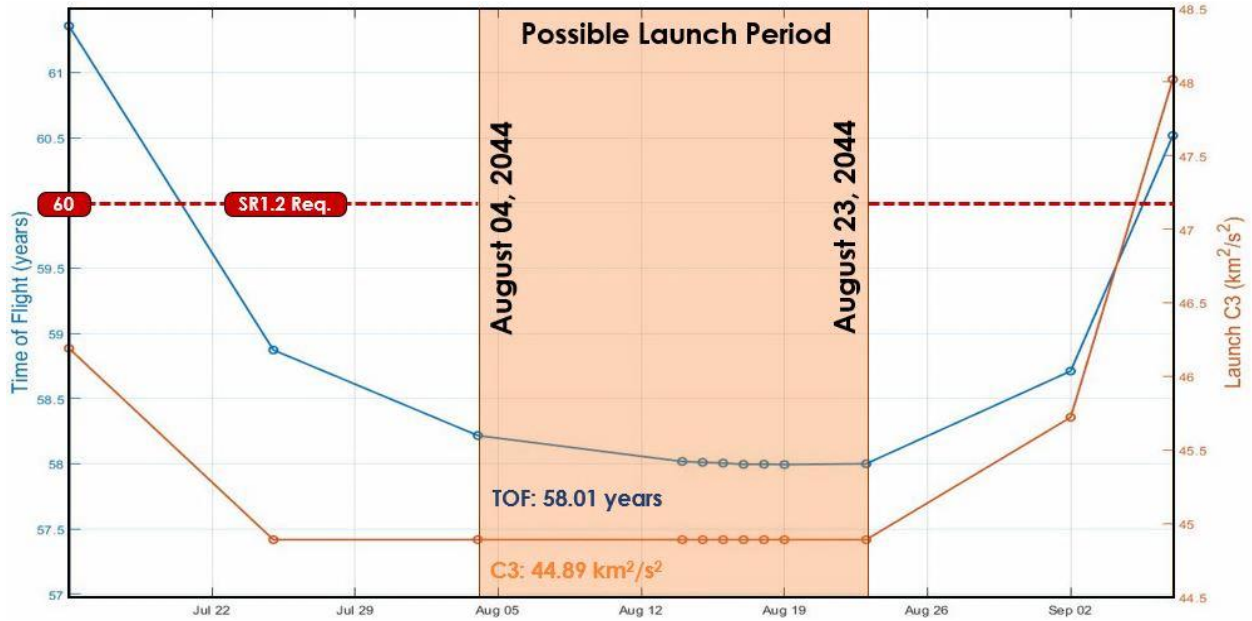


Figure 4-9 2044 Launch Opportunity

Based on the parametric results study, a launch opportunity between August 04 and August 23, 2044 was selected. It is expected that the launch date will be sensitive because of Jupiter’s heliocentric right ascension. The trajectory relies on Jupiter’s position in order to reduce the amount of propellant spent correcting the solar system escape leg’s right ascension.

5 Propulsion Sub-System

The propulsion subsystem relies heavily on the trajectory and the mass of the spacecraft. When designing the trajectory of the mission, the type of propulsion system is kept in mind to ensure that the mission is feasible. Initially, all forms of propulsion were considered, but due to the mass and power properties of RETRIEVER, it was possible to start ruling out some types of propulsion.

5.1 Selecting a Propulsion System

Chemical and electric propulsion were both considered for the propulsion system for the spacecraft. Due to the large mass of the payload, solar sails were not considered.

5.1.1 Chemical Propulsion

The first type of propulsion that was considered was chemical propulsion. Chemical propulsion consists of the burning of a fuel and an oxidizer to produce thrust. Chemical propulsion is the oldest form of propulsion dating back to the thirteenth century in the form of fireworks. Since then, chemical boosters have become very efficient and well understood. In general, there are three different types of chemical propulsion: solid, liquid, and a hybrid between the two.

The main characteristic of a solid rocket booster is that the propellant is made into a casted solid grain. This means that the system is much less complex to liquid propellants due to a lack of need for pumping the fuel. Also, a solid propellant is much easier to store than liquid propellant. Once a solid rocket booster has ignited, it cannot be shut off. Therefore, they cannot be used to make fine trajectory correction maneuvers and attitude adjustments. Solid rocket boosters are primarily used in conjunction with another source of propulsion or for primary burns, which then another form of propulsion is used to make any corrections.

Liquid fueled engines are much more complex than their solid counterparts. The most common forms of liquid engines use either monopropellant or bipropellant. Monopropellant thrusters are much more reliable and less complex than bipropellant thrusters, however they lack the ability to generate large amounts of impulse. Therefore, monopropellants are most commonly used in attitude control systems. Bipropellant thrusters are much more complex due to the need for two different liquids to operate. The two propellants are a fuel and an oxidizer. When the two liquids are mixed, it becomes extremely combustible, so they are stored in separate tanks and are not allowed to interact until they meet in the combustion chamber. In general, bipropellant engines perform better than both solid and

monopropellant thrusters. There are two main types of liquids that can be used for these engines. The first are cryogenic liquids. The most common cryogenic oxidizer used is liquid oxygen (or LOX) and a common cryogenic fuel is liquid hydrogen (or LH2). Because these fuels are cryogenic, they need to be kept at very low temperatures (<100 K) and they are very susceptible to outgassing. Therefore, cryogenic propellants are used most commonly in two situations: on launch vehicles where it is easier to maintain their temperatures and when the storage durations are short enough where boil off can be mitigated. The second type of liquid is hypergolic liquid. These liquids can be kept at warmer temperatures and are less susceptible to outgassing. On the downside, they do not perform quite as well as cryogenic fuels, but on long deep-space missions such as Voyager III, it is the only option.

5.1.2 Electric Propulsion

The second type of propulsion that was analyzed for this mission was electric propulsion. There are many different forms of electric thrusters such as Ion Thrusters and Hall Effect Thrusters. This form of propulsion is newer than chemical propulsion, but its popularity has been growing in the recent years. Electric thrusters can only generate a fraction of a Newton of thrust, but they can achieve ten times the specific impulse than the chemical thrusters can. This means that electric thrusters need less fuel to complete the same maneuver as chemical thrusters. The only downside is that that same maneuver would take many years longer to complete. The benefit to this is that electric thrusters can be on for multiple years, which would generate a large amount of thrust over time. The main drawback to electric propulsion thrusters is the large amount power required to operate them. Currently, their main use is in small course corrections on satellites, such as orbit maintenance on GEO satellites, but they have been used on interplanetary missions. In 1998, Deep Space 1 carried the first interplanetary electric engine. The longest an electric engine has been powered continuously is six years which could provide a huge benefit to the spacecraft.

5.1.3 Propulsion System Requirements and Constraints

The propulsion system onboard the RETRIEVER will need to be able to meet the requirements of our trajectory. This calls for a large ΔV maneuver after the Jupiter flyby. The system will also need to make course corrections to counteract any propulsive errors. However, the spacecraft must be able to be light enough to launch on the SLS, so it cannot use too much propellant.

5.1.4 Propulsion System Down Selection

Due to the high precision required for our spacecraft to reach an optimal position to perform solar gravitational lensing on TRAPPIST-1, solid rocket boosters cannot solely get the job done to get RETRIEVER to 550 AU. There is still a possibility of them being able to assist the primary propulsion system, but the propulsion system needs the ability to throttle its thrusters for precise maneuvers. Monopropellant liquid engines also cannot take our spacecraft to the interstellar medium because they do not perform as efficiently as bipropellant liquid engines. If a liquid engine is considered, it would have to be a bipropellant engine. Cryogenic propellants aren't a viable option because the amount of power required to cool the propellants would be unachievable. Hypergolic propellants can be used; however, they do not perform as well as cryogenic fuels, but they are storable. The only problem is the amount of propellant that would need to be brought onboard would be significantly more than any launch vehicle can handle. Therefore, liquid propulsion cannot meet the demands of the trajectory. Electric propulsion can achieve our trajectory. This is mainly due to the ability to a lack of constraint of the burn time. A small amount of thrust over multiple years can build up the ΔV needed to allow RETRIEVER to reach 550 AU within 60 years. Therefore, electric propulsion will be the type of propulsion that will be used by the RETRIEVER.

5.2 Selecting a Thruster

There are many electric thrusters that are currently in use as well as in development. Only thrusters that were TRL 4 and above were considered. With the launch date set in 2044, a thruster with a TRL of 4 should be sufficient. Three thrusters were ultimately selected to down select from. One that is flight proven, and two that are still in development, but offer much higher performance.

5.2.1 Electric Thruster Options

The first engine that was considered was the NSTAR ion thruster. This thruster is the safe option for the mission. It will not perform the best, but it requires a low amount of power and is the only one that has been flown on an interplanetary mission. It was first flown in 1998 on the Deep Space 1 mission where it accumulated 6,630 hours of operation [26].

The NEXT Ion Thruster was the second thruster considered for the propulsion system. While this thruster has not flown on a mission, it has been tested for almost 6 years of continuous operation [27]. This thruster requires triple the power input as the NSTAR engine.

The last engine that was considered was the Busek BHT-8000. The big difference between this thruster and the other two is that it is a Hall Effect thruster. It also requires the most input power, but in turn, produces the most amount of thrust.

5.2.2 Electric Thruster Down Selection

The highest importance in selecting a thruster was its ability to burn all of the propellant without taking up too much time. Unfortunately, high thrust electric thrusters require large amounts of power to operate. Using electric thruster data, it was possible to plot the relationship between the specific impulse, thrust, and input power. This plot can be found in **Figure 5-1**. After the creation of this contour plot, it was discovered that the specific impulse and thrust had an inverse relationship with the input power. To help select a thruster, a design space was created and placed on the graph. This design space contained the range of necessary properties that the thruster would need to have while still making it have a low enough power to be usable on the spacecraft. This design space ensured that all thrusters would have at least 400 mN of thrust and require no more than 9 kW of power. Those three engines were then plotted on the chart. The only engine that was found inside the design space was the Busek BHT-8000.

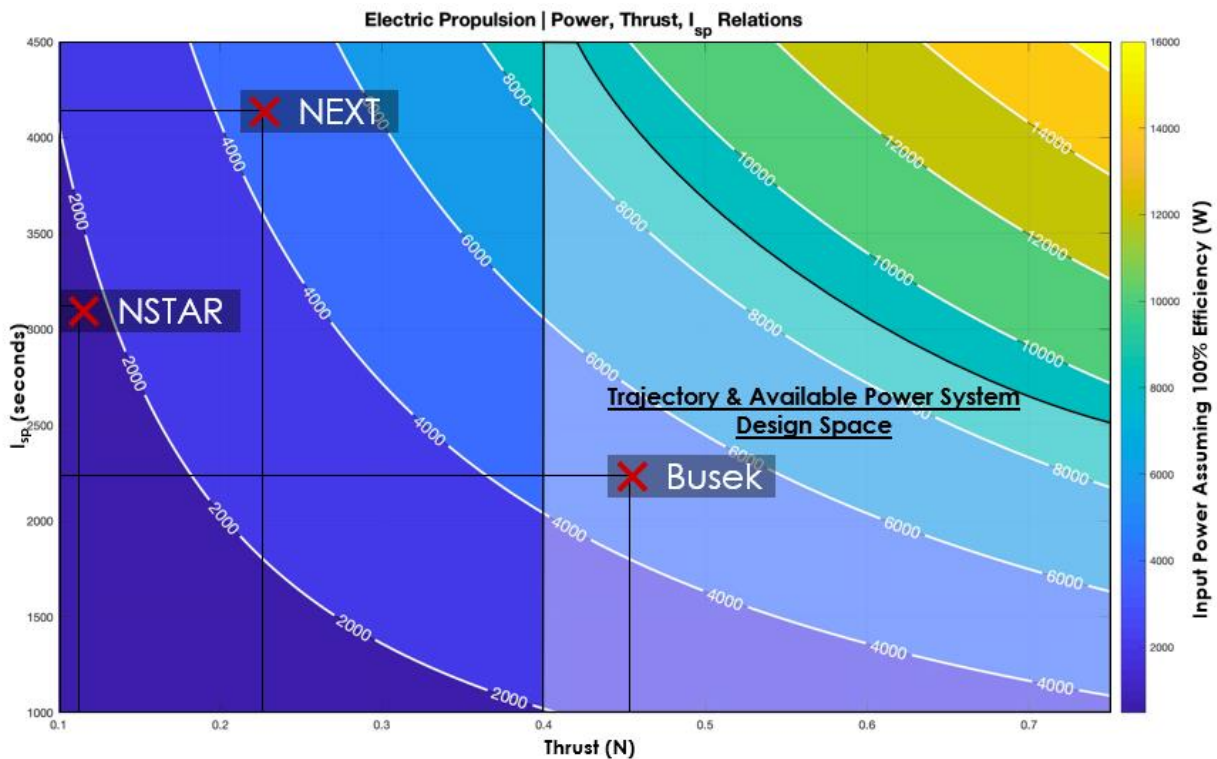


Figure 5-1 Contour Plot Demonstrating the Relationships Between I_{sp} , Thrust, and Power

More analysis was performed to ensure that the BHT-8000 would be able to meet trajectory requirements. One of the most important aspects of the desired thruster was the total amount of time that it would take each thruster to burn all the propellant onboard the spacecraft. The NSTAR would take 115 years to burn our 10,800 kg of propellant. Since requirement SR1.2 calls for the spacecraft to arrive at 550 AU within 60 years, this confirms that the NSTAR cannot be used for this mission. The NEXT can burn through all the needed propellant within 61 years. This is still above the 60-year arrival time, but if multiple thrusters were used simultaneously, this burn time could decrease to a reasonable time frame. The only problem with this situation is that more thrusters would call for more power and the NEXT is already on the upper limits of what the spacecraft can handle. The last thruster looked at was the Busek BHT-8000. This thruster could burn through all the propellant within 17 years. This thruster has a TRL of 5, so it should be operational by 2044 [28]. The input power is on the larger side with 8 kW, but there are power systems available to achieve it. Therefore, the thruster that will be used by the spacecraft is the Busek BHT-8000.

5.3 Propulsion System in Detail

For the selected thruster to meet the needs of the trajectory, it required 10,800 kg of xenon to reach the required ΔV . With this much propellant, the subsystem will have to be designed in a way to effectively handle it.

5.3.1 Required components

The BHT-8000 will require some components for its operation. The first is it will need a power processing unit. The PPU will need to be able to process 8 kW of power. These PPUs are currently available [29] and since the launch is in 2044, a selection of a specific PPU is unnecessary. Other components that are required are solenoid valves, proportional flow control valves, pressure transducers, thermocouples, and regulators. The exact count of these components can be found in the mass breakdown of the propulsion system in Section 5.3.3.

5.3.2 Piping and Instrumentation Diagram

The piping and instrumentation of the propulsion subsystem was designed to resemble Busek's patented design that is currently used on a satellite in orbit [30]. This diagram can be found in **Figure 5-2**. To maximize the lifespan of the thruster, a second thruster has been added for redundancy. Both thrusters will be used throughout the burn, but at different times. Instead, each thruster will be cycled between. The primary thruster will burn for a set time before cycling to the secondary thruster which will be on for

the same amount of time and so forth. This will help expand the life of the propulsion system to 17 years. All the xenon will be in one tank which will be then be piped to either thruster. Solenoid and proportional flow control valves will be used to limit the amount of xenon that will go into the thruster. Each thruster will have its own power processing unit. The KiloPower reactor will provide power to either PPU which will then be directed to their respective thrusters.

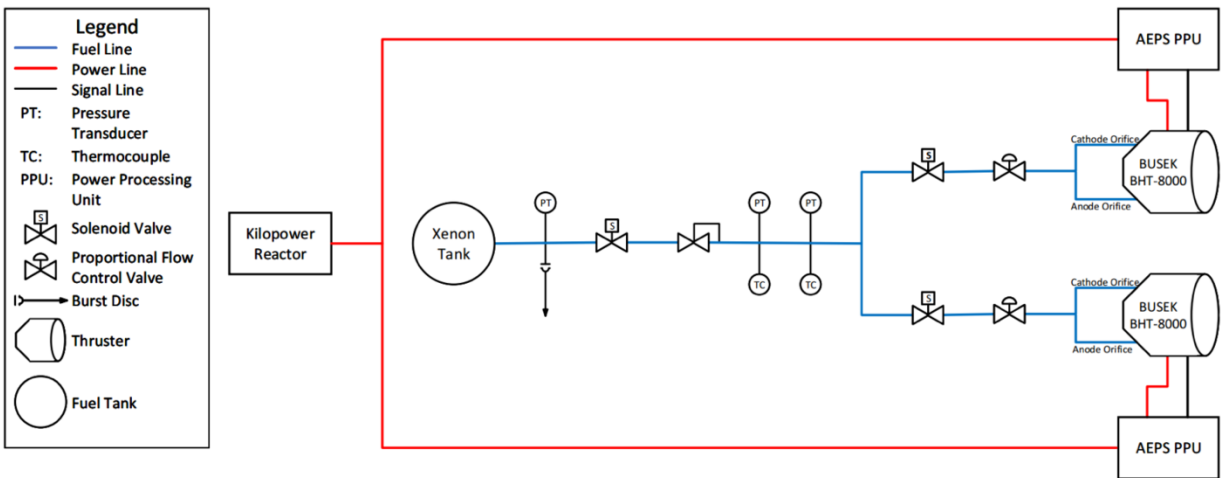


Figure 5-2 Piping and Instrumentation Diagram

5.3.3 Subsystem Mass Breakdown

The last aspect of this subsystem is the mass breakdown. The breakdown listed by components can be found in **Table 5-1**. The dry mass of the subsystem is 290 kg. The xenon tank makes up most of the subsystem mass, but that is to be expected with the quantity of xenon that is being launched onboard the spacecraft.

Table 5-1 Propulsion Subsystem Mass Breakdown

Component	Count	Mass (kg)	Total Mass (kg)
Engine	2	25	50
Xenon Tank	1	171	171
PPU	2	30	60
Fuel Lines	n/a	0.3	0.3
Piping Components	n/a	18.8	18.8
Subsystem Dry Mass			290
Xenon Propellant			10,800
Subsystem Wet Mass			11,090

6 Power Sub-System

One key aspect that defines the lifetime for any interplanetary robotic mission is the power required to accomplish the science and mission objectives. The power subsystem of a spacecraft is typically designed for the End of Life (EOL) scenario with the appropriate margins are applied to the power subsystem design. The three main types of power sources considered when designing this subsystem for a spacecraft are: chemical, solar, and nuclear. These power sources are shown in **Figure 6-1** in which a contour plot compares electric power level vs duration of use.

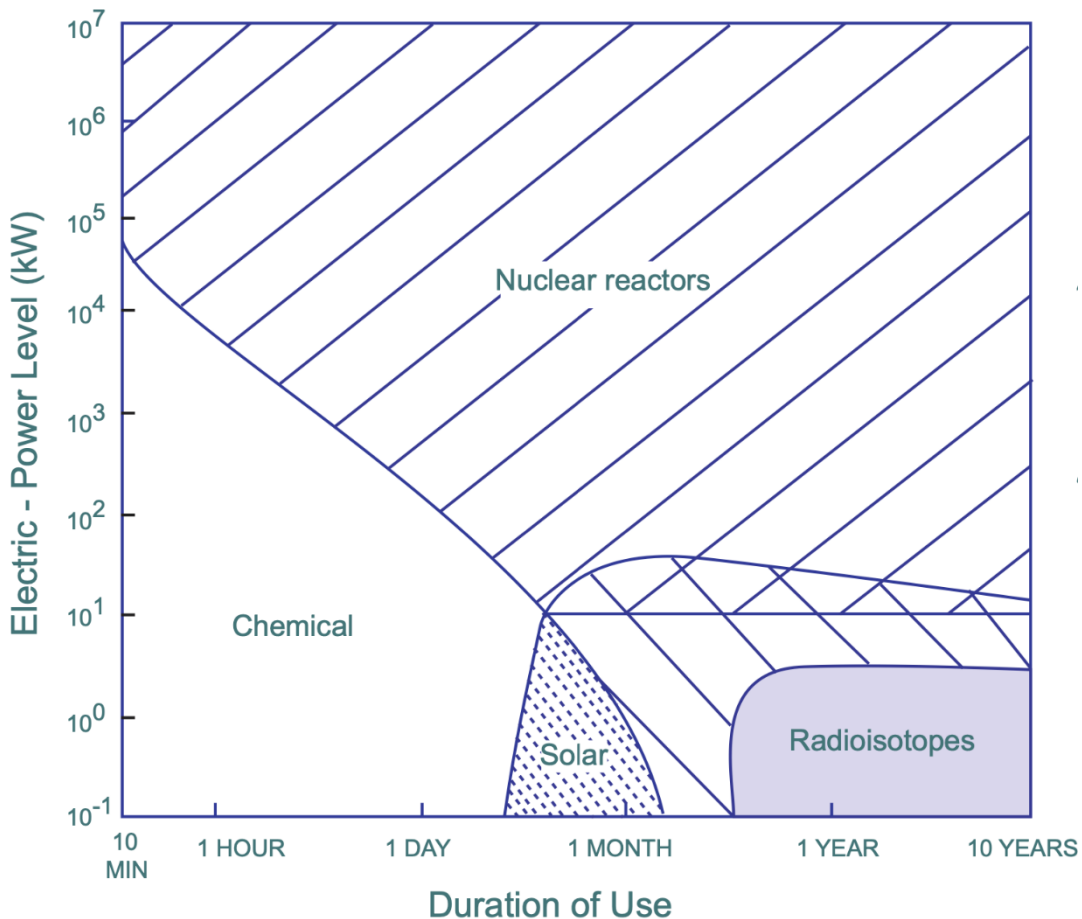


Figure 6-1 Power Sources Lifetime vs Output Power Level [31]

Chemical sources such as lithium ion batteries have been used previously in spacecrafts, satellites, and rovers. These power sources are typically used in conjunction with solar arrays, power distribution units and Radioisotope Thermoelectric Generators (RTG). There are two types of batteries: primary and secondary. Primary batteries are single use, as they cannot be recharged. Secondary batteries can be recharged. One cycle of the secondary batteries can be categorized as follows: during the illuminated

period, the solar arrays or any other primary source of power charge the batteries of the spacecraft and provide power to feed the rest of the subsystems. During this period, the number of tasks increases in order to maximize efficiency and data acquisition. During the eclipse time, the charged batteries are then used to maintain the spacecraft’s minimum required systems. The power distribution unit (PDU) is used throughout both of these times in order to properly manage the power output from the power sources and assign it to the different components as necessary.

Batteries were not considered as a primary source of power during the design of RETRIEVER. Due to their high discharge rate no amount of batteries would be able to meet the mission power requirements. The flight time of the mission is approximately 60 years and no battery source could provide the amount of power necessary for that long. A table of common batteries used in spacecraft missions can be seen in **Table 6-1**.

Table 6-1 Primary Battery Characteristics [31]

	Silver Zinc	Nickel Cadmium	Nickel Hydrogen
Energy Density (Wh/kg)	90	35	75
Energy Density (Wh/dm ³)	245	90	60
Oper Temp (deg C)	0-20	0-20	0-40
Storage Temp (deg C)	0-30	0-30	0-30
Dry Storage Life	5 yr	5 yr	5 yr
Wet Storage Life	30-90 days	2 yr	2 yr
Max Cycle Life	200	20,000	20,000
Open Circuit (V/cell)	1.9	1.35	1.55
Discharge (V/cell)	1.8-1.5	1.25	1.25
Charge (V/cell)	2.0	1.45	1.50
Manufacturers	Eagle-Pitcher, Yardney Technical Prod	Eagle-Pitcher, Gates Aerospace Batteries	Eagle-Pitcher, Yardney, Gates, Hughes

Unlike deep space mission orbiters such as Dawn, Juno and Cassini, RETRIEVER will have to undergo both, a long flight time and a rapid increase in its heliocentric velocity to escape the solar systems gravitational forces. Having arrived at interstellar space and passed the heliopause, the spacecraft will finally conduct its science at the 550 AU mark. Primarily due to the distance of the mission, solar arrays were considered unfeasible. In order for solar arrays to provide enough electrical power to run the science instrumentation and power the ion engines, they would need to have a total area of about 7.85km² and a mass of 31,425mT. The calculation can be seen in **Table 6-2** and **Table 6-3** assuming a required power output of 1100 W_e. Additionally, the mass of the attachments required for the solar arrays was not included in the mass of the arrays.

Table 6-2 Battery and Solar Array Physical Values

# of Strings	
$V_{peak} (V)$	2.05
% _{head}	115%
$V_{array} (V)$	31.625
# Cells/String	16
# of Strings	160,593,293
Solar Array Mass	
$\rho_{panel} (kg/m^2)$	4
$m_{panel} (kg)$	31,414,840.95
$m_{attach} (kg)$	4,712,226.14

Table 6-3 Solar Array Efficiencies

Solar Array Area	Power (W)
η_{p-f}	92%
η_{rad}	70%
η_{temp}	56.5%
η_{UV}	98%
η_{cy}	99%
η_m	97.5%
η_L	98%
η_{con}	99%
η_{total}	0.33
$P_{eff-cell} (W)$	0.00
# Cells	2,569,492,680.9
Cells/m ²	327.17
$A_{total} (m^2)$	7,853,710.24

All the power systems mentioned previously, meet and surpass the amount of power needed by the scientific instrumentation shown in **Table 6-4**. Only two, however, the KiloPower Nuclear Reactor and Radioisotope Thermo-electric Generators could be considered given their output power-weight ratio and long-lasting durability.

Table 6-4 Payload Power Required

Instrument	Power (W)
Mag-3	0.03 [9]
Solar Wind Ion Composition Spectrometer (SWICS)	6 [10]
Cosmic Dust Analyzer	16 [11]
Ariel Telescope & Coronagraph	180 [12]
Total	202

A hybrid power system was considered to form a combination of both a nuclear reactor and a determined amount of RTG's. The nuclear reactor would be used mainly to provide power to the ion engines enabling them to thrust at a higher benchmark and for a long period of time. Once the spacecraft reaches the 550 AU mark the propulsion assembly alongside the nuclear reactor would disengage from the bus. From this point forward, RTG's would supply direct power to the remaining subsystems of the bus as well as the science instruments. The problem with this hybrid power design is the fact that one cannot control the output power of the RTG's. Once connected, they will constantly provide power to the spacecraft. If both of these systems would be on at the same time, complications such as power surges due to a power overload could potentially damage the electronics and flight computers.

As the power source was narrowed down to two choices, a trade study was conducted between these two systems to decide which would be best suited for RETRIEVER. This trade study can be best summarized in **Table 6-5**. It was calculated that the amount of RTG's required in order to meet mission power requirements was about 20 units compared to one unit from the nuclear reactor. It was noted however, that nuclear reactors are not typically used to power spacecraft. The only nuclear reactor ever flown by the United States was SNAP-10A in 1965 [32]. Los Angeles National Laboratory, however, has been leading the design and testing of a new reactor technology called the KiloPower Reactor Using Sterling Technology (KRUSTY). This system is to undergo ground and flight testing in the upcoming years [33].

Although having a high TRL level and cost the system chosen for RETRIEVER was the KiloPower reactor. This system meets the power levels necessary for the spacecraft to throttle and perform its science objectives throughout the mission. The main reason why the reactor is successful is due to its fuel specific power, thermal control, and geometry.

Table 6-5 Power Sources Trade Study

Category	Units	KiloPower Reactor [34]	Next-Gen RTG [35]
Launch Power	W	10,000	378-472
Mass/Unit	Kg	1445	62
Dimensions (diameter x length)	m	1.5x3	0.4x1.4
Cost	\$FY2020	43M	77M
Heat Dissipation	n/a	Radiators 20m ²	Fins Mounted on RTG
Fissile Substance	Kg	²³⁵ U	²³⁸ Pu
TRL	n/a	5	3
Exp. Availability	Year	2030 (Artemis)	2028
No. Units Required	n/a	1	20

The core of the reactor is made up of 93% enriched ²³⁵U alloyed with 7% Mo by weight. This solid cast of uranium molybdenum alloy is stated to provide optimum thermal power while as well reducing the amount of fuel needed, radiator geometry and size, giving the system a higher specific power (W/kg) than other forms of fuel [33]. The reactor uses Advanced Sterling Radioisotope Generators (ASRTG) for generate electricity. The thermal dissipation system for the nuclear reactor is based on sodium heat pipes. The heat generated through the fission reaction is conducted through the core and into the heat pipe evaporator which vaporizes the liquid sodium. Sodium vapor then travels up the heat pipe into the sterling convertors. At this stage the vapor is condensed back to liquid and its temperature decreases. This cycle then repeats. RETRIEVER will be using a similar system but will differ from the traditional pedal radiator arrangement. Instead the radiators for the KiloPower reactor of RETRIEVER will extend not from the top in a circular pattern but from the sides linearly spaced in the form of panels. In order to meet the same radiator area criteria as the pedal shaped radiators, retriever has three radiator assemblies. These assemblies are configured in a T-shaped manner with two rigid panels and the last one being able to fold in order to fit within the SLS fairing. The power system requirements were met.

7 Space Environment

Throughout the RETRIEVER’s journey to the ISM, the spacecraft will encounter many different hazardous environments, from the high temperatures around Earth, to the dense radiation belts at Jupiter, even to the unknown environment in interstellar space.

7.1 Thermal Environments

The thermal environments throughout the mission can be broken up into five major categories, Earth (Sun-facing & eclipse), Jupiter (Sun-facing and eclipse), and finally interstellar space. Before evaluating the steady state temperatures, the spacecraft will achieve in each environment, it must be noted the different parameters taken into account. First is the heat generated by the spacecrafts own onboard power system. Due to the RETRIEVERs high power output, the actual heat conducted to the rest of the spacecraft is reduced by the spacecrafts inclusion of radiator panels. Next is heating due to solar flux hitting the spacecraft. This value is calculated based of a 1 AU reference heating and drop off based off the Inverse Square Law. The final concern is heating due to orbiting body albedo. Below in **Table 7-1** of each contribution to the spacecrafts heating at each phase of the mission.

Table 7-1 Heating Considerations per Mission Phase

Planet	Internal Power Gen.	Solar Heating	Orbit Body Heating
Earth – Sun Facing	✓	✓	✓
Earth – Eclipse	✓	✗	✓
Jupiter – Sun Facing	✓	✓	✓
Jupiter – Eclipse	✓	✗	✓
Interstellar Medium	✓	✓	✗

7.1.1 Steady-State Heating Analysis

In order to put the steady-state, equilibrium, temperature into context, first the operational and non-operational limits of all of RETRIEVER’s heat sensitive components must be documented. In **Figure 7-1**, it can be seen, apart from ARIEL which will be discussed later in detail in **Section 7.1.2**, that all of the spacecrafts components will be safe at 300 K.

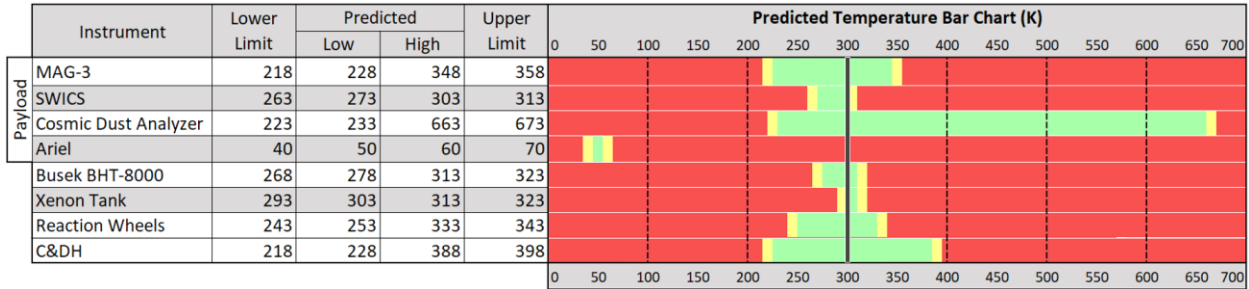


Figure 7-1 Temperature Envelope for Mission Instruments

Now that a desired spacecraft temperature has been established, it must be compared against all of the steady state temperatures at each phase of the mission. In **Table 7-2** below, shows the equilibrium temperatures for each planet at their hot and cold cases, with the ISM just being a cold case. Also highlighted, is the worst case for both cold and hot conditions, these will be the design points for later in the paper when thermal management is discussed in more detail. As well listed below is the equations used to calculate each case, do note that the spacecraft is assumed to be a uniform sphere [36].

Table 7-2 Steady State Heating Conditions (Cold and Hot)

Location	G_s (W/m ²)	$q_{\text{planet,IR}}$ (W/m ²)	T_{min} (K)	T_{max} (K)
Earth	1367.6	237	220	289
Jupiter	49.6	8.37	188	226
ISM (550AU)	0.00452	N/A	124	

$$T_{\text{max}} = \left[\frac{G_s \left(\frac{\alpha_s}{4} + a\alpha_s K_a F_{s-e} \right) + q_{\text{IR}} \epsilon_{\text{IR}} F_{s-e} + \frac{P}{\pi D^2}}{\sigma \epsilon_{\text{IR}}} \right]^{\frac{1}{4}} \quad \text{(Equation 7-1)}$$

$$T_{\text{min}} = \left[\frac{q_{\text{IR}} \epsilon_{\text{IR}} F_{s-e} + \frac{P}{\pi D^2}}{\sigma \epsilon_{\text{IR}}} \right]^{\frac{1}{4}} \quad \text{(Equation 7-2)}$$

7.1.1.1 Mitigation Strategies for Worst Cases

For each of these cases, since they are underneath the required temperature of 300 K, RETRIEVER will require a heating element to keep all components at their operating temperature. To accomplish this, the spacecraft will utilize the 10-kW reactor on board, which has existing heat piping running to its radiator paneling. Using this passive heat source, RETRIEVER will be able to keep all of its systems function and operating, while incurring no active thermal control measures.

7.1.2 ARIEL Thermal Management

Due to ARIEL analyzing spectrum including infrared radiation, in order to reduce signal noise, the image sensor involved must be kept at as low of a temperature as possible. In **Figure 7-1** above, ARIEL's computers must be kept at a temperature of 50 K [12], which will require special considerations as compared to the rest of the spacecraft. In the effort to decouple ARIEL's temperature from the rest of the spacecraft, multiple methods were introduced to isolate all thermal conduction and radiation. The fixtures that hold up the ARIEL enclosure will be thermally isolated, as well as a set of fins at increasing angles will be set below the instrument, as seen in **Figure 7-2** below. These panels have a highly reflective coating that allows thermally radiation to be reflected away from the telescope, further increasing thermal isolation. Finally, the telescope itself is painted in a black paint in maximize its thermal emissivity.

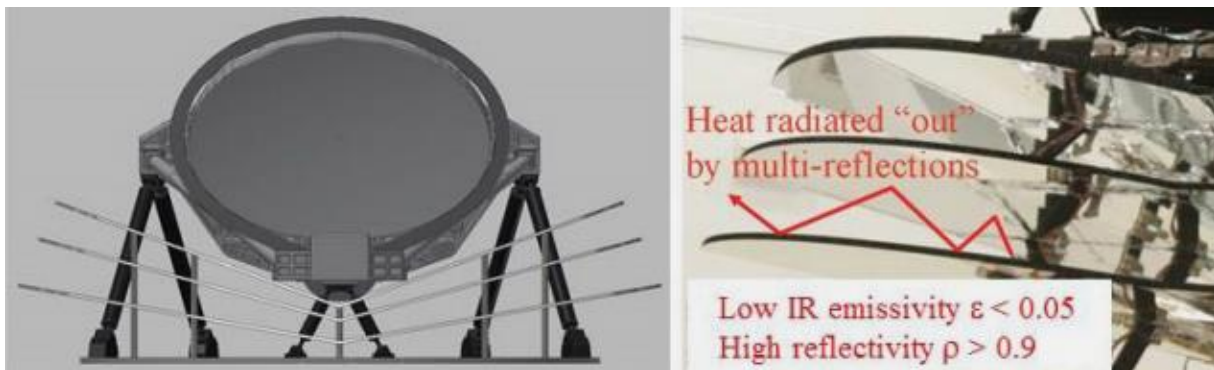


Figure 7-2 Layout and effects of ARIEL's radiation dissipation fins

To demonstrate the capabilities of this system, below, in **Figure 7-3**, it can be seen that the temperature gradient from the spacecraft bus to the instrument properly keeps the spacecraft cool in its environment. The thermal analysis, performed by ESA, shows two cases, on top is the cold case and on bottom is the hot case [12]. In both cases the telescope is kept at or below a temperature of 50 K. Another finding of note is that even after a 50 K increase in the temperature of the spacecraft bus, the temperature of the telescope increased by 1 K. With this analysis, along with the rest of the spacecraft, ARIEL will be able to survive the thermal environment at both the worst-case cold and hot conditions of the RETRIEVER spacecraft throughout its journey.

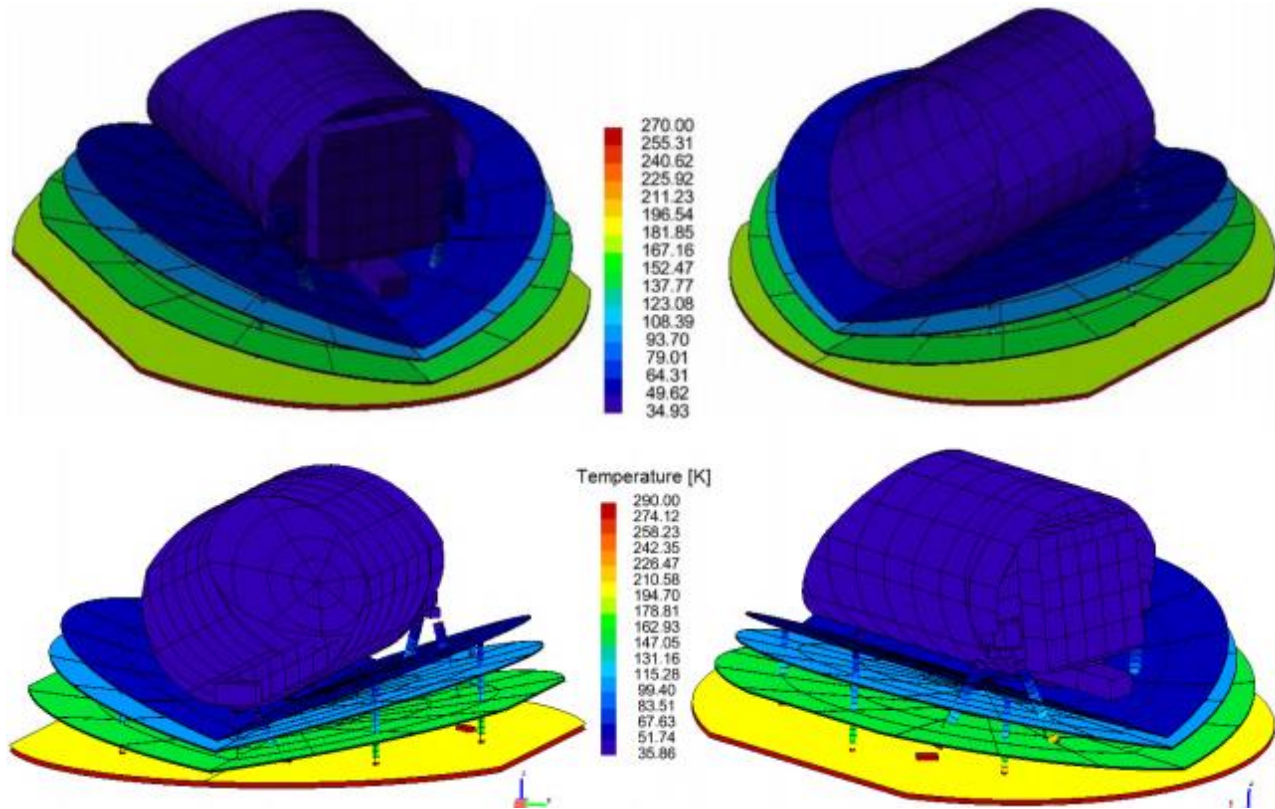


Figure 7-3 Finite Analysis of ARIELs Thermal Isolation Techniques [12]

7.1.3 Additional Thermal Equipment

Along with the equipment used to manage ARIEL, RETRIEVER employs multiple other systems where the reactor heating is either insufficient or infeasible. For the magnetometer instrument, due to its distance away from the main spacecraft bus, running heat pipes is non-ideal. To supplement this problem, the spacecraft will employ general purpose heating units (GPHUs) to keep warm this equipment without the need of a piping run. Additionally, for the case where the inside of the bus enclosure or propulsion housing gets too hot, RETRIEVER will also have a set of passive louvers which will activate when the components exceed a heat of 300 K. Finally, for the reactor itself, in order to cool the generated 10 kW of power, 20 m² of radiator panels will be required [37]. These panels are oriented in a T-shaped pattern to allow for the space of the high-gain antenna.

By utilizing all of this equipment and analysis, the RETRIEVER spacecraft will be able to thermally survive its journey out to 550 AU.

7.2 Radiation Environments

Similarly, the thermal environment, RETRIEVER will be subjected to multiple different radiation environment that could compromise the electronic equipment and render the spacecraft inoperable.

7.2.1 Environments Considered

Of the three environments considered, Earth, Jupiter, and the ISM, only two pose a threat to the spacecraft. The first and largest threat is Jupiter, due to having the largest magnetic field outside of the Sun, this also traps a large quantity of ionizing radiation within its equatorial belts. As well since RETRIEVER will be performing an equatorial flyby, the spacecraft will be exposed for a large period of time to the harshest part of the radiation belt. The only other historical precedent is the JUNO spacecraft which is performing a series of polar orbits through the belts. The second environment of consideration is the Interstellar Medium. The reason for inclusion is due to the fact that not much is known about the radiation environment outside of our solar system.

7.2.2 Worst-Case Analysis

The path of the spacecraft during its flyby of Jupiter is be propagated over time, from trajectory data, generating an orbital altitude over time. By utilizing height maps of Jupiter’s radiation belts which yield radiation over a set period of time, the spacecraft total accumulated dosage can be found [38]. In **Figure 7-4** on the right, are the different levels of radiation exposure depending on the areal density of the shield material. Before consider mitigation methods, it was evaluated that the spacecraft would be exposed to over 5 Mrads during its flyby through Jupiter’s radiation belt. This is compared to the limits of the flight electronics of 100 krad at minimum and 300 krad at maximum [39] [40]. In order to reduce the spacecraft radiation exposure by over fifty times, a radiation vault must be considered.

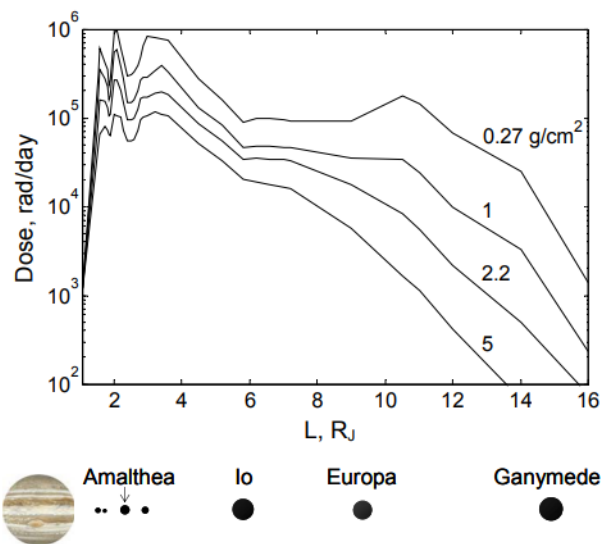


Figure 7-4 Model of Radiation Dosage Rate vs Jupiter Orbit Altitude with Varying Shielding [38]

For historical reference, the JUNO spacecraft also carried on board a radiation vault made 1 cm thick titanium, weighing 200 kg, in order to protect its equipment through its orbits. For RETRIEVER a similar system will be considered. Materials such as Aluminum, Titanium, and Nickel Beryllium Titanium alloys were considered, but due to the minimizing the volume of material required and the manufacturing complexity, titanium was selected.

From there the spacecraft's orbit was propagated and evaluated for varying titanium thicknesses until the required radiation limits were achieved. In the **Figure 7-5** below, the results from the radiation exposure analysis can be found. For the electronics vault, a thickness of 1.4 cm was required to meet the 100 krad limit. Additionally, for the reaction wheel assemblies, which require less than 300 krad, will be enclosed in 0.8 cm thick vaults. In total the electronics vault weighed in at 165 kg, while the two reaction wheel vaults weighed 38 kg each, making the total radiation protection mass 241 kg.

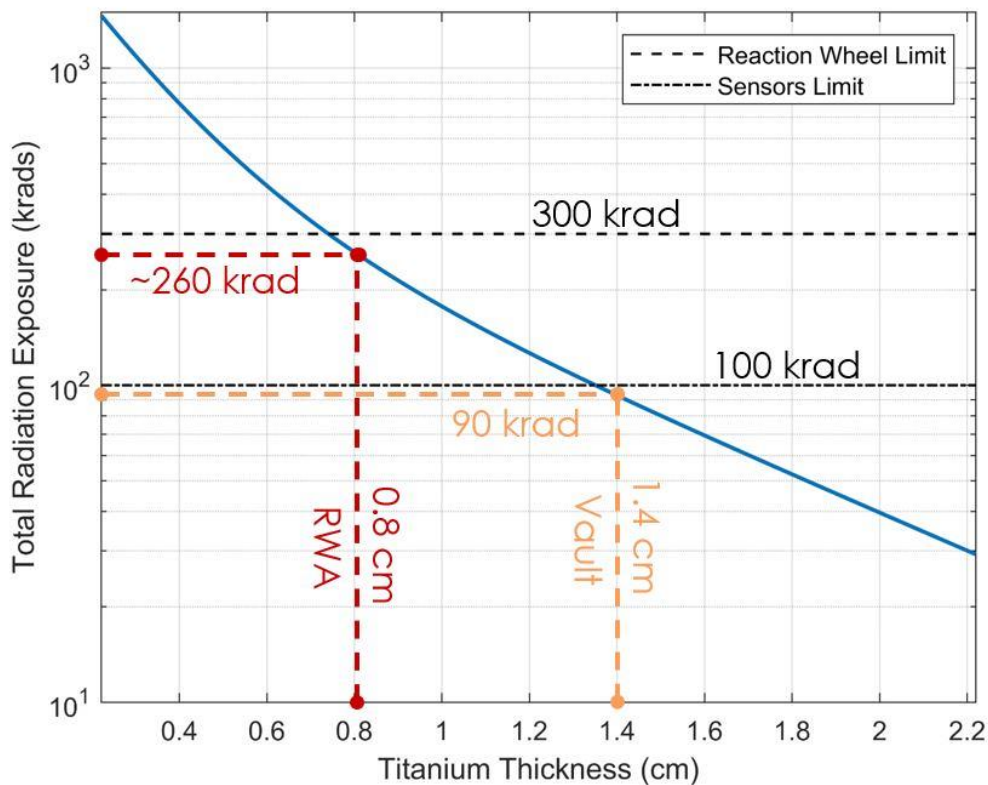


Figure 7-5 Radiation Experienced Through Jupiter Flyby vs Titanium Thickness

8 Structures Sub-System

8.1 Intro / Primary Structure Overview

The primary structure of the spacecraft was not only designed to survive the expected launch loads, but to also provide steady observation capabilities at the solar focal line. Similar to launch vehicles and aircraft fuselages, vertical stringers and skin was used to enclose the highest load bearing structures. Panel is being used to mount components and close out the enclosures. Due to the heat generated from the reactor, the intermediate structure between the bus and propulsion house was designed with tie-rods to reduce the impact the primary structure might have on heat dissipation.

8.2 Material Choices

The materials used for the spacecraft consists of 2024 and 7075 Aluminum in various forms. The components of the primary structure were designed with simplicity and ease of manufacturing in mind to reduce the cost of fabrication. The extrusions used on the spacecraft are Army Navy Drawing (AND) shapes which can be purchased in bulk length and cut down to size to fit the design [41]. The bends of the sheet metal found in the design are bent at the minimum radius allowed for the thickness of sheet for 7075 Aluminum. Keeping the bend radii at or above this minimum bend radius will ensure that the spacecraft will not require any additional manufacturing costs to bend the metal in O-condition and then heat treat to the required temper. The only machined parts found in the primary structure are the clevises which interface the tie-rods to the panels. The number of machined parts for the primary structure was kept to a minimal number to reduce the cost of manufacturing. The two most expensive set of components to manufacture are going to be the vented aluminum honeycomb panels and the titanium propulsion tank mount assembly. The honeycomb panels are fabricated with 7075 aluminum facing and 1/8" cell size 5052 aluminum honeycomb core. The support structure for the propulsion tank was designed with Ti-6V Al titanium tubing for the struts which interface with a set of titanium rings that interface the struts to the top and bottom panels of the propulsion house. The mechanical properties and strengths of our materials were referenced from MMPDS-09.

8.3 Model Definition

The mesh of the FEMAP model was generated by hand by examining the defining nodes of the primary structure. The defining nodes can be defined as places where geometry changes, where another component interfaces with the mesh, or where a point load needs to be applied. With the defining nodes

determined, the size of the mesh could be established based of the closest distance between any two of the defining nodes.

As an example, for the spacecraft FEMAP model the closest defining nodes were the distance between two of the vertical stiffeners on the primary structure. By measuring the distance between the two vertical stiffeners, it was determined that two elements would be enough to display the behavior of the intermediate elements. The distance between the two vertical stiffeners was then halved and used to mesh the geometry for the top of the bus at that mesh size. The distance between another pair of defining nodes was first measured, then divided by the predetermined mesh size. This would determine the number of elements that should be meshed along that curve to preserve the desired mesh size.

Loads were applied to the model using a combination of body acceleration, distributed element loads, and nodal point loads. Only the primary structure was modeled and the secondary components of the spacecraft with the significant inertial loads were modeled as applied loads. The model was restrained with “pinned” constraints at 18 points along the circumference of the bottom ring of the payload adaptor. Pinned constraints were used to restrain the model to ensure that they behaved as fasteners which would not carry bending at the interface points to the launch vehicle.

8.4 Load Cases

The load factors which the spacecraft was designed to the enveloped design load factors provided in the SLS Mission Planner’s Guide for various phases in the launch vehicle’s ascent. The table of the combined load factors that were considered can be seen below [42]. Two sets of load factors were considered for one case having the highest axial load and the other having the highest lateral load. The highest axial load is experienced during the Main Engine Cut Off (MECO) and the highest lateral load is experienced during maximum dynamic pressure (Max Q).

The two load cases were assessed separately, but the two associated load factors were combined and applied to the model, resulting in an inertial acceleration off axis from one of the vehicles principle axes. The inertial loads were represented in the model in various ways, depending on what component the inertial load was associated with. The model only consisted of the primary structure with the components being represented in the model by their inertial loads.

The inertial loads of the primary structure were present in the model by assigning each element property with the correct density of the material. With the densities and dimensions of the elements

defined, NASTRAN was able to apply an acceleration to the entire model and the elements would carry their own inertial load.

The radiation vault for the spacecraft’s electronics, reactor, and the ARIEL Telescope were all represented using elemental loads with uniform distribution. The presentation of these elements as inertial loads started with an assessment of how much area each component occupied to determine the number of elements which would have the elemental load applied. The load distribution of the ARIEL telescope and the reactor were idealized as circular uniform distributed loads on the top panel of the bus and the top panel of the propulsion house, respectively. The radius of the interface area of ARIEL was approximated to be around 36 inches, providing an area of 4,072 in². The radius of the interface area of the reactor was approximated to be around 24.75 inches, providing an area of 1,924 in². The interface area of the radiation vault was approximated as 1,710 in² in a rectangular area inside the bus, behind the panel which the high gain antenna was mounted to. The pressure that was required to be applied to the selected elements was determined by dividing the mass of the component with the load factor by the measured area. The two perpendicular distributed loads for each combined load case were then used to determine an equivalent resulting load factor which would be in the direction the resultant load vector.

Point loads were used to represent the tank and high gain antenna’s inertial loads. The interfaced to the struts of its support structure in a radial array, at the midspan of each strut. The node at the mid span of each of the struts was selected to have the nodal load applied. The value of the nodal load was determined by dividing the factored weight of the propellant assembly amount each strut equally, which assumes that the tank acted as a rigid body. The high gain antenna’s point loads were determined by sketching a free body of the antenna and reacting the inertial load of the antenna at the location of each of the inserts which tied it down. The high gain antenna’s center of mass had a 12-inch eccentricity from the interface with the panel inserts so the overturning moment of the antenna for the download case was combined with the tensile load on the inserts from the lateral load.

Table 8-1 Block 1B PPL/CPL Combined Load Factors [42]

Case	Vehicle Axial (G)	Vehicle Lateral (G)
Liftoff	+1.0	±1.5
Liftoff / Transonic	-2.0	±2.0
Max Q	-2.3	±2.0
Core Stage Flight	-3.5	±0.5
MECO	-4.1	±0.5

8.5 Properties

8.5.1 Sheet Metal

The central structure of the bus was designed using 0.063" thick 7075-T6 sheet metal with a minimum bend radius of 0.310" per industry standards [43]. The central structure consists of 6 bent facets that have flanges to be fastened along the edges of each facet to form an extruded hexagonal tube made from bent sheet metal. The ends have flanges that are bent to interface the central structure to the top and bottom panels using inserts. The center of the webs of the central structure has been designed to be chemically milled down to 0.032" thick for weight reduction.

The sides of the propulsion house are fabricated using 0.047" thick 7075-T6 aluminum. These facets are used to strictly carry shear while the stiffeners, which will be covered in a later section, carry the vertical load. The sheets of the propulsion house can be fastened to the vertical stiffeners using #10 rivets with 3.5-inch pitch.

The construction and design purpose of the skin of the payload adapter is like the propulsion housing facets, where the sheets are only used to carry shear while stiffeners carry the axial load. The skin of the payload adapter is 0.063" thick 7075-T6 aluminum.

The sheet metal was modeled using CQUAD4 elements with the thickness and material properties matching the design specifications.

8.5.2 Extrusions / Stiffeners

The extrusions used on the central structure help carry the axial load of the telescope during any down loads. Without the central structure, the top panel of the instrument bus would have to carry the axial load from the telescope entirely in bending. The Army Navy Drawing (AND) shape chosen for the vertical stiffeners of the central structure was AND10138-1402. This unequal leg, zee extrusion was used to have the outward flange to mount any additional, lightweight equipment.

The vertical stiffeners of the propulsion house and payload adapter use the same shape. The shape was inspired by standard Boeing stringer "hat channels" fabricated from bent 0.063" thick 7075-T6 sheet metal. The shape of the stringer can be found below. The stringer was designed to be mounted to the inside faces of the sheets it supported with rivets through the centerline cap of the hat-section. The fastener pattern used to tie the stringers to the sheet could be #10 rivets at 2.5" pitch.

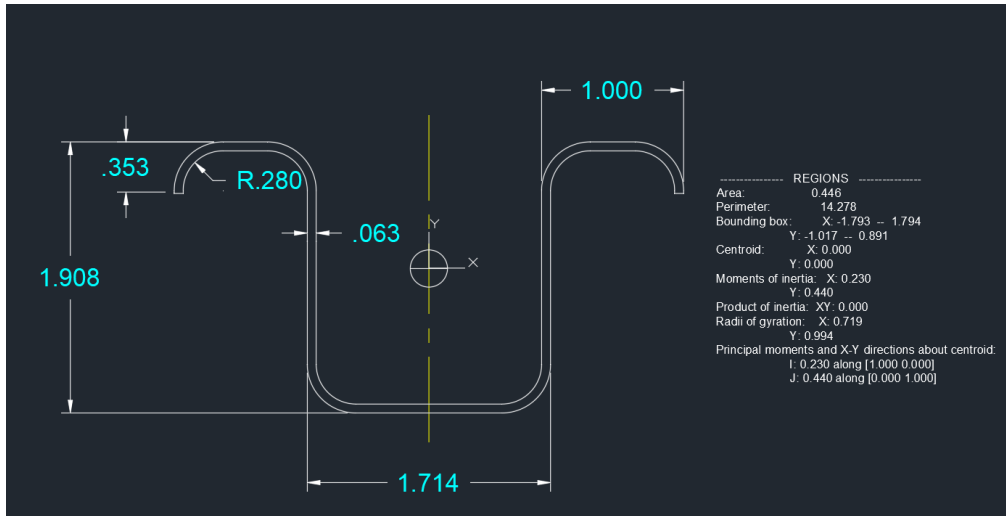
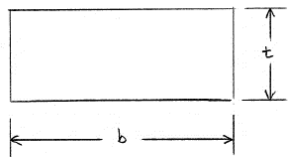


Figure 8-1 Vertical Stiffener Cross Section

8.5.3 Panels

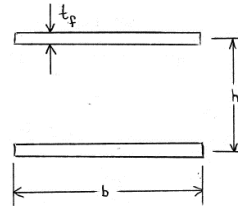
Panels were used for the top and bottom facets of the instrument bus and the propulsion house. The instrument bus had 1" thick panels with 0.02" face sheets while the propulsion house used 3" thick panels with 0.04" thick face sheet. The reason for the propulsion house using thicker panels was due to the propulsion house having to carry much more load than the instrument bus in bending. The aluminum honeycomb panels were designed to be fabricated using 7075 for the face sheets and 5052 for the core. The panels were also designed to be vented in order to accommodate for decompression by having the cells of the core perforated and having small 1/16" diameter holes spread 3 inches from one another on the face sheets to follow the JPL 2000 volume to area ratio for decompression [44].

The panels of the spacecraft were modeled using CTRIA3 plate elements with the properties generated by determining an equivalent thickness. To determine the equivalent thickness of the CQUAD4 to model the sandwich panel, the two equations shown below were set equal to one another and solved for the thickness term in the rectangular section equation. The two equations shown below are the equations for the moment of inertia for a rectangular section and the moment of inertia for a sandwich section. The effective thickness equation below was used to model the sandwich panels using plates. It is important to note that this relation shown above is only valid if the top and bottom face sheets have the same thickness.



$$I_{rect} = \frac{1}{12} b(t^3)$$

Figure 8-3 Moment of Inertia of a Rectangular Section



$$I_{panel} = \frac{t_f h^2 b}{2}$$

Figure 8-2 Effective Moment of Inertia of a Sandwich Panel Section

$$t_{eff} = \sqrt[3]{6t_f h^2} \quad \text{(Equation 8-1)}$$

8.5.4 Tie-Rods

The tie rods of the spacecraft assembly were modeled using CBAR elements with the area dimensions set to the cross section of the tie rod tubes, while the moment of inertias were set to 0.0001 in⁴ to ensure that the rods would not carry any bending. Tie rods were used in the instrument bus in lieu of side panels to alleviate weight and were also used in the intermediate structure to provide as little of impingement on the heat dissipation system of the reactor as possible.

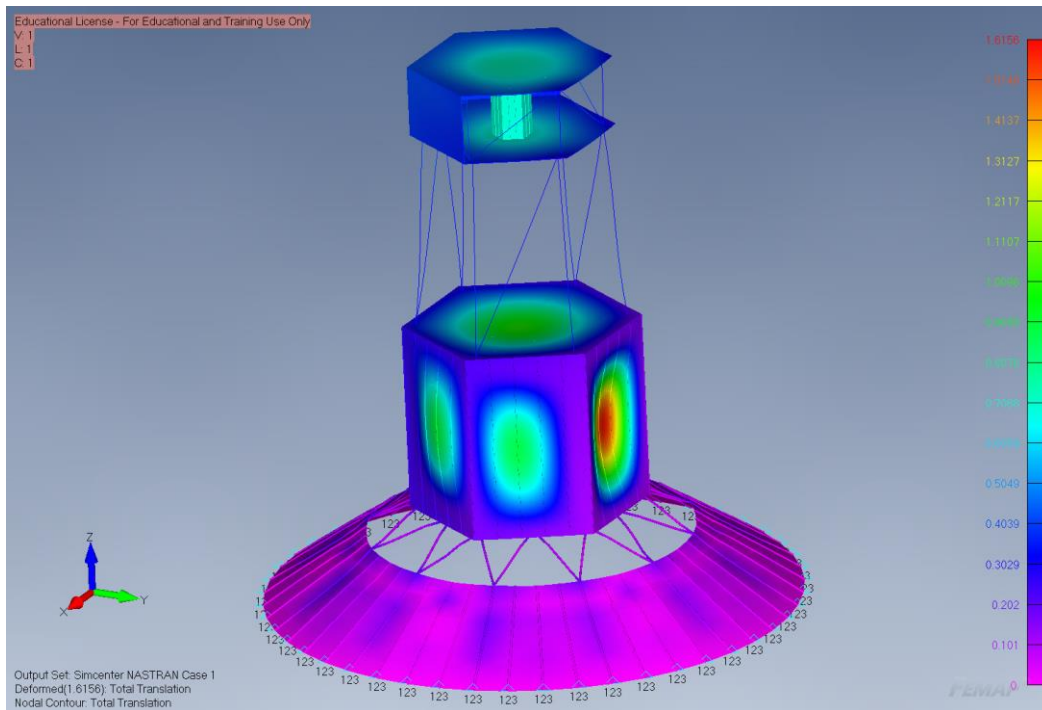
8.5.5 Tank Struts

The tank struts were designed to mimic the mounting style of spherical tanks found on most spherical pressure vessels. A polar array of twelve cylindrical tubes were used to support the 11 metric ton tank of xenon in both the axial and lateral load cases. The sizing of the tank struts was determined by dividing the total mass of the tank by the number of struts and examining a single strut as a simply supported beam. The bending stress was determine using the axial load to load the beam midspan where it interfaces with the tank. The bending stress was combined with the axial load generated from the down component of the inertial load to get the maximum tensile stress on the strut cross-section. The maximum tensile stress on the strut cross section was then compared to the yield strength of Ti-6V Al titanium to generate a margin of safety. An additional 25% load was added to applied load during assessment of these struts for conservative analysis. Calculations showed that the struts required to have an outer diameter

of 3.5 inches and a wall thickness of 0.12 inches. These tubes were modeled using CBAR elements with all associated dimensions and properties of the annular cross-section.

8.6 MECO

The results of the MECO load case FEMAP model can be found below. The MECO combined load case consisted of 4.1G axial and 0.5G lateral accelerations [42]. The maximum total translation of the model was 1.616 inches on the side panels of the propulsion house. The maximum bending moment on the panels was 3,173 in-lbs/in which resulted in a face sheet stress of 26.4 ksi. Using 0.04" thick 7075 face sheets on 3" thick panel leaves a margin of 1.61. The maximum shear stress found on the model was found in the skin of the payload adapter with a value of 10.91 ksi which remains below the shear allowable for 7075-T6. The highest axial load found on the CBAR element of the model was 10.08 kips in tension along the top ring of the payload adapter. The 0.20 in² area of the payload adapter upper ring presents a tensile stress of 50.4 ksi stress and a margin from yield of 0.03.



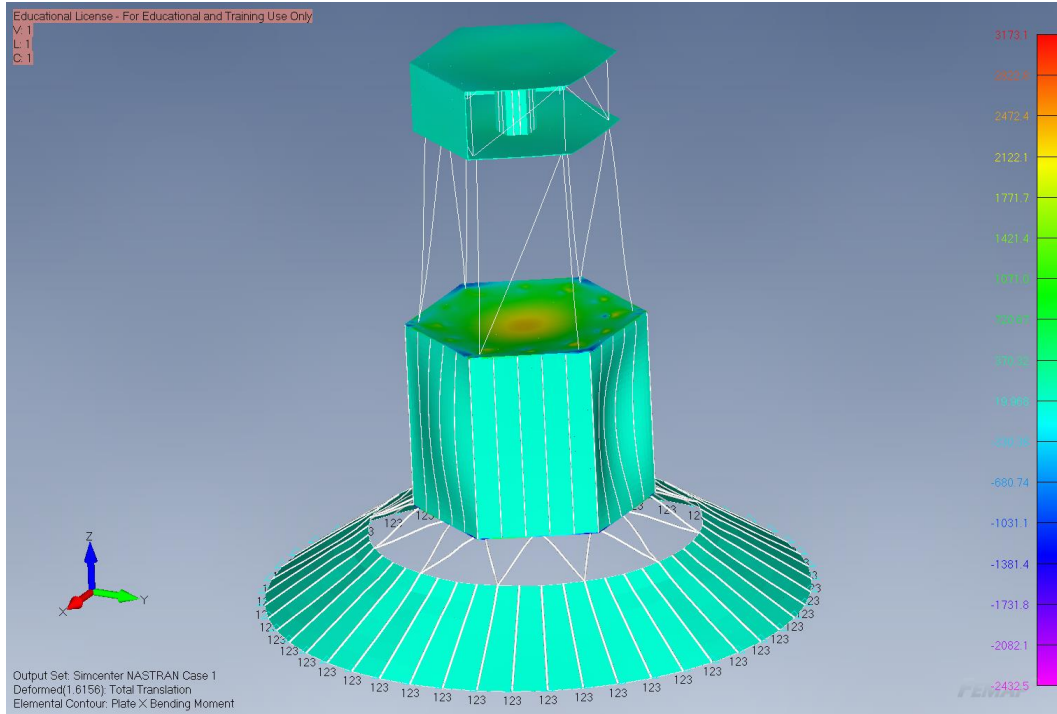


Figure 8-5 MECO - Plate Bending Moment X

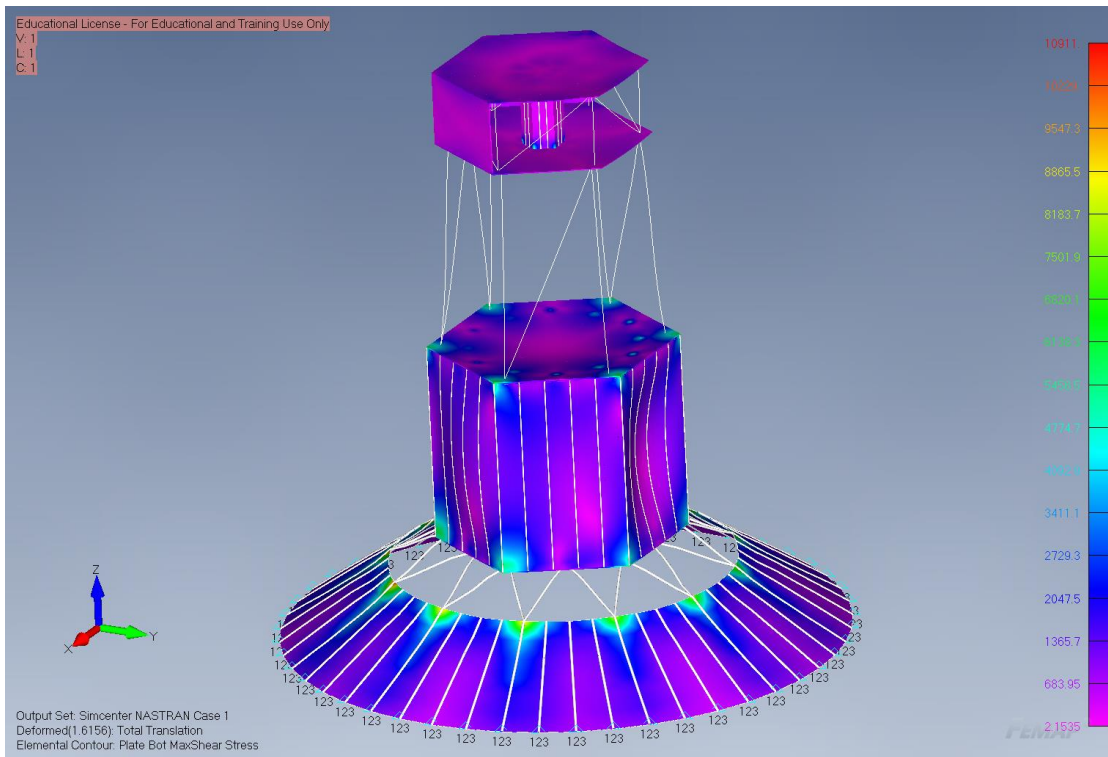


Figure 8-6 MECO - PLATE Bottom Max Shear Stress

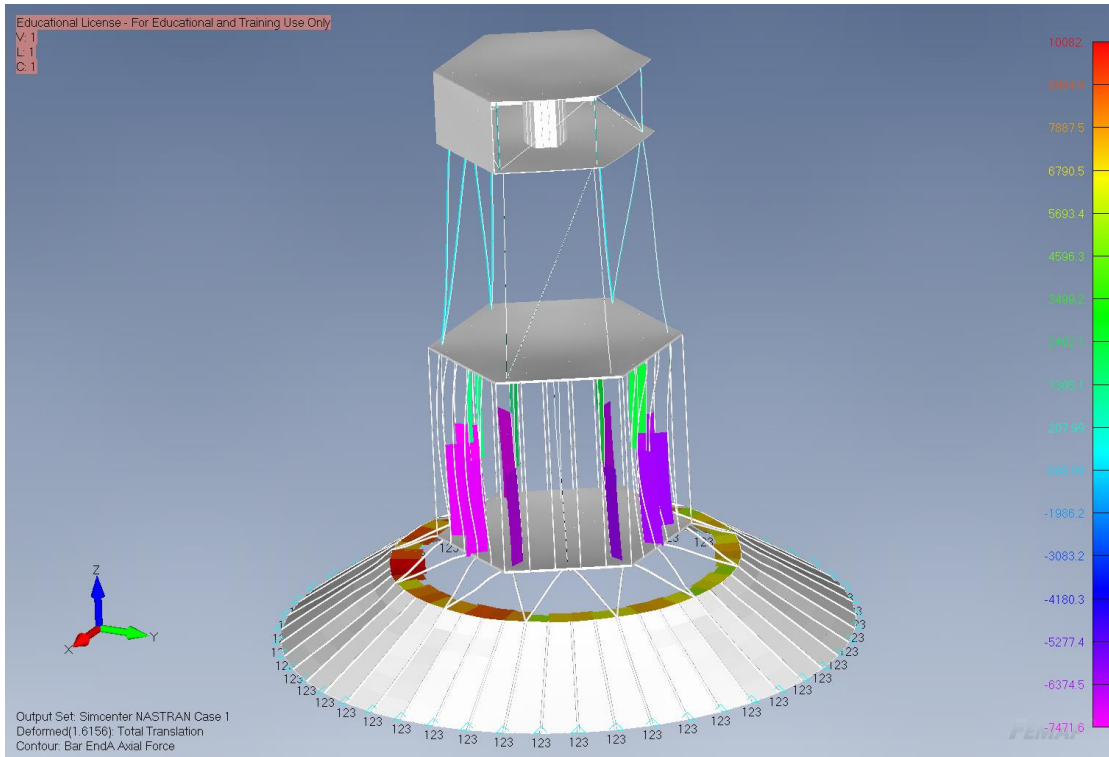


Figure 8-7 MECO - CBAR Axial Load

8.7 Max Q

The results of the Max Q load case FEMAP model can be found below. The Max Q combined load case consisted of 2.3G axial and 2.0G lateral accelerations [42]. The maximum total translation of the model was 2.10 inches on instrument bus. The maximum bending moment on the panels was 4,636 in-lbs/in which resulted in a face sheet stress of 38.6 ksi. Using 0.04" thick 7075 face sheets on 3" thick panel leaves a margin of 0.787. The maximum shear stress found on the model was found in the skin of the payload adapter with a value of 16.88 ksi which remains below the shear allowable for 7075-T6. The highest axial load found on the CBAR element of the model was 13.55 kips in tension along the top ring of the payload adapter. The 0.15 in² area of the payload adapter upper ring presents a tensile stress of 67.8 ksi stress and a margin from yield of 0.017.

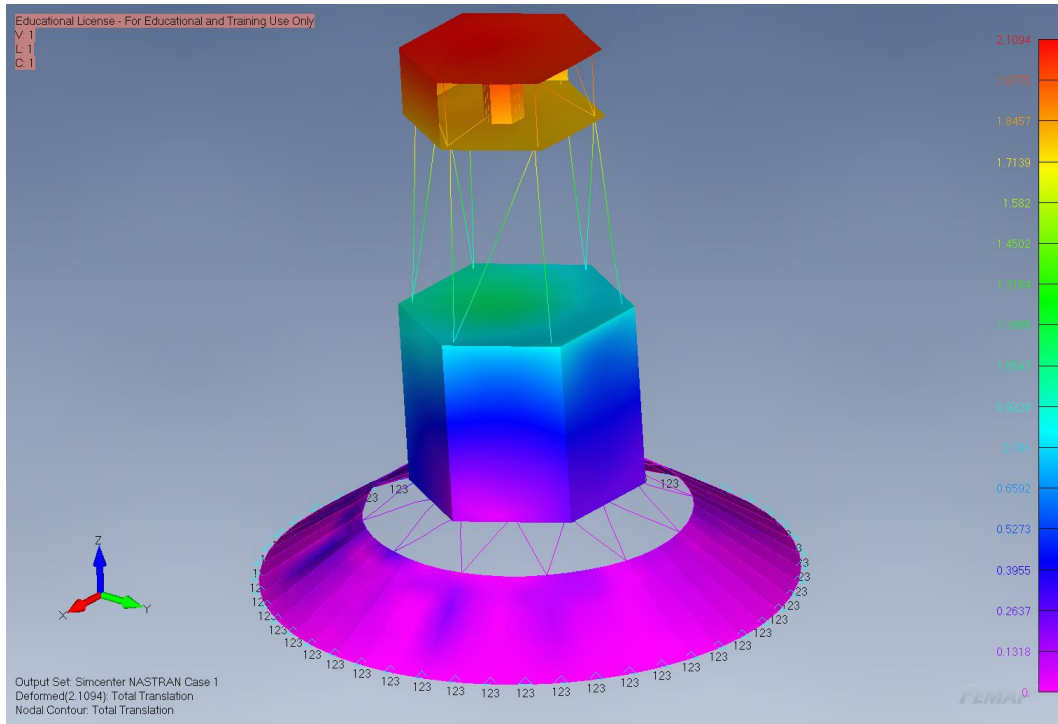


Figure 8-8 Max Q - Total Translation

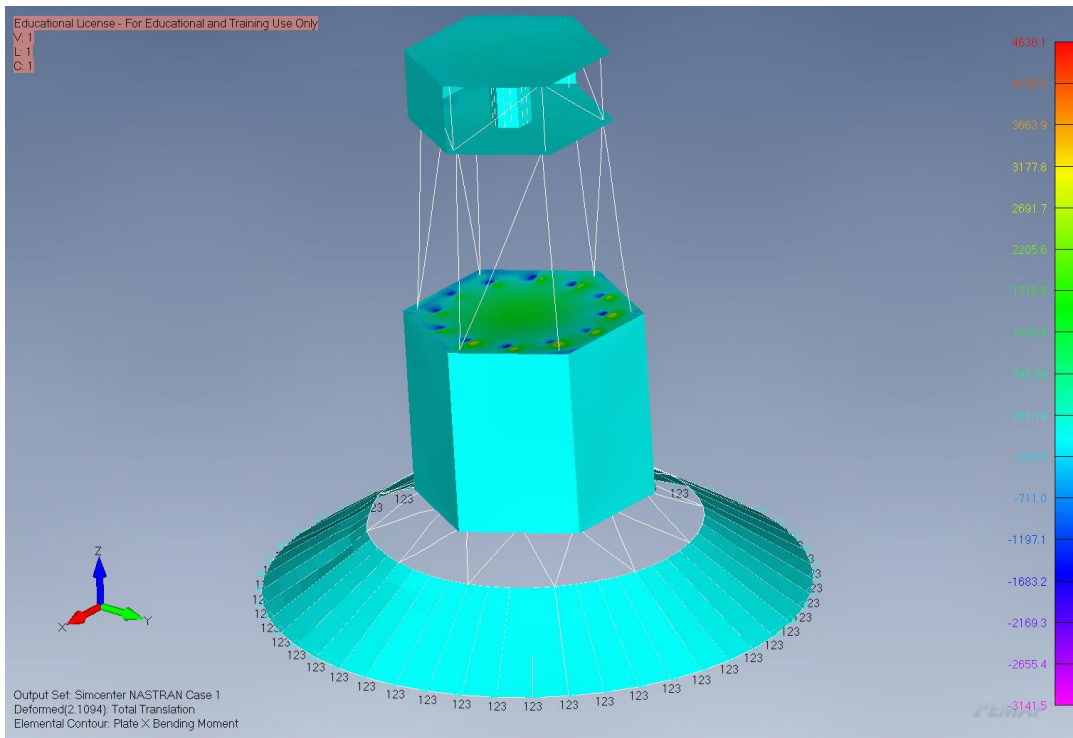


Figure 8-9 Max Q - Plate Bending Moment X

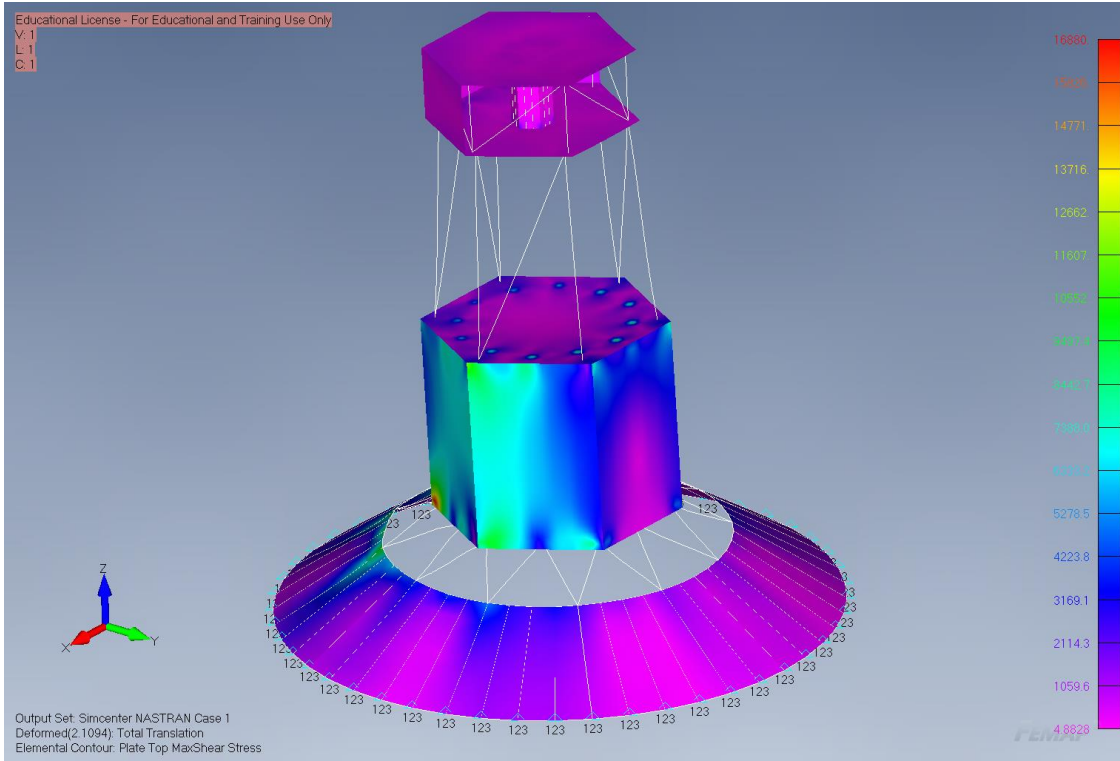


Figure 8-10 Max Q - Plate Top Max Shear Stress

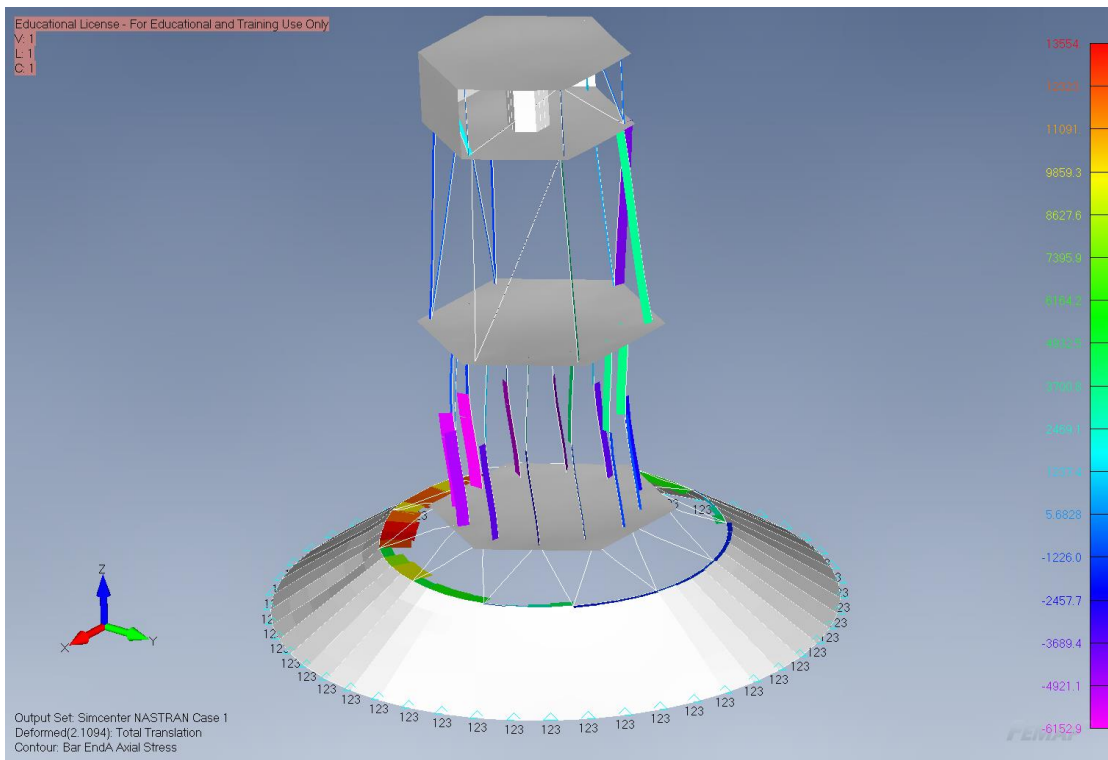


Figure 8-11 Max Q - CBAR Axial Load

8.8 First Mode Approximation

To ensure the applicability of the load factors used, the SLS Mission Planner’s Guide suggests assessing the payload cantilevered fundamental load frequencies. The fundamental first mode frequencies can be estimated using a 1G static assessment in each of the principal directions [45]. The model used to analyze the structure for the combined load factors discussed earlier was modified to determine the displacement of the center of mass during each of the 1G acceleration in the principal directions. The relation shown below used the 1G displacement of the center of mass to estimate the payload’s fundamental mode frequency in that direction. The results from the 1G static load assessment can be found in the table below along with the determined fundamental frequencies. The determined fundamental mode frequencies are below the minimum suggested frequencies, so the load factors used for the MECO and Max Q load case cannot be substantiated until the design of both the SLS and spacecraft mature [42].

$$f_n = \frac{\sqrt{G/D_n}}{2\pi} \quad \text{(Equation 8-2)}$$

Table 8-2 First Mode Approximations

Normal [n]	1G CM Displacement [Dn] (in)	First Mode Frequency [fn] (Hz)	Recommended Minimum Fundamental Mode Frequencies [Fn] (Hz) [42]
X	0.602	4.03	8
Y	0.325	5.48	8
Z	0.1045	9.67	15

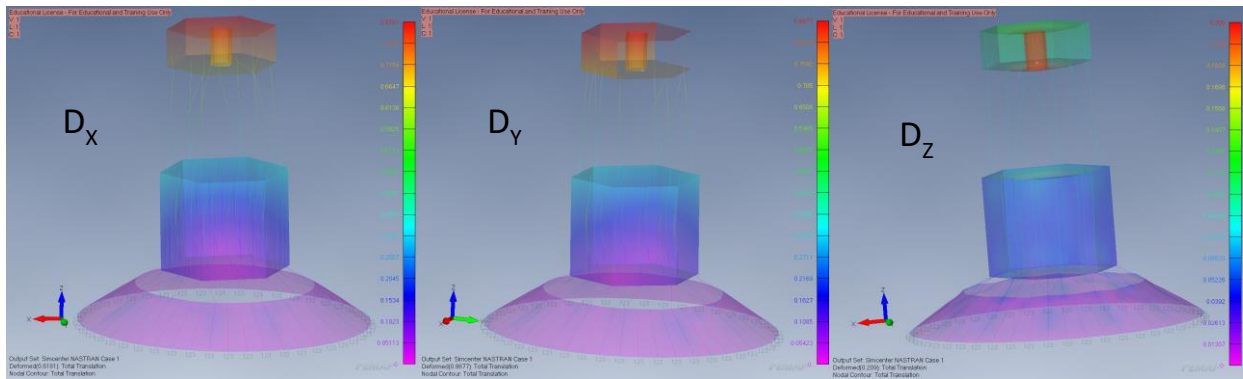


Figure 8-12 1G Displacements

9 Attitude Control Sub-System

The attitude and control system of the spacecraft must be able to provide accuracy and stability through a whole host of operations modes. Of these modes the ones with the most stringent requirements were chosen to be examined further. First, RETRIEVER must meet the point accuracy requirements of the telescope of 17 arcsec. Second, the spacecraft must be stable in cruise. Lastly, the attitude control system must be robust enough to withstand the long mission duration.

Different types of attitude control system are shown in **Table 9-1** [46]. Examining the types of ACS available it was quickly apparent that the only attitude system capable of meeting the pointing accuracy requirement of the telescope was a 3-axis reaction wheel stabilized system. Furthermore, by meeting the telescope pointing requirement the spacecraft will be able to meet the HGA pointing accuracy requirement of 360 arcsec.

Table 9-1 Characteristics of Different Control Systems

Control System	Pointing Accuracy (+/- arcsec)	Propellant Usage	Mass
Spin Stabilization	360	Low	Low
Dual Spin Stabilization	360	Low	Low
Momentum Bias	360	Low	Low
3-axis Thruster Stabilized	360	High	Low
3-axis Control Moment Gyro Stabilized	3.6	Low	High
3-axis Reaction Wheel Stabilized	0.36	Low	Low

9.1 Actuators and Sensors

The system uses two different types of actuators for different purposes. The main actuators of the spacecraft control system are the reaction wheel assemblies. They are used for major attitude maneuvers and for fine pointing maneuvers. The other actuator in the attitude control system are the thrusters. They are used for desaturation of the reaction wheels and for performing trajectory correction maneuvers. The locations of the ACS components are indicated in **Figure 9-1**.

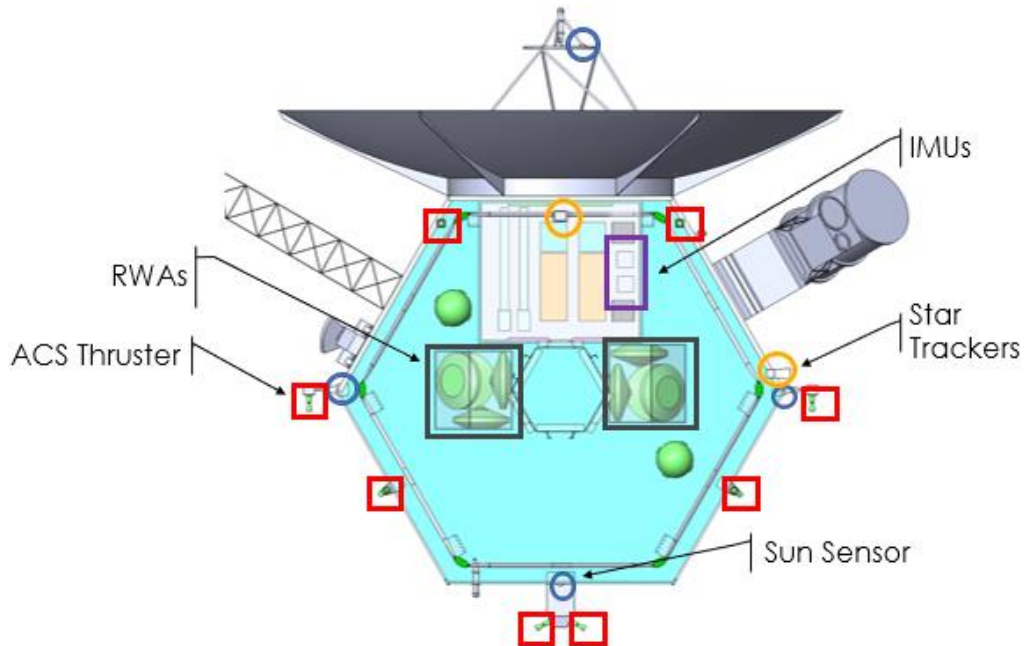


Figure 9-1 Placement of ACS Components in Bus

9.1.1 RWA

The reaction wheel assembly that was selected was the Honeywell H16 [40]. These reaction wheels showed to have the longest lifespan out of any of the reaction wheels. Furthermore, they were Rad hardened up to 300 kRad. Lastly, they were chosen because of their high momentum storage capabilities. The H16 are able to store 150 N-m-s of impulse, so desaturation maneuvers can be performed less frequently.

The reactions wheel assemblies are set up in such a way that one is pointed in each principal axis and there is one that is point off axis to provide a redundancy in each assembly. There is further redundancy in the fact that the spacecraft is using 2 reaction wheel assemblies for a total of 8 reaction wheels on the entire spacecraft.

9.1.2 Thruster

The thrusters that were selected for the spacecraft attitude control system were the MR-106L engines from Aerojet Rocketdyne [47]. They were selected because they provide 22N of thrust and are individual thrusters allowing for the placement of the thrusters in many different angles to accommodate the geometry of the spacecraft. The spacecraft contains 16 different thrusters to provide the ability to desaturate in all axes.

Due to the fact that the spacecraft contained 3 large components, the 3.5 meter high gain antenna, the telescope and the reactor assembly, Due to the fact that the spacecraft contained 3 large components the thrusters were placed in an unconventional manner around the spacecraft. **Figure 9-2** on the right shows the placement of the ACS thrusters on RETRIEVER. Four of the thrusters are pointing in the aft direction and four are point in the forward direction to provide the ability to desaturate the spacecraft in pitch and yaw. The other eight thrusters are solely to provide the ability to desaturate in the reaction wheels in roll.

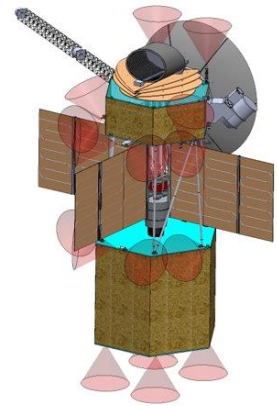


Figure 9-2 ACS Thruster Placement

9.1.2.1 Sensors

The spacecraft must include sensors capable of performing the mission and uses 3 different types of sensors to perform the mission.

9.1.2.2 IMU

The spacecraft will be equipped with the Honeywell Miniature IMU [48] [39] [49]. The IMU is capable of taking rotational rate data and translational data. An example of the Fiber Optic Gyroscope used in the MIMU is shown in **Figure 9-3** to the right.



Figure 9-3 Gyroscope used in MIMU [39]

9.1.3 Star Tracker

The star tracker gives the spacecraft an inertial reference in space. Retriever uses the DTU MicroASC star trackers as the inertial sensors [50]. Each star tracker was designed to have built in dual redundancy. Each star tracker has two camera heads and data processing units. **Figure 9-4** shows the one of the camera head units that would be a part of the star tracker. Furthermore, the spacecraft is using two of these star trackers. By using two MicroASC star trackers the spacecraft effectively has four on-board star trackers.



Figure 9-4 MicroASC Star Tracker without Baffle [50]

9.1.4 Sun Sensor

The sun sensor indicates to the spacecraft the position of the sun. The sun is mostly use for safing events. The sun sensors have a 60°x60° FOV [51]. We are using four SSOC-A60 2-Axis Analog Sun Sensors for our design. **Figure 9-5** shows the sun sensor chosen for RETRIEVER.

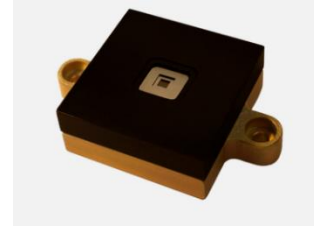


Figure 9-5 SSOC-A60 Sun Sensor [51]

9.2 Performance

Aside from point the spacecraft towards the sun for SGL the spacecraft needs to be able to perform large maneuvers and reject disturbance torques introduced into the system.

9.2.1 ACS Maneuvers

The spacecraft maneuvers shown in **Figure 9-6** and **Figure 9-7** are at 550 AU and assume that all disturbance torques are essentially zero. Furthermore, due to the shape of the spacecraft it can be assumed that the spacecraft is axially symmetric. Therefore, I_y and I_z were both equal to 33,760 kg-m² and I_x was equal to 8,180 kg-m². The motion of the spacecraft in **Figure 9-6** is 18 minutes and motion of the spacecraft in **Figure 9-7** is 13 minutes. The maneuvers are done with the reaction wheel assemblies due to that and the fact that the moments of inertia are so large contribute to the maneuvers taking between 10-20 minutes.

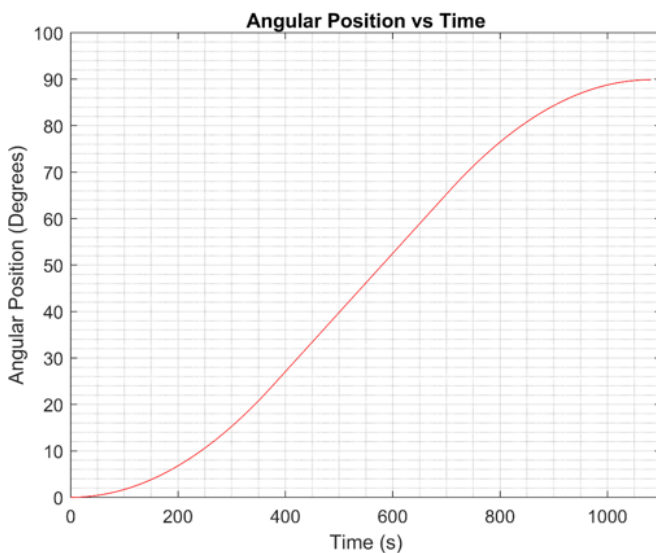


Figure 9-6 Pitch 90° to go from Interstellar Cruise to SGL

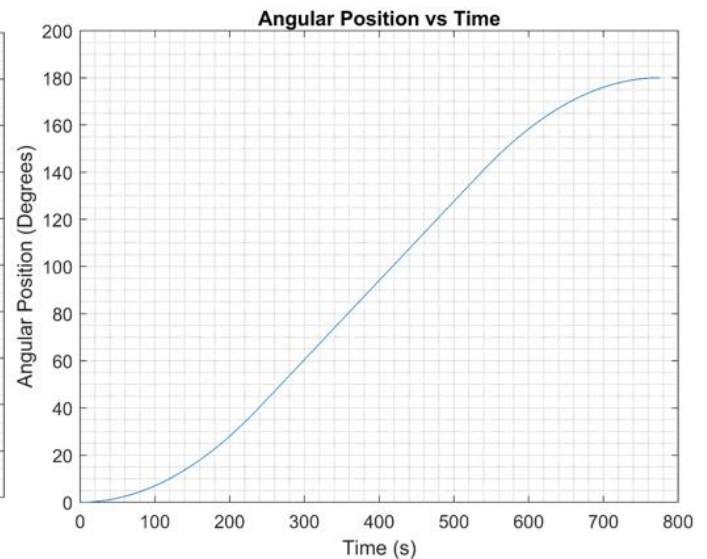


Figure 9-7 Roll 180° to go from SGL to Science Data Downlink

9.2.2 Orbit Torques

The spacecraft will experience the majority of the orbit torques in the first 4 years of operation. After that period, the spacecraft will be past Jupiter and not experience much disturbance torque as shown in **Figure 9-8**. Due to the fact that the spacecraft will not be experiencing significant orbit torques throughout the entire lifetime, the spacecraft will use the reaction wheels periodically to ensure that they are still

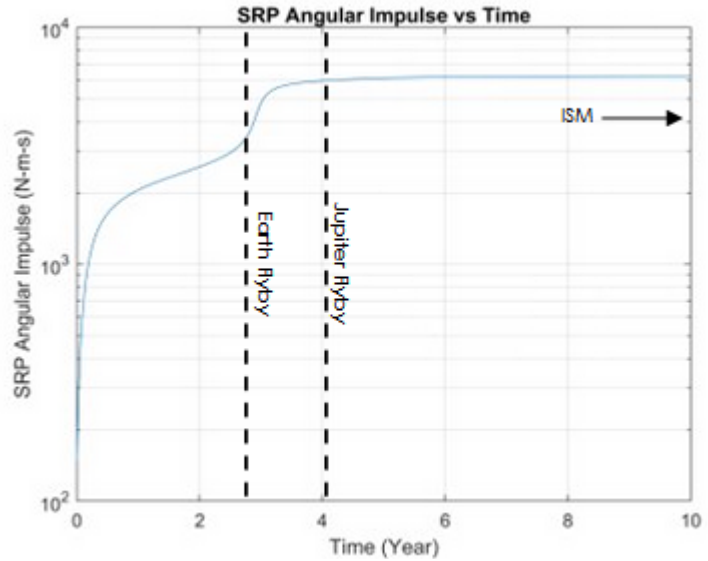


Figure 9-8 SRP Angular Impulse vs Time

functional. The HR16 reaction wheels have a 15 year plus lifetime when in GEO. **Table 9-2** shows the angular impulse built up by the orbit torques over the entire spacecraft primary mission. Furthermore, **Table 9-2** contains an example of the angular impulse experienced by a small satellite in MEO. The values were of torque were from a small satellite at a 20,000 km circular orbit around Earth and were integrated over the typical mission lifetime of 15 years [52]. RETRIEVER will experience nearly double the amount of orbit torques through its lifetime when compared to a small earth orbiting satellite. For this reason, the spacecraft will have two sets of reaction wheel assemblies for a total of 8 reaction wheels.

Table 9-2 Expected Lifetime Orbit Torques

Category	RETREIVER	RETREIVER	SCS Example	SCS Example
	Angular Impulse (N·m·s)	Fuel Req. (kg)	Angular Impulse (N·m·s)	Fuel Req. (kg)
Solar Radiation Pressure	6258	2	3124	1
Jupiter				
Gravity Gradient	75.1	0.02	N/A	N/A
Magnetic Torque	35.5	0.01	N/A	N/A
Earth				
Gravity Gradient	23.3	≈ 0	217.7	≈ 0.06
Magnetic Torque	0.9	≈ 0	142	≈ 0.04
Total	6393	2.03	3484	1.1

9.3 Mass and Power Breakdown

The power for the ACS power breakdown assumes that two reaction wheels, two thrusters, one IMU, one Star tracker, and 1 Sun Sensor is on. **Table 9-3** contains the ACS subsystem Power and Mass CBE.

Table 9-3 ACS Mass and Power Current Best Estimate

Component	Mass (kg)	Power (W)	Quantity	Mass Subtotal	Power Subtotal
RWA	12	22	8	96	44
Star Tracker	0.425	3.7	2	0.85	3.7
IMU	5	2.08	2	10	2.08
Thruster	0.59	36	16	9.44	72
Sun Sensor	0.025	0.35	4	0.1	1.4
			Total	116.39	123.18

10 Command and Data Handling Sub-System

To be able to have the spacecraft over the 60-year mission, it is required that RETRIEVER have a C&DH system that is robust. The C&DH system was designed to meet DR4.1 in order to complete the mission.

10.1 Components

10.1.1 Computers

RETRIEVER will be equipped with 4 BAE RAD750 Single Board Computers they are single board computers that have been used on many missions. They have been used on many missions such as MRO, LRO, and Europa Clipper [53] [54] [55]. The main reason that these computers were selected was their long heritage and reliability. The MRO has been operational for 14 years and continues to operate [56]. Two of the RAD750 SBCs will be used for the Command and Data Handling System. The other two systems will be used strictly for the attitude control system.

The RAD750 is capable of running VxWorks operating system for the spacecraft which also has a long heritage of spacecraft mission. VxWorks has a multitude of fault protection in the coding and has been used for spacecraft at JPL, such as MRO and MSL [57].

10.1.2 Payload Data Handling Unit

The Payload Data Handling Unit (PDHU) was taken from the GAIA spacecraft. The PDHU can store 1 TB of data [58]. GAIA was launched in 2019 will perform Exoplanet observation. Consequently, the GAIA PDHU is of TRL 9.

10.2 Performance

While performing the SGL portion of the mission the spacecraft will produce 11.4 GB of science data per day. Over the 30 days that the spacecraft is performing SGL the spacecraft will produce 43 GB of data. The spacecraft then needs to store that data along with other instrument data until able to transmit the data back to earth. **Table 10-1** shows that the amount of science data the spacecraft could possibly collect during the mission. The information is based on the data rates of the instruments and the amount of time each instrument is expected to be on shown in the instrument schedule. The spacecraft produces more information than it could possibly store. Therefore, the spacecraft will downlink the science data using the HGA after the electric propulsion burnout.

Table 10-1 Amount of Data Possible to Collect

Instrument	Data Produced Through Mission Lifetime (GB)
MAG – 3	3108
SWICS	15.76
CDA	28.91
ARIEL	43
Total	3195.67

10.3 Fault Protection

To prevent the spacecraft from being vulnerable to single modes of failure, the spacecraft implements dual redundancy wherever possible for mission critical components. The RAD750 chosen for this mission are shown resistant to single event upset [59]. To prevent failure to high levels of radiation all the components chosen are radiation hardened to at least 100 krad.

10.4 Mass and Power Estimate

The power estimate calculation assumes that only one of each of the computers will be on at any given moment. For example, one ACS computer and one C&DH computer are on at the same time resulting in a total power draw of 20 W. **Table 10-2** shows the current best mass and power estimates of the C&DH system.

Table 10-2 C&DH Mass and Power Estimate

Component	Power (W)	Mass (kg)	Quantity	Mass (kg)	Power (W)
ACS RAD 750 SBC	10	2	2	4	10
C&DH RAD 750 SBC	10	2	2	4	10
GAIA PDHU	26	14	2	28	26
Misc. Equipment Estimate	20	30	2	60	20
			Total	96	66

11 Telecommunications

The spacecraft is required to be able to communicate all the science data at 550 AU. The spacecraft uses a 3.5 m high gain antenna for communication of at high bit rates. The spacecraft also has three low gain antennas for the communication of data at lower bit rates to or from the spacecraft. **Figure 11-1** shows how the entire telecommunications system will operate.

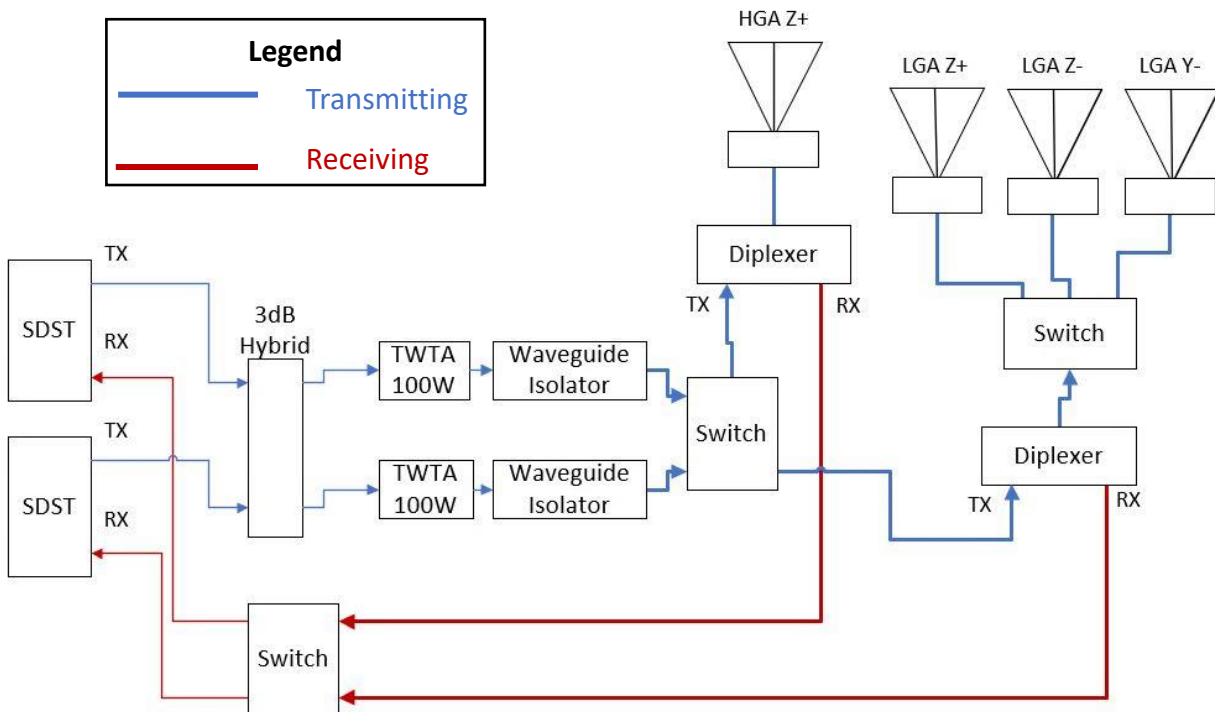


Figure 11-1 Telecommunications System Block Diagram

11.1 Antennas

RETREIVER uses traditional methods of communication with Earth. The spacecraft uses 2 different types of antennas to achieve meet communication requirements.

11.1.1 DSN Antennas

The spacecraft will be communicating to Earth using the Deep Space Network system. The DSN communication stations are located approximately 120 degrees around Earth allowing constant coverage of the spacecraft [60]. The spacecraft will utilize the 34 m DSN antenna for both sending commands to the spacecraft and transmitting engineering and science data. The DSN is able to communicate currently

in X, S, and Ka band. For the X-Band communication that RETRIEVER will be using the DSN 34 m antenna provides 68 dB of gain.

11.2 High Gain Antenna

The spacecraft has a 3.5 m Cassegrain antenna. The antenna was selected because the Cassegrain antennas provide the largest amount of gain for their given weight [61]. The HGA is based on the DAWN spacecraft design albeit at a much larger size [62]. **Figure 11-2** below shows the location of all the antennae on the spacecraft.

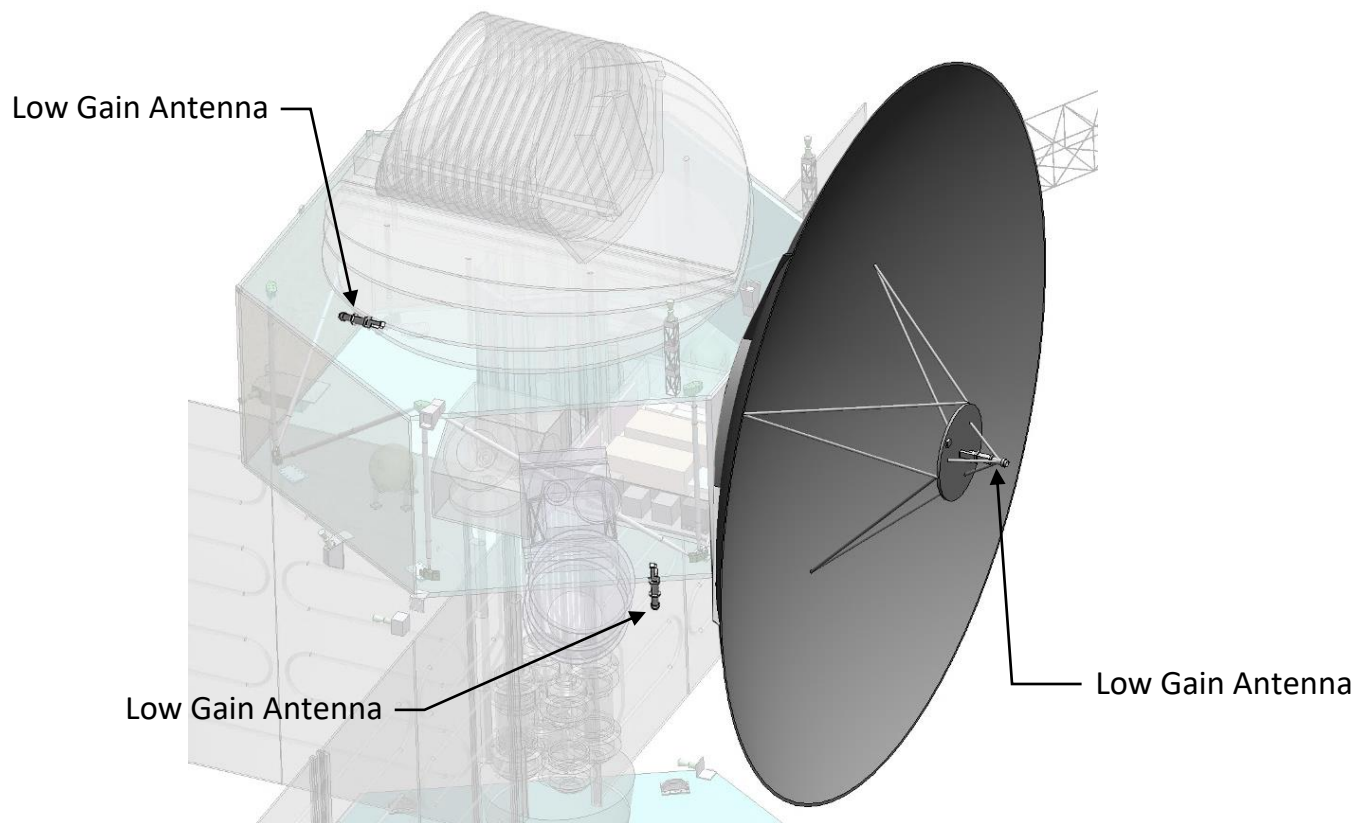


Figure 11-2 Antennas of the Communications System

11.2.1 Low Gain Antenna

The spacecraft has three low gain horn antennae based on the design of the DAWN spacecraft. Each of the LGAs are pointed in a different direction. One is pointed in the -Y direction, so that when the spacecraft is performing the electric propulsion burnout it will be able to communicate with Earth. As shown in **Figure 11-2** there is an LGA pointing in the same direction as the HGA, the Z+ direction. The LGA is pointing that direction in case the spacecraft goes into a safing event. The likelihood of it making contact

with the LGA as opposed to the HGA is much larger. The last LGA is pointing in the Z- direction and the reason for this is to allow the spacecraft to communicate while it is performing SGL. The spacecraft will be able to receive commands and transmit engineering data back to Mission Control.

11.3 Electronics

11.3.1 Small Deep Space Transponder

RETRIEVER employs the use of the Small Deep Space Transponder (SDST) for the purposes of communicating with Earth. The SDST has been used on every deep space mission at JPL since Cassini and is derived from the Deep Space Transponder (DST) used on Cassini [63]. The SDST allows the spacecraft to communicate to Earth using X Band.

11.3.2 Traveling Wave Tube Amplifiers

RETRIEVER uses a Travelling Wave Tube Amplifier (TWTA) that was used on DAWN. This particular TWTA is capable of producing a transmitter power of 100W. The author has found that this is currently the highest power TWTA that has been found on and is of TRL 9.

11.4 Performance

The communications system's performance is dictated by the link budget. For uplink there are two different conditions that the spacecraft may have. The first is that the spacecraft is using the LGA to receive commands and the other is that it is using the HGA to receive commands. If the spacecraft were to enter into a safing event at any point during the mission it will use the HGA to try and locate Earth. During cruise the spacecraft will use the LGA that points in the -Y direction to receive commands. As shown in **Table 11-1**, RETRIEVER is able to perform both of these task at 550 AU. JUNO currently uses 7.8 bps for sending commands during safing events [64]. Therefore, the spacecraft will be able to be recovered if it enters a safing at 550 AU.

Table 11-1 Uplink to the RETRIEVER at 550 AU

Parameter	LGA Value	HGA Value
Transmitter Facility	34 m DSN Antenna	34 m DSN Antenna
Transmitter Power (W)	20,000	20,000
Receiver	Horn	3.5 m HGA
Bit Rate	75 bps	2 kbps
Symbol Rate	200 sps	5 ksps
Bit Error Rate	10^{-6}	10^{-6}
Coding	Reed-Solomon Convolution	Reed-Solomon Convolution
SNR Achieved (dB)	5.5	32
SNR Required (dB)	3	3
Data Link Margin	2.5	29

Table 11-2 shows the scientific data downlink budget at 550 AU. Reed-Solomon Convolution coding is being used. The spacecraft has a bit error rate of 5×10^{-3} which is acceptable for science data [63]. While Cassini was performing its main mission the spacecraft used the same type of coding along with the BER and SNR to complete its mission [63]. With that given BER, the SNR required drops to 0.31 dB allowing the spacecraft to communicate at a much higher data rate. RETRIEVER will use the same BER and coding type as Cassini and as a result is able to have the same SNR requirement.

The DSN antenna selected for this portion of the mission is the 70m series of antennae. They are the only ones capable of achieve an acceptable bit rate. If the 34m series of DSN antenna are used for this portion of the mission the amount of time necessary to communicate the SGL data would increase nearly four-fold.

Table 11-2 Science Data Downlink Budget from 550 AU

Parameter	70 m DSN Antenna Value	34 m DSN Antenna Value
Transmitter	3.5 m HGA	3.5 m HGA
Transmitter Power (W)	100	100
Receiver	70 m DSN Antenna	34 m DSN Antenna
Bit Rate	80 kbps	23 kbps
Symbol Rate	203 ksps	58.4 ksps
Bit Error Rate	5×10^{-3}	5×10^{-3}
Coding	Reed-Solomon Convolution	Reed-Solomon Convolution
SNR Achieved (dB)	1.76	0.97
SNR Required (dB)	0.31	0.31
Data Link Margin	1.45	0.66
Communication w/ DSN	5 hr/day	5 hr/day
Downlink SGL Data Time	0.66 years	2.28 years

11.5 Subsystem Mass and Power Estimate

The mass and power estimate for the telecommunications system is shown in **Table 11-3**. The power estimate for the telecommunications system assumes that one SDST is on and one TWTA is on.

Table 11-3 Telecomm Mass and Power Estimate

Component	Mass (kg)	Power (W)	Quantity	Mass Subtotal	Power Subtotal
SDST	2.7	11.7	2	5.4	11.7
HGA	41	0	1	41	0
TWTA	2.3	187	2	4.6	187
LGA	0.5	0	3	1.5	0
			Total	52.5	198.7

12 Systems Engineering

12.1 System Disposal

In concern for both the effects of orbital debris and radioactive substance there are two phases of the mission that are affected. First is the Earth SOI ejection, completed by the SLS's boost stage, which will be thrown into a highly elliptical Sun-centered orbit with the chance of returning to Earth, much like one of the Apollo mission's third stages. Measures will be taken to evaluate and monitor the stage to gain knowledge on its expected orbit before it falls out of perceivable range. The second phase of concern is the end of life for RETRIEVER itself. By the 550 AU point, the spacecraft is on a course to never return to the solar system and the time towards another star system is on the order of tens of thousands of years to millions.

12.2 Risk Analysis and Mitigation

As previously stated, the Voyager III concept is not a normal mission in terms of risks, the long cruise duration tops even that currently seen on the Voyager 1 & 2 probes. In **Figure 12-1** are the five largest risks posed to the mission throughout the development, manufacturing, and operation of RETRIEVER, sorted by their likelihood and consequence.

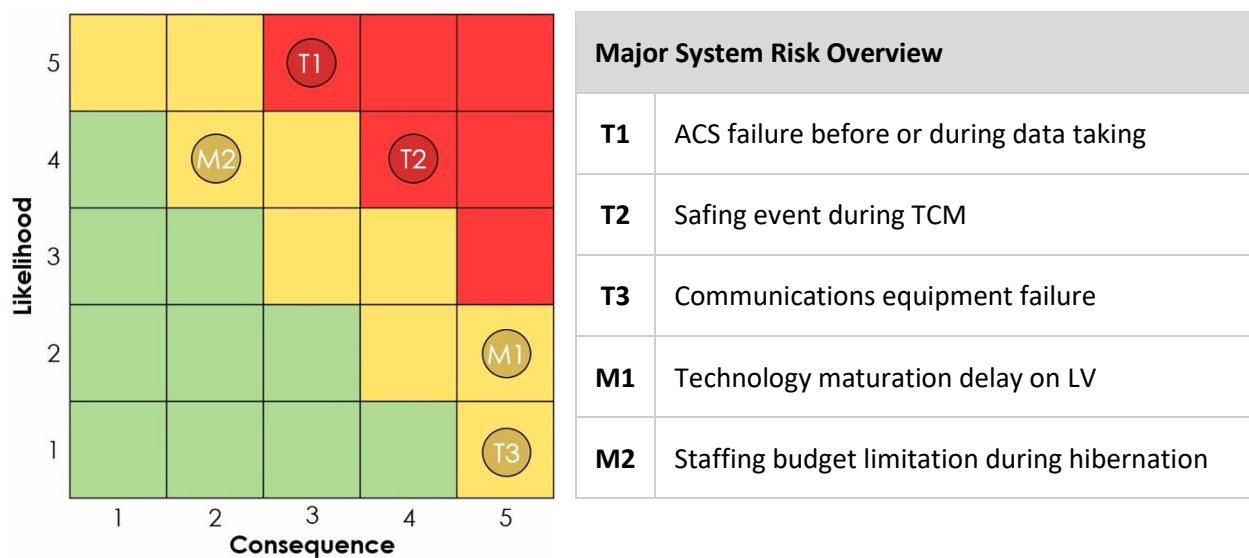


Figure 12-1 Architecture Risks Sorted by Likelihood and Consequence Matrix

Each associated risk also has a mitigation path in order to counter or reduce the consequences of possible failures or budget cuts. As an example, in order to mitigate risk T2, the spacecraft will be flown on trajectories to accommodate at least one missed day of low thrust in 100 days of operation, as well as have TCMs made prior by the low-thrust system itself.

12.3 Cost Breakdown

The spacecraft and project cost estimation was conducted as per requirement SR1.4.

12.3.1 Projected Cost Estimation

Work Breakdown Structure (WBS) based component cost breakdowns were analyzed using the NASA Project Cost Estimation Capability (PCEC) tool. PCEC is designed to handle up to non-nuclear interplanetary missions, and so several assumptions and considerations had to be made in order to use the tool for this nuclear, solar system escape mission.

The power system production cost for the flight hardware was estimated externally from PCEC as this was the nuclear component for the design. Operational cost for the reactor was estimated by PCEC's end of life (EOL) model with the assumption that the total amount of power is what is required for the SGL mission, and not the total reactor output. This was done to ensure that the operations cost of the subsystem would not be associated with the nearly 10 kW of output power the reactor can provide. The NASA Glenn Research Center's Kilopower reactor is an essential technology for this mission. To date, \$20M have been allocated for a ground based 1 kW reactor prototype [65], but the development cost for a space rated version has not announced. It is expected that NASA's Artemis program will include the development and use of the Kilopower reactor [66], but to be conservative, it was assumed that RETREIVER would cover this cost. Reference [67] was used to estimate the cost based off of data from Cassini's GPHS-RTG and MSL's MMRTG development. Kilopower utilizes Advanced Sterling Radioisotope Generators (ASRG) for its power generation, and it is included in the reference. It was assumed that costs for this technology type with the scaling factors from the legacy systems would be reasonable for preliminary analysis. **Table 12-1** highlights the process used to estimate the development sum total.

Table 12-1 Estimation of ASRG Development and Manufacturing

Cost Element	Development Sum \$M FY2015	Development Escalation \$M FY2015	Production Sum \$M FY2015	Production Escalation \$M FY2015	Sum Total \$M FY2015 (Includes cost escalation factor)	Sum Total \$M FY2020
GPHS-RTG	-	-	-	-	352.78	384.18
MMRTG	66.85	15.78	93.99	15.11	191.73	208.8
ASRG	188.22	21.22	264.63*	20.32*	452.85	493.16

The asterisked numbers indicate estimates that were derived from the MMRTG’s development/product costs and factored into the ASRG development cost. This underlying assumption was made to approximate the total cost of \$493.16M FY2020. The sum total was added to the flight system hardware cost. It is important to note that this is a preliminary cost analysis. Schedule overruns, or even cooperation with existing NASA projects may increase or decrease this development and manufacturing cost as it is a shared technology among future missions.

Other considerations and assumptions for the PCEC model include the total prime mission duration being limited to the SGL mission only, and the total accumulated radiation would be of the components inside the radiation vault. Miscellaneous costs were lumped into public and outreach, and reserve costs were not added as lumped percentages to the total cost. **Figure 12-2** is the cost breakdown of the flight system. Note that the electrical and power distribution subsystem accounts for nearly 73.5% of the total cost and can be considered as an area for cost reduction. The reactor development and integration costs as well as its operation through the mission were considered in these assumptions.

Component	\$M (FY2020)
F.S. Project Management	10.23
F.S. Systems Engineering	36.20
F.S. Product Assurance	10.19
Structures	19.75
Thermal Management	6.49
Power Management	493.16
GN&C	18.61
Propulsion (w/o Xenon propellant cost)	3.19
Telecommunications	43.79
Command & Data Handling	18.00
Flight System I&T	11.66
Total Flight System Cost	671.28

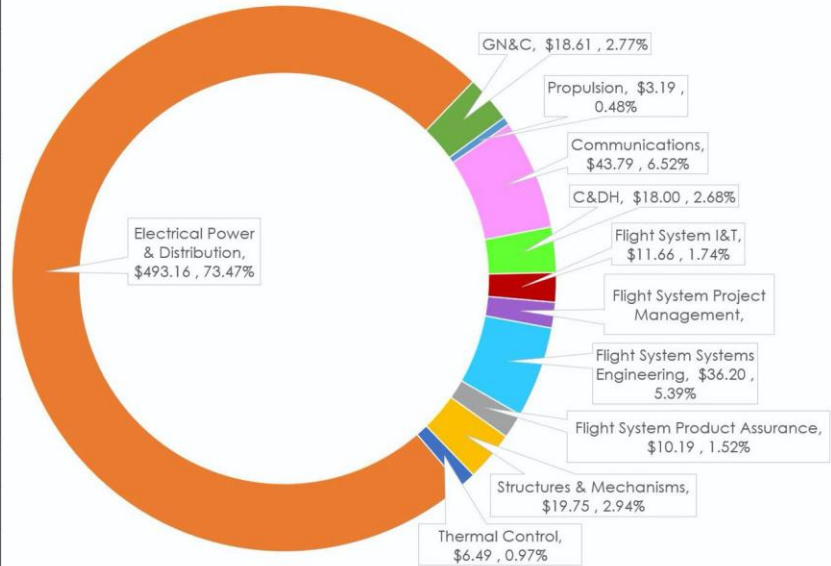


Figure 12-2 Total Flight System Cost Breakdown

Figure 12-3 breaks down the entire project cost estimation. Mission operations is clearly the largest cost in the model as it requires nearly \$1.25 billion. However, it must be noted that this is estimated using PCEC's cruise phase cost estimation component. This certainly can be reduced with limited communication with the spacecraft during its cruise after the Jupiter flyby. Periodic equipment exercising and state reporting can be done with the Deep Space Network, but further investigation into very long duration, low communication states need to be investigated. Finally, the operations cost can be further reduced by keeping a smaller number of staff to the project in the cruise phase of the mission. The PCEC model would have to be adjusted or replaced to estimate the cost difference for this phase of the mission.

Component	\$M (FY2020)
Project Management	18.51
Systems Engineering	65.47
Mission Assurance	18.43
Science/Technology	17.32
Payload	26.40
Flight System	671.28
Mission Operations	1,248.72
Launch Services (w/o LV)	195.08
Ground Data Systems	168.24
System Integration, Test, & Checkout	21.08
Outreach	0.56
Total \$M FY2020	2,451.07

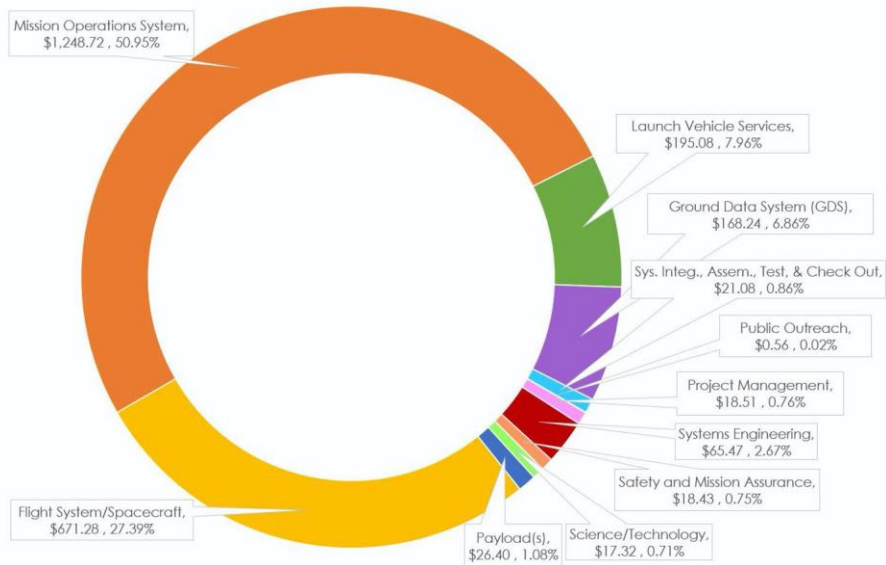


Figure 12-3 Total Project Cost Breakdown

12.3.2 Comparing Total Cost

To put the customized PCEC model into perspective, the project cost was estimated using two alternate methods. These models have the same limitations as PCEC in terms of the nuclear power system and mission type. QuickCost from SMAD is a system level CER that was referenced to provide an idea of how the projected cost of the mission would change as the proposal study continued. The model relies on a single CER that assumes various project and hardware components such as: dry mass and power, mission type and duration, team experience, and instrument properties. It assumes a high standard error rate of 41% as it is a broad stroke tool. One modification that needed to be made was the beginning of life (BOL) power. Like PCEC, QuickCost is not able to handle nuclear power sources, and so the EOL maximum expected power draw was entered. The USMC 8.0 model, Large Satellite Cost Model, and NASA Instrument Cost Model (NICM) were coupled together to have a preliminary estimation for all project cost excluding operations. **Table 12-2** compiles the respective costs from the three models based on their capabilities.

Table 12-2 Cost Estimation Comparison (FY2020)

Model	Total Cost w/o Operations \$B	Total Cost \$B
PCEC	1.202	2.451
QuickCost	-	2.670
USMC 8.0	1.739	-

12.4 System Mass & Power Breakdown

Table 12-3 includes a breakdown of the spacecraft’s mass and power requirements. The asterisked masses for the subsystems are those that were not considered for the additional 15% margin. It is important to note that despite the large power draw, this is in the absolute worst case scenario when all the instruments are active.

Table 12-3 RETRIEVER Mass and Power System Summary

Sub System	Mass (kg)	Power (W)
Structure/Mechanisms	440	10
Radiation Management	240	0
Thermal Management	50	10
Attitude Control	150	125
Power Management	1445*	120
Cabling	80	0
Propulsion	290	8000
Telecommunications	50	395
Command & Data Handling	75*	55
Sub-Total	With 15% Margin 3000	With 20% Margin 9440
Payload	200	150
Propellant	10800	0
Launch Vehicle Adapter	415	0
Total	Launch Mass 14415	Total Power 9590

12.5 System Compliance

As follows in **Table 12-4**, is the breakdown of the architectures compliance with each of the system level requirements. RETRIEVER proves to be fully compatible with all mission requirements, with a small note for SR3.4. ARIEL’s mirror size is 0.95m while the RFP was negotiated to have a requirement of 1.0m diameter, down from 1.5m as shown in the RFPs original document. The systems compliance was approved by the RFP issuer after showing the spacecraft exceeds requirement DR2.4, an image resolution of 10 km/pixel, by over a factor of five, 1.8 km/pixel.

Table 12-4 Architecture System Level Requirement Compliance Matrix

Req.#	Requirement	Capability	Compliance
SR1.0	Trajectory		
SR1.1	The launch shall be conducted on today's available launch vehicles (including the SLS).	SLS Block 1B LV	Compliant
SR1.2	The spacecraft shall reach 550 AU in less than 60 years from launch.	58.01 years	Compliant
SR1.3	The spacecraft shall remain in LoS for at least 30 days at 550 AU for SGL.	Final RA: 166.62 Final Dec: 5.04	Compliant
SR1.4	All required maneuvers shall be addressed and corrections to the orbit.	✓	Compliant
SR2.0	Observations		
SR2.1	All scientific objectives shall be met by the spacecraft.	✓	Compliant
SR2.2	An exoplanet system shall be selected for observation.	TRAPPIST-1	Compliant
SR2.3	An exoplanet shall be directly imaged using solar gravitational lensing (SGL).	✓	Compliant
SR2.4	A schedule shall be provided for all major scientific experiments.	✓	Compliant
SR3.0	Vehicle		
SR3.1	The spacecraft shall withstand both the launch vehicle and space environment.	✓	Compliant
SR3.2	The spacecraft power supply shall be capable of transmitting all scientific data back to Earth.	10 kW	Compliant
SR3.3	The spacecraft's attitude control system shall be capable of maneuvering the telescope to perform SGL for at least 30 days.	✓	Compliant
SR3.4	The spacecraft shall be equipped with a 1.0 m diameter telescope and coronagraph at 550 AU.	0.95 m	Compliant*
SR4.0	Management		
SR4.1	Cost estimates shall be provided for all subsystems and operations of the mission.	Total: \$2.451B FY2020 (w/o LV)	Compliant
SR4.2	A timeline of all major events and stages of the mission shall be provided.	✓	Compliant

13 Future Improvements and Conclusion

13.1 Future Improvements

Major weight reductions could be made to the design by using laminates. Changing the face sheets of each sandwich panel and the sheets enclosing the propulsion house a carbon fiber laminate with the same thickness would result in a structural mass decrease of approximately 50 kilograms [68]. The initial hesitation in the design to use laminates come from the unpredictability of the lamination of each ply after half a century in space. Future research into the behavior of laminates and potting compounds in a deep space environment for extended durations of time would be required in order to gain more confidence in the use of these materials for the mission.

The mission duration can be reduced by roughly 15 years if powered flybys of either Jupiter or the Sun are implemented. Trajectories can be in excess of 9 AU/year for Jupiter flybys with an applied ΔV of 8 km/s, and 12 AU/year for Perihelion flybys with an applied ΔV of 7 km/s [15]. These options were not considered in this mission design due to execution errors being amplified through the flyby. When maneuver design technology improves and such large-scale burns can be applied with limited error uncertainty, these options become interesting possibilities to expedite the mission.

13.2 Conclusion

In order to meet mission requirements of this magnitude and difficulty, radical design philosophies must be considered to go further and faster than any man-made object before it. Similar to the previous Voyager missions, Voyager III continues their legacy in advancing the use of new technologies to solve previously impossible problems. The most forefront risk of the whole mission was its reliability to last 58 years, almost 50% more than that of Voyager 1 and 2 [1]. To address this, every system on RETRIEVER either has additional redundant systems or mitigation paths that still provide limited mission capabilities. RETRIEVER itself has proved that it is a more than capable architecture that is able to reach the interstellar medium and 550 AU. The combination of the Hall-Effect propulsion and fission reactor allow spacecraft to reach its mission point in a safe and reliable manner, and the ARIEL telescope will return images of the surface, in well over 1,000,000x the detail ever seen previously. In conclusion, RETRIEVER is a JPL NASA mission architecture that will expand the bounds of our current knowledge of the universe and allow for increased capabilities in the search for life on other planets.

Acknowledgements

The STARWORKS team would like to thank:

- Dr. Nakhjiri of Cal Poly Pomona for his mentorship and support through this senior design class.
- Dr. Try Lam and Dr. Damon Landau of JPL Mission Design and Navigation for their guidance and advice for the Star broad search and trajectory design.
- Dr. Scott and the rest of the Voyager III science team at JPL for their feedback from the beginning to the end of the design period.
- All the review teams and individual reviewers from Jet Propulsion Laboratory, Cal Poly Pomona, Lockheed Martin, and Northrup Grumman.

References

- [1] NASA JPL, "Voyager Did You Know," [Online]. Available: <https://voyager.jpl.nasa.gov/mission/did-you-know/>. [Accessed 07 April 2020].
- [2] J.-R. C. Cook, "Juno Armored Up to Go to Jupiter," NASA, 12 August 2010. [Online]. Available: https://www.nasa.gov/mission_pages/juno/news/juno20100712.html. [Accessed 2020].
- [3] NASA Technology Transfer Program, "Project Cost Estimating Capability (PCEC)," NASA, May 2020. [Online]. Available: <https://software.nasa.gov/featuredsoftware/pcec>. [Accessed May 2020].
- [4] NASA, "The Planetary Society," [Online]. Available: <https://www.planetary.org/blogs/casey-dreier/images/nasa-flight-mission-project-life-cycle.html>.
- [5] R. A. T. a. C. H. Jaroschek, "The Heliospheric Termination Shock," 25 July 2008. [Online]. Available: <https://arxiv.org/pdf/0807.4170.pdf>. [Accessed 2020].
- [6] S. G. Turyshev, M. Shao, V. T. Toth, L. D. Friedman and L. Alkalai, "Direct Multipixel Imaging and Spectroscopy of an Exoplanet with Solar Gravity Lens Mission (NIAC Phase II Study)," NASA Innovation Advanced Concepts, 18 March 2020. [Online]. Available: <https://arxiv.org/ftp/arxiv/papers/2002/2002.11871.pdf>. [Accessed 2020].
- [7] G. A. Landis, "Mission to the Gravitational Focus of the Sun,," [Online]. Available: <https://arxiv.org/ftp/arxiv/papers/1604/1604.06351.pdf>. [Accessed 2020].
- [8] N. A. A. S. ADMINISTRATION, "Cassini Launch," october 1997. [Online]. Available: https://www.jpl.nasa.gov/news/press_kits/cassini.pdf. [Accessed 2020].
- [9] SpaceQuest, Ltd., "MAG-3 Satellite Magnetometer," Fairfax.
- [10] G. Gloecker, "The Solar Wind Ion Composition Spectrometer," *Astronomy and Astrophysics Supplement Series*, vol. 92, no. 2, pp. 267-289, 1992.
- [11] S. R. A. N and L. D., "THE CASSINI COSMIC DUST ANALYZER," Kluwer Academic, Netherlands, 2004.

- [12] P. Eccleston and K. Middleton, "ARIEL Payload Design Description," RAL Space, 2017.
- [13] C. Maccone, *Deep Space Flight and Communications - Exploiting the Sun as a Gravitational Lens*, Chichester, UK: Praxis Publishing Ltd. , 2009.
- [14] National Aeronautics and Space Administration, "Space Launch System (SLS) Program Vehicle Data Summary," [Online]. Available: <https://ntrs.nasa.gov/archive/nasa/casi.ntrs.nasa.gov/20120014495.pdf>.
- [15] N. Arrora, N. Strange and L. Alkalai, "Trajectories for a Near Term Mission to the Interstellar Medium," JPL Technical Report Server, Pasadena, 2015.
- [16] P. Blanco and M. Carl, "Rocket Propulsion, Classical Relativity, and the Oberth Effect," *The Physics Teacher*, vol. 57, no. 7, p. 439, 2019.
- [17] D. Landau and T. Lam, "Broad Search and Optimization of Solar Electric Propulsion Trajectories to Uranus and Neptune," *Advances in Astronautical Sciences*, vol. 135, pp. 2093-2112, 2010.
- [18] N. Strange, D. Landau, R. Hofer, S. Snyder, T. Randolph, S. Campagnolar, J. Szabo and B. Pote, "Solar Electric Propulsion Gravity-Assist Tours For Jupiter Missions," *AIAA/AAS Astrodynamics Specialist Conference*, pp. 1-9, 2012.
- [19] T. A. Pavlak, R. B. Frauenholz, J. J. Bordi, J. A. Kangas and C. E. Helfrich, "Maneuver Design for the Juno Mission: Inner Cruise," American Institute of Aeronautics and Astronautics, 2014.
- [20] J. A. Sims and J. M. Longuski, "Analysis of V_{∞} Leveraging for Interplanetary Missions," American Institute of Aeronautics and Astronautics, West Lafayette, 1994.
- [21] L. Weiss, "Cassini Controversy," *Mother Jones*, 30 September 1997. [Online]. Available: <https://www.motherjones.com/politics/1997/09/cassini-controversy/>. [Accessed 20 April 2020].
- [22] Technische Universitat Braunschweig, "MASTER (Meteoroid And Space debris Terrestrial Environment Reference)," Technische Universitat Braunschweig, [Online]. Available: <http://www.space-systems.eu/index.php/de/master>. [Accessed 27 March 2020].
- [23] SpaceX, "SpaceX Falcon Heavy Users Guide," January 2020. [Online]. Available: https://www.spacex.com/sites/spacex/files/falcon_users_guide_10_2019.pdf.
- [24] United Launch Alliance, "ULA Delta IV Heavy User's Guide," January 2020. [Online]. Available: <https://www.ulalaunch.com/docs/default-source/rockets/delta-iv-user%27s-guide.pdf>.
- [25] United Launch Alliance, "ULA Atlas V-551 Users Guide," January 2020. [Online]. Available: <https://www.ulalaunch.com/docs/default-source/rockets/atlasusersguide2010.pdf>.
- [26] J. S. R. V. K. a. P. M. J. Sovey, "Ion Propulsion Development Projects in the U.S.: Space Electric Rocket Test I to Deep Space 1," AIAA, Cleveland, 2011.
- [27] W. A. Hosknis, R. S. Aadland, N. J. Mecjel, L. A. Talerico and J. M. Monheiser, "NEXT Ion Propulsion System Production Readiness," AIAA, Cincinnati, 2007.
- [28] J. Szabo, B. Pote and L. Byrne, "Eight Kilowatt Hall Thruster System Characterization," IEPC, Washington D.C., 2013.
- [29] J. Jackson, J. Cassidy, M. Allen and R. Myers, "Development of High Power Hall Thruster Systems to Enable the NASA Exploration Vision," NASA, Seville, 2018.

- [30] I. Busek Co., "GEOSAT Propulsion System Architecture with Electric Apogee Motor". United States of America Patent 15/138,748, 22 December 2016.
- [31] D. W. Miller and J. Keesee, "Spacecraft Power Systems," [Online]. Available: https://ocw.mit.edu/courses/aeronautics-and-astronautics/16-851-satellite-engineering-fall-2003/lecture-notes/l3_scpowersys_dm_done2.pdf.
- [32] Idaho National Laboratory, "Atomic Power in Space II," 2015.
- [33] M. A. Gibson, L. Mason and C. Bowman, "Development of NASA's Small Fission Power System for Science and Human Exploration," American Institute of Aeronautics and Astronautics, Oak Ridge.
- [34] M. A. Gibson, D. I. Poston and P. McClure, "NASA's Kilowatt Reactor Development and the Path to Higher Power Missions," NASA.
- [35] J. F. Zakrajsek, D. F. Woerner and J.-P. Fleurial, "NASA SPECIAL SESSION: NEXT-GENERATION RADIOISOTOPE THERMOELECTRIC GENERATOR (RTG) DISCUSSION," NASA.
- [36] D. Edberg, Introduction to Spacecraft Design & System Engineering, Cognella, 2006.
- [37] M. Gibson, D. Palac, L. Mason and M. Houts, "Nuclear Systems Kilowatt Overview," NASA, 22 February 2016. [Online]. Available: <https://ntrs.nasa.gov/archive/nasa/casi.ntrs.nasa.gov/20160012354.pdf>. [Accessed 2020].
- [38] M. V. Podzolko, I. V. Getselev, Y. I. Gubar, I. S. Veselovsky and A. A. Sukhanov, "Charged Particle Fluxes and Radiation Does in Earth-Jupiter-Europa Spacecraft's Trajectory," February 2009. [Online]. Available: http://www.iki.rssi.ru/conf/2009elw/presentations/presentations_pdf/session2/podzolko_getselev_ELW.pdf. [Accessed 2020].
- [39] Honeywell, "GG1320AN Digital Laser Gyro," [Online]. Available: <https://aerospace.honeywell.com/content/dam/aero/en-us/documents/learn/products/sensors/brochures/GG1320ANDigitalLaserGyro-bro.pdf?download=true>. [Accessed 2020].
- [40] Honeywell, "Constellation Series Reaction Wheels," Honeywell.
- [41] U.S. Army-Navy, "AND10139," in *Aeronautical Design Standards*, 1983.
- [42] NASA, "Space Launch System (SLS) Mission Planner's Guide - Rev A," [Online]. Available: <https://ntrs.nasa.gov/archive/nasa/casi.ntrs.nasa.gov/20170005323.pdf>. [Accessed 10 May 2020].
- [43] eMarketAmerica, "Bend Radius," American Machine Tools Co., 2011-2019. [Online]. Available: https://www.americanmachinetools.com/bend_radius.htm. [Accessed 22 October 2019].
- [44] "Ames Technical Standard," [Online]. Available: <https://www.nasa.gov/sites/default/files/atoms/files/std8070.1.pdf>.
- [45] MSC Software, Dynamic Analysis User's Guide: MSC Nastran 2012, 2011.
- [46] W. J. Larson, Space Mission Analysis and Design 3rd Edition, Kluwer Academic Publishers, 1999.
- [47] Aerojet Rocketdyne, "In-Space Propulsion Data Sheets: Monopropellant and Bipropellant Engines".
- [48] Honeywell, "Honeywell Delivers 250th Miniature Inertial Measurement Unit For Space Missions," Honeywell, [Online]. Available: <http://www51.honeywell.com/honeywell/news-events/press-releases-details/03.31.09MIMU.html>. [Accessed 2020].

- [49] Honeywell, "Q-Flex® QA-2000 Accelerometer," [Online]. Available: https://aerospace.honeywell.com/content/dam/aero/en-us/documents/learn/products/sensors/brochures/Q-FlexQA-2000Accelerometer_bro.pdf?download=true. [Accessed 2020].
- [50] J. J. T. D. Peter Jorgenson, "MicroASC: A Miniature Star Tracker," Technical University of Denmark.
- [51] SolarMEMS Technologies, "SSOC-A60 Technical Specification, Interfaces & Operation," [Online]. Available: <https://www.cubesatshop.com/wp-content/uploads/2016/06/SSOCA60-Technical-Specifications.pdf>. [Accessed 2020].
- [52] J. E. Scott R. Starin, "19.1 Attitude Determination and Control Systems," [Online]. Available: <https://ntrs.nasa.gov/archive/nasa/casi.ntrs.nasa.gov/20110007876.pdf>. [Accessed 2020].
- [53] NASA, "Mars Reconnaissance Orbiter Command and Data Handling Systems," [Online]. Available: <https://mars.nasa.gov/mro/mission/spacecraft/parts/command/>. [Accessed 2020].
- [54] A. D. D. E. S. M. J. R. D. S. Richard Berger, "RAD750TM SPACEWIRE-ENABLED FLIGHT COMPUTER FOR LUNAR RECONNAISSANCE ORBITER," BAE.
- [55] NASA, "Europa Study 2012 Report: Europa Orbiter Mission," 2012. [Online]. Available: <https://www.lpi.usra.edu/opag/europa2012/ES%202012%20Report%20B%20Orbiter%20-%20Final%20-%202020120501.pdf>. [Accessed 2020].
- [56] NASA, "Mars Reconnaissance Orbiter," [Online]. Available: <https://mars.nasa.gov/mro/>. [Accessed 2020].
- [57] M. M. Ed Benowitz, "Patching Flight Software on Mars," 2015. [Online]. Available: https://www-robotics.jpl.nasa.gov/publications/Mark_Maimone/FSW2015_Benowitz_Maimone_4.pdf. [Accessed 2020].
- [58] Sharing Earth Observation Resources, "Gaia Astrometry Mission," [Online]. Available: <https://directory.eoportal.org/web/eoportal/satellite-missions/g/gaia>. [Accessed 2020].
- [59] BAE Systems, "RAD750® 6U CompactPCI Single Board Computer," [Online]. Available: <https://www.baesystems.com/en-us/our-company/inc-businesses/electronic-systems/product-sites/space-products-and-processing/radiation-hardened-electronics>.
- [60] JPL, "Deep Space Network Services Catalog," 2015.
- [61] C. D. Brown, Elements of Spacecraft Design, AIAA Education Series, 2002.
- [62] J. Taylor, "Dawn Telecommunications: DESCANSO Design and Performance Summary Series," JPL.
- [63] J. Taylor, "Cassini Orbiter/Huygens Probe Telecommunications: DESCANSO Design and Performance Summary Series," JPL, 2002.
- [64] J. Talor, "JUNO Telecommunications: DESCANSO Design and Performance Summary Series," JPL, 2017.
- [65] M. Gibson, D. Poston, P. McClure, T. Godfroy, M. Briggs and J. Sanzi, "The Kilowatt Reactor Using Stirling Technology (KRUSTY) Nuclear Ground Test Results and Lessons Learned," NASA Technical Report Server, 2017.
- [66] M. Wall, "Nuclear Reactor for Mars Outpost Could Be Ready to Fly by 2022," Space.com, 12 August 2019. [Online]. Available: <https://www.space.com/nuclear-reactor-for-mars-outpost-2022.html>. [Accessed 21 January 2020].

- [67] J. E. Werner, S. G. Johnson, C. C. Dwight and K. L. Lively, "Cost Comparison in 2015 Dollars for Radioisotope Power Systems—Cassini and Mars Science Laboratory," Idaho National Laboratory, Idaho Falls, 2016.
- [68] S. K. M. Minus, "The Processing, Properties, and Structure of Carbon Fibers," *JOM*, vol. 57, no. 2, pp. 52-58, 2005.
- [69] J. R. Brophy, "Ion Propulsion System (NSTAR) DS1 Technology Validation Report," Jet Propulsion Laboratory, Pasadena, 1995.
- [70] M. J. Patterson and S. W. Benson, "NEXT Ion Propulsion System Development Status and Performance," AIAA, Cincinnati, 2007.
- [71] J. R. Brophy and M. G. Marucci, "Implementation of the Dawn Ion Propulsion System," AIAA, Tucson, 2005.
- [72] A. Hawkes, "Kepler's Final Image Shows a Galaxy Full of Possibilities," NASA, 06 February 2019. [Online]. Available: <https://www.nasa.gov/image-feature/ames/kepler-s-final-image-shows-a-galaxy-full-of-possibilities>. [Accessed 2020].
- [73] T. Greicius, "Interstellar: Crossing the Cosmic Void," NASA, 21 December 2016. [Online]. Available: <https://www.nasa.gov/feature/jpl/interstellar-crossing-the-cosmic-void>. [Accessed 2020].